Engineering Formulations for the Treatment of Periodontal Disease

by

Ashlee Chennicia Greene

B.S., Massachusetts Institute of Technology, 2013

M.Eng., Cornell University, 2014

M.S., Cornell University, 2015

Submitted to the Graduate Faculty of the

Swanson School of Engineering in partial fulfillment

of the requirements for the degree of

Doctor of Philosophy

University of Pittsburgh

2021

UNIVERSITY OF PITTSBURGH

SWANSON SCHOOL OF ENGINEERING

This dissertation was presented

by

Ashlee Chennicia Greene

It was defended on

August 23, 2021

and approved by

Morgan V. DiLeo, Ph.D., Assistant Professor, Department of Ophthalmology, Bioengineering, Chemical Engineering, and Clinical and Translational Science

Tagbo Niepa, Ph.D., Assistant Professor, Department of Chemical and Petroleum Engineering

Charles Sfeir, Ph.D., D.D.S., Associate Professor, Department of Oral Biology, Periodontics and Bioengineering

Dissertation Director: Steven R. Little, Ph.D., Professor and Chair,
Department of Chemical and Petroleum Engineering, Bioengineering, Pharmaceutical Sciences, Opthalmology and Immunology

Engineering Formulations for the Treatment of Periodontal Disease

Ashlee Chennicia Greene, PhD

University of Pittsburgh, 2021

Periodontal disease (periodontitis) is a common disease that impacts approximately 46% of US adults over the age of 30 (~141 million people). Characterized by an overburden of invasive oral bacteria that triggers gum inflammation and plaque buildup, periodontitis results in pocket formation around the teeth and eventual gum and tooth loss. Current treatment options either combat the invasive bacteria and biofilm growth or target the inflammation and underlying immune imbalance. However, with recent advances in the field of controlled drug delivery and new understanding of the biological environment of the periodontium, new and revamped formulations could improve disease outcomes. Therefore, we developed three types of extended release, bioerodible microsphere formulations that can each resolve the unmet needs of currently available treatments with translational value for patients with varying forms of periodontitis.

In aim 1, in anticipation of FDA generic (ANDA) drug applications to replace a common periodontal adjunct antibiotic therapy (Arestin®), we use reverse engineering to determine critical microsphere design parameters. We then develop a panel of possible generics/comparator microsphere formulations to validate a novel dissolution device for FDA bioequivalence testing. In aim 2, we develop a one-pot formulation that encapsulates a natural product (cranberry extract) with stearic acid (SA) for a new, potential Johnson & Johnson consumer healthcare product. The addition of a bioadhesive (polyvinylpyrrolidone (PVP) or ethyl lauroyl arginate (LAE)) is studied for tooth surface/pellicle targeting and the prevention of biofilm growth *in vitro*. Lastly, in aim 3, we take a next generation approach to modulate a patient's own immune balance to resolve disease.

We develop a formulation with a combination of factors (IL2, TGFβ and rapamycin) for the local induction of regulatory T cells to bring the periodontium back to homeostasis. A murine, ligature-induced periodontitis animal model is used to assess the potential impact of our immunomodulatory formulation on periodontal disease prevention.

Table of Contents

List of Tables

List of Figures

Acknowledgments

I would like to first and foremost thank my PhD advisor and mentor Dr. Steve Little for his 6+ years of invaluable guidance and sincere support. From the moment I was welcomed into the Chemical Engineering department at the University of Pittsburgh and the Little lab, I have felt a sense of belonging. The nurturing environment that Steve has fostered within the department and the lab has been critical to my success. Although my PhD journey has been long (and especially difficult during the COVID19 pandemic), it has been extremely rewarding. I have grown tremendously both personally and professionally from all my experiences and numerous collaborators along the way. A special thanks goes to an essential collaborator, Dr. Charles Sfeir, for his role as a committee member and for all of his assistance and periodontal disease clinical expertise that he has shared throughout the years. Additional thanks and appreciation go to my committee members Dr. Tagbo Niepa and Dr. Morgan Fedorchak for all of their support and for their feedback that also helped to strengthen my dissertation.

Many thanks also to the numerous project collaborators that I have worked with along the years. Dr. Lisa Rohan and Dr. Sravan Patel were invaluable collaborators on our project with the FDA and taught me so much about dissolution and general pharmaceutical product development. Dr. Sayuri Smith and Dr. Gustavo Garlet were of particular help in my training at the beginning of my PhD when I was troubleshooting a lack disease induction in the murine gavage animal model I started out with before switching to the ligature model. Additionally, Dr. Mostafa Shehabeldin and Dr. Jin Gao of Sfeir lab were instrumental to all the protocol development, animal work and sample analysis performed in Aim 3.

In many ways, your lab becomes your family, so many thanks also go to my labmates both past (Alice Liang, Dr. Abhinav Acharya, Dr. Ethan Bassin, Dr. Sang Beom Lee, Dr. Andrew Glowacki, Dr. Riccardo Gottardi, Dr. Michelle Ratay, Dr. Sam Rothstein, and undergraduates Nick Yuhas, Kayla Lemaster) and present (Dr. Stephen Balmert, Lizzy Bentley, Matt Borrelli, Julie Kobyra, Dr. Andrea Schilling and Dr. Nihan Yonet Tanyeri) who have helped to shape my PhD experience- I cannot say thank you enough.

On a personal note, last but certainly not least, a huge thank you goes to my family who has been my support system from the very beginning. We have been on this journey towards a PhD for a long time and I could not have made it without their constant encouragement, support and prayers. To my husband Jeremy, thank you for taking this journey with me even after completing your own PhD! Words are not enough to say how you have made the long days and nights, uncertainties, small and big wins all the better. To my parents Jennifer and Lemuel, thank you for raising me to continually strive for my best and to be tenacious in the face of difficult challenges. To my siblings Brittany and Lemuel and dog Cleo, thank you for all of your emotional support and for being a constant source of laughter. To my in-laws Ron and Nancy, thank you for giving me a home away from home, in Pittsburgh. Lastly, to my grandparents Julian & Margaret and Thomas & Francis who are not here today but forever in my heart, this PhD is just the beginning and I hope I continue to make you proud.

1.0 Introduction

1.1 Formulation Development

Pharmaceuticals play an important role in everyday life; from maintaining health to curing ailments. This has been made possible by the continuous drug discoveries throughout the last 200 years[1]. Yet, with so many critical discoveries focused on elucidating drug mechanisms and effects, it is easy to forget that these main ingredients rarely work best when administered alone. Instead, they are often administered as a combined product with other "inert" ingredients for better patient outcomes. This essential interplay between an active pharmaceutical ingredient (API) of interest with inactive components (excipients)[2] to create a final drug product, is the fundamental nature of formulation development. Furthermore, designating excipients as inactive does not mean they are inconsequential. On the contrary, excipients can provide beneficial effects such as pH control, increased API solubility, extended API stability, or enhanced processability of the drug product[3,4].

The role of excipients can also be guided by the dosage form of the drug product. Dosage forms are product-suited specific routes of administration like aerosols, capsules, gels, emulsions or powders (lyophilized microspheres fall into these categories)[5]. Accordingly, each dosage has its own limitations that excipients can help address. A bitter tasting tablet that's administered orally, undergoes degradation by atmospheric moisture or oxygen exposure easily, and needs protection against gastric acid would then dictate the addition of excipients that are humectants[6] or antioxidants[7], with a sweetener to mask the taste[8] and coating agents[9] to give some gastric acid protection and control release.

1.1.1 Microsphere Formulation Development

Of the many dosage forms used for controlled release, polymeric microspheres are common due to their easily tunable properties[10]. In the range of 1-1000um, these systems are considered microspheres but when less than 1um, they are nanoparticles. Additionally, polymeric microspheres can be made from naturally occurring materials such as collagen, chitosan, poly dextran or they can be synthetic and made of poly methyl methacrylate (PMMA) (non-biodegradable) vs PLGA (biodegradable)[11,12].

Biodegradable microspheres like PLGA microspheres offer the additional advantage of their well-characterized, tri-phasic release[13]. The first phase of release is an initial burst which is influenced by factors such as drug dispersion throughout matrix, co-encapsulation with excipients, osmotic pressure, initial drug loading and porosity. The second phase, the lag phase (with a near zero release rate), can be tuned by adjusting the degradation rate with catalytic excipients or the polymer molecular weight. And lastly, phase three is the final release phase where release is normally dictated by diffusion can be altered by changing the polymer blend[14].

Nevertheless, while there are a wide variety of benefits to incorporating excipients into formulations, it is also remains critical to recognize how excipient-induced effects may also have disease specific consequences. This was best demonstrated in the Australian 1968-9 phenytoin intoxication incident where excipient diluent calcium sulphate was replaced by lactose[15]. What was considered a harmless substitution resulted in a large increase in mean serum phenytoin concentration above the toxic threshold due to the increase in solubility with the incorporation of lactose in the formulation.

There is both versatility and a delicate balance of incorporating excipients in formulations. Herein, we explore how to harness this understanding for developing treatments for periodontal disease.

1.2 Periodontal Disease; Etiology and Pathogenesis

Periodontal disease (periodontitis) is the sixth-most prevalent condition in the world[16], with over 11% of individuals worldwide suffering from the most severe form of the disease[16,17]. In the U.S. alone, approximately 46% of US adults over the age of 30 (~141 million people)[18,19] are impacted. This high prevalence not only corresponds to a high healthcare burden but a large global economic burden as well. It is estimated that direct (treatment) and indirect costs (as measured by lack of productivity/absenteeism as tooth loss can impact nutrition and quality of life) together accounted for an annual economic impact of 442 billion USD/yr cost in 2010[20] and is rising.

Contributing to the high prevalence of periodontitis is its multifactorial nature whereby many factors can augment disease development and clinical outcomes. Genetic, environmental and acquired risk factors such as; pre-existing diseases, age, gender, medications, smoking and general oral hygiene can all influence disease progression[21]. Additionally, socioeconomic status has emerged as another risk factor as those without accessibility to dental care are disproportionately impacted by periodontitis[22]. Conversely, with oral health tied to general health, periodontal disease has also been associated with higher incidences of other diseases like diabetes, cardiovascular disease, miscarriages[23–27], and Alzheimer's disease[28–30]. Interestingly, with the COVID-19 pandemic, there have been several studies indicating links between periodontitis and COVID-19 severity[31,32] as well.

Symptoms of periodontitis can vary but many of the effects are bacterial burden driven. The main periodontal pathogens responsible for the initiation and propagation of periodontitis from a bacterial perspective are anaerobes *Aggregatibacter actinomycetemcomitans, Tannerella forsythia*, and *Porphyromonas gingivalis*[33–35]. An overburden of these bacterial pathogens causes an accumulation of biofilm and plaque that triggers inflammation of the tooth supporting structures. This inflammation then leads to a loss of gingiva and periodontal ligament attachment, bleeding, pain, pocket formation and eventual bone and tooth loss[36]. While patients can sometimes take notice of these symptoms at home during their oral health care routine, it takes a clinical evaluation from a general dentist/periodontitis for a diagnosis.

1.3 Clinical Interventions

To diagnose a patient with periodontitis, they receive a comprehensive periodontal evaluation[37]. This evaluation consists of an assessment of the patient's overall health including dental history, medical history and occurrence of any periodontal risk factors. Furthermore, an evaluation of the teeth and soft tissues is performed to determine clinical parameters such as tooth mobility, probing depth, plaque score, gingival attachment level and bleeding on probing[38,39]. Based on these clinical parameters, disease severity or "case type" can then be categorized as either mild, moderate or severe with the treatment modality determined accordingly[38,40,41]. In a mild case, with shallow probing depths (<4mm pockets) and/or calculus and plaque deposits only on the enamel without evidence of bone loss in radiographs, a prophylaxis cleaning may be performed with an emphasis on at home oral health maintenance[42]. For moderate cases with clinical loss of periodontal attachment and/or radiographic evidence of bone loss and/or radiographic evidence of

root surface calculus, a scaling and root planing procedure would be performed with the addition of an antibiotic adjunct therapy. For severe cases, treatment usually requires dental surgery that may include; flap surgery-to more effectively clean the root surface with sutures to reduce pocket size, soft tissue grafts- for a receding gumline, bone grafting- to regrow bone destroyed surrounding the tooth root or guided tissue regeneration- where biocompatible material is inserted to repair periodontal defects[43,44].

1.3.1 First line of action- Adjunct Therapy Treatment for moderate Periodontitis

With periodontal pathogens thought to be one of the primary agitators and initiators of disease, many initial periodontitis treatments target the local oral bacterial burden. A procedure known as scaling and root planning (SRP) is often first performed for the physical debridement and removal of bacterial plaque and calculus from the tooth and root surfaces[43,45,46]. The complex nature of bacterial biofilms on teeth creates a challenge for the development of treatment strategies. Biofilms consist of microbial cells enclosed in a multi-component anionic matrix of extracellular polymeric substances (mostly polysaccharides)[47,48]. Classic antimicrobial strategies for more extreme cases of oral disease have focused on bactericidal action through the use of antibiotics[49–51]. However, many of these classic antibiotics target the biosynthetic processes of actively growing bacteria and are consequently ineffective in treating persistent infections (like in periodontitis) where the bacteria have become quiescent[52,53]. Moreover, the matrix of the biofilm is known to impart shielding by deactivating antimicrobial and antibiotic agents, further limiting susceptibility of biofilms to these antimicrobial approaches as demonstrated by Anderl et al.[54] and others[55–58]. Nevertheless, for patient cases where SRP may not be enough, a systemic or local adjunct antibiotic therapy may also be prescribed or administered. Common local adjuncts include;

PerioChip® (chlorhexidine gluconate)[59–61], Atridox® (doxycycline)[62,63], Periostat®(doxycycline hyclate)[64,65] and Arestin® (minocycline hydrochloride)[43,66].

Of all the options for local, oral adjunct therapies, Arestin® is the only extended release (longer than 10days) periodontal product currently available[67]. Arestin is a subgingival product that contains 1 mg of the tetracycline antibiotic minocycline hydrochloride (MIN) incorporated into bioresorbable, polymeric (PLGA) microspheres. The active ingredient, minocycline, is a broad spectrum antibiotic that inhibits microbial protein synthesis. Major periodontal pathogens such as *Porphyromonas gingivalis*, *Prevotella intermedia, Fusobacterium nucleatum*, *Eikenella corrodens,* and *Actinobacillus actinomycetemcomitans* are susceptible to minocycline at minimal concentrations (<8mcg/mL)[68].

1.3.1.1 FDA ANDAs and dissolution testing

With a pending patent expiration, there will soon be generic versions of Arestin® (minocycline hydrochloride microsphere formulations) seeking FDA Abbreviated New Drug Application (ANDA) approval. As part of the approval process for an ANDA or even Investigation New Drug (IND) and New Drug Application (NDA) applications, drug release/dissolution data is required[69].

Dissolution testing of drug product remains one of the major performance tests used for control of batch quality, determination of effect of composition and processing, elucidating mechanism of drug release, and predicting in vivo performance[70–72]. Since its introduction in the pharmaceutical industry, the focus of dissolution testing[70] has undergone several changes and now encompasses not only providing adequate discrimination amongst formulations with manufacturing differences but also predicting clinical performance of drug products[72] by establishing in vitro-in vivo correlations (IVIVCs). This shift has encouraged the development of

more biorelevant dissolution methods, which are in vitro dissolution methods that simulate conditions a drug product will encounter after in vivo administration[71].

Yet, developing dissolution methods for controlled release products such as poly(lactic-co-glycolic acid) (PLGA) microspheres has remained challenging. There is a lot of difficulty due to the length of studies ranging from weeks to months, stability of the active molecule and media components during study duration, and detection limits of analytical methods. The latter is particularly true for low dose and hydrophobic drugs. Burgess' group has developed several dissolution methods based on sample and separate, dialysis, and continuous flow methods for particulate PLGA dosage forms applied parenterally[73–75]. Of these, the USP apparatus 4 dissolution system has been widely shown to be most discriminatory for particulate dosage forms.

Nevertheless, for PLGA microspheres applied specifically in the small anatomical crevice of periodontal pocket, the USP apparatus 4 device is not biorelevant. Development of a biorelevant dissolution method requires understanding of the in vivo environment of the periodontal space and replication of it during dissolution testing. There have been limited attempts to simulate the environment of the periodontal pocket i.e. the small region between the tooth and the inflamed gum for the purpose of dissolution studies. Recently, Ren et al.[76] reported a miniaturized flow-through system for dissolution of PerioChip®, a long-acting periodontal insert. However, this system is not suitable for particulates because the set-up will lead to undissolved particles traveling into dissolution samples due to the lack of filtration system. The periodontal pocket amounts to an extremely small volume of around 0.5 µL. The flow rate of the gingival crevicular fluid (GCF) present in the pocket was reported to be anywhere from 0.33 – 2.28 µL/min, depending on the disease stage[77].

This understanding of key parameters in the periodontal pocket has become more critical as 'new' generic minocycline hydrochloride microsphere formulations are required to be compared for bioequivalence to the relevant reference drug product- Arestin®. To determine bioequivalence, the FDA assesses measurements of the qualitative (Q1) and quantitative (Q2) sameness and changes of manufacturing process and excipient composition. Any new biorelevant dissolution device must take these key parameters into account.

1.3.2 Consumer Oral Health Care: Johnson & Johnson Products with a Natural Therapeutic Edge

Regardless of periodontitis disease severity, as both a prophylactic measure and as maintenance after SRP, a consistent oral hygiene regimen is always recommended[78]. Although periodontitis is highly prevalent, in the absence of other risk factors, it is easily preventable with twice daily toothbrushing, regular flossing and the use of a therapeutic mouthrinse (for the areas difficult to reach with a toothbrush)[79]. However, not all mouthrinses are made equal. While many therapeutic mouthrinses contain strong antiseptic ingredients like cetylpyridinium chloride (CPC) and chlorhexidine (CHX) for activity[80,81], others like Johnson & Johnson's Listerine® use a combination essential oils with natural antibacterial and antiseptic properties as the active ingredients[80,82,83]. Fittingly, a possible new natural active ingredient of growing interest is cranberry extract. Cranberry extract (CE15) is a derivative from cranberries/cranberry juice and contains 3 key active components; anthocyanins (A), proanthocyanins (PAC) and flavonols (FLAV)[84]. These components have been shown to have natural antibacterial/antibiofilm properties against many bacterial strains including *Helicobacter pylori*, *Streptococcus mutans*[84], *Staphylococcus aureus* and *Pseudomonas*[85], in a manner that is concentration dependent[86–88].

While these findings suggest cranberry extracts should be explored for oral/periodontal applications, there are several drawbacks. The first drawback is the working concentration needed for CE15 in a perinodal product. To be in the bulk concentration range of 5-10mg/mL of CE15 for biofilm inhibition (10mg/mL yields bactericidal activity which is undesired), with the average human saliva production rate of 1mL/min when stimulated, approximately 7.2 grams of CE15 would be required per day. However, delivering gram quantities of CE15 is not practical. This issue could be amended with a controlled release formulation that delivers locally, in the proximity of the biofilm, but the encapsulation of extracts can also be challenging[89–93].

Extracts like cranberry extract also present encapsulation challenges due to its multi-component nature. A diverse array of encapsulation methods have been used to microencapsulate extracts, each tailored to the composition and desired extract/formulation properties. Cyclodextrin-extract complexation has been used by Hill et al. [89] and others [94,95] for various applications in food products and supplements. Specifically, this complexation has been used to increase solubility while masking taste for cinnamon and clove extracts [89]. Cyclodextrin-extract complexation has also improved the physical/chemical stability of natural and synthetic coffee flavor extracts [94] and lemon oil and peppermint oil volatile liquid aroma extracts [95] while maintaining their antioxidant or antimicrobial activity (extract dependent). Several groups have also explored alginate-based delivery [90–92], poly(lactide)/poly(lactic-co-glycolic acid) (PLA/PLGA) nano- and microsphere delivery [96–100], liposomes [101,102] or lipid-based nanodelivery [93], to increase extract solubility, loading and antioxidant activity. Deladino et al. [92] resorted to the use of calcium alginate and calcium alginate-chitosan beads to encapsulate aqueous extracts from *Ilex paraguariensis* to retain polyphenol antioxidant activity. Separately, Kumari et al. [100] fabricated PLA nanoparticles by

solvent evaporation to encapsulate the hydrophobic cranberry extract flavonoid component quercetin.

While these strategies of alginate-based, or PLA/PLGA delivery could be useful for the selective encapsulation of aqueous soluble polyphenols (hydrophilic) or hydrophobic/lipophilic components individually, neither of these methods allow for the full encapsulation and high loading of all components into a single formulation. CE15 is particularly challenging to encapsulate as this extract contains a variety of compounds (known and unknown) including; flavonol glycosides (primarily myricetin-3-galactoside and quercetin-3-galactoside) [103], phenolic acids (primarily 3- and 5-caffeoylquinic acid) [104] along with coumaroyl iridoid glycosides [105] and fatty acids like linolenic acid [106,107]. These various CE15 extract components have different properties making encapsulation into a single formulation difficult. In addition to overcoming these challenges, to ensure targeted local delivery and increased oral residence time, any CE15 formulation would also need to bind directly to the tooth surface or pellicle- all specifications that are unprecedented for the delivery of cranberry extract.

1.3.3 Immune Modulation as an Alternative to Surgical Intervention

The above strategies of encapsulating an antibiotic or natural extract may be useful for cases of mild to moderate periodontitis but unfortunately for patients with severe periodontitis, treatment options are limited. Approximately 9% of patients with periodontitis are unresponsive to SRP treatment even in conjunction with adjunct treatments[18]. These patients are categorized as severe or refractory and surgical intervention with gingival flap surgery or bone/soft tissue grafts may be necessary[108–110].

1.3.3.1 Small Molecules for Immune Modulation

While an overburden of periodontal pathogens can initiate oral dysbiosis of the microbiome, literature suggests it is actually the immune system's (unbalanced) inflammatory response that causes the severity of symptoms and destruction[111,112]. This new understanding has led to the development of immune modulation strategies as alternative treatment modalities. Specifically, an early approach of immune modulation was to block instead of regulate the inflammatory process[113]. However, solely dampening host immune response can lead to systemic infections and previous studies of blocking inflammatory response increased bacterial burden and disseminated infection[114]. Another approach has been to use pro-resolving molecules like lipoxins and resolvins which have shown promise in neutralizing lymphocyte recruitment and initiating disease resolution[115–117]. Additionally, tetracyclines like minocycline and doxycycline intriguingly not only have a primary antibiotic function but a secondary effect of inhibiting tissue destroying matrix metalloproteinases[118].

1.3.3.2 Cell Inspired Approaches for Immune Modulation

There has also been tremendous work focused on the various cell types involved in the immune-mediated inflammation and how to modulate their activity. Osteoclasts have been a key cell population as osteoclast-related mediators like matrix metalloproteinases (MMPs) and cathepsins that are downstream factors of osteoclasts are responsible for the degradation of bone and soft tissue[119,120]. Others have focused on cell type populations like dendritic cells[121,122] or the polarization of macrophages[123,124] and their roles in influencing the local microenvironment.

Yet, the body has a natural immune regulation system that can also be harnessed using regulatory T cells (Tregs). Tregs are an immune T cell type subset ($CD4^+CD25^+FOXP3^+$) that can suppress other immune cells including other CD4 T cells (Tcons). Mechanisms of suppression can

be both direct and indirect. For direct suppression, Tregs can secrete immunosuppressive soluble factors like IL10 or TGFβ cytokines. Tregs can also act through direct cell-cell contact and inhibit T cell receptor (TCR) induced proliferation. Indirectly, Tregs can suppress the activation of antigen presenting cells (APCs) (dendritic cells, macrophages and B cells) that normally display antigen for T cell recognition[125,126].

With their immune regulation abilities, regulatory T cells (Tregs) are naturally positioned to counteract immune imbalance and inflammatory destruction [127], especially in periodontitis. Specifically, Tregs are known to accumulate in gingival tissues during flare-ups of periodontal disease in both human and animal models, emerging as key natural regulators of *local* inflammation [128]. In previous studies[129], controlled drug delivery for the recruitment of Tregs in the local periodontium environment aided in the reestablishment of homeostasis in periodontal disease. Using a formulation that encapsulated the chemokine CCL22 in a murine oral gavage model [129], Tregs were locally recruited and enriched such that the ratio of Treg to effector T cells favored resolution of inflammation, bone loss was reduced and there was a microenvironment shift towards regeneration. However, Treg recruitment strategies have limited application in patients with systemic diseases that may alter the suppressive ability of any Tregs already present[130–132].

Opportunely, studies suggest a combination of factors (IL2, TGFβ and Rapamycin) can cause the local induction of Tregs from naïve T cells present at the site of administration[133–135]. IL2 and TGFβ are cytokines known to promote the growth and differentiation of naïve T cells into regulatory T cells [136]. Rapamycin is a small molecule, mTorr inhibitor capable of preventing the differentiation of naïve T cells into other T cell types[137,138]. Thus, it remains to be determined if the development of a drug delivery formulation with this combination of three factors could potentially have an impact when administered as a preventative treatment for periodontal disease.

1.4 Hypothesis: Excipient composition in polymeric microsphere formulations can be modified to tune for desired drug delivery application

As noted in section 1.1, the contribution of excipients to the overall properties of a drug product is complex but important. Although APIs provide the primary drug activity functions, excipients can modify key parameters including overall performance and release kinetics to make treatments disease targeted. ***To this end, we hypothesize that excipient composition and fabrication method could be modified to engineer extended-release formulations (that take advantage of advances in the field of controlled drug delivery and new understanding of the biological environment of the periodontium) for the; 1) generation of an Arestin® generics/comparator panel and validation of a novel dissolution test, 2) encapsulation of a natural product (cranberry extract) to counteract bacteria biofilm growth and 3) encapsulation of a combination of factors to target the underlying immunological imbalance, that can each resolve the unmet needs of currently available treatments for patients with varying forms of periodontitis (from mild to severe).***

2.0 Controlled Release of an Antibiotic for the Treatment of Periodontal Disease

This chapter is adapted with copyright permission, from: Sravan Kumar Patel, Ashlee C. Greene, Stuti M. Desai, Sam Rothstein, Iman Taj Basha, James Scott MacPherson, Yan Wang, Yuan Zou, Mostafa Shehabeldin, Charles Sfeir, Steven R. Little, Lisa C. Rohan. (2021) Biorelevant and Screening Dissolution Methods for Minocycline Hydrochloride Microspheres Intended for Periodontal Administration. *International Journal of Pharmaceutics*. https://doi.org/10.1016/j.ijpharm.2021.120261

Specific Aim 1: To Engineer Arestin® Comparator Products for Biorelevant Dissolution Testing Mimicking the Periodontal Pocket for the FDA.

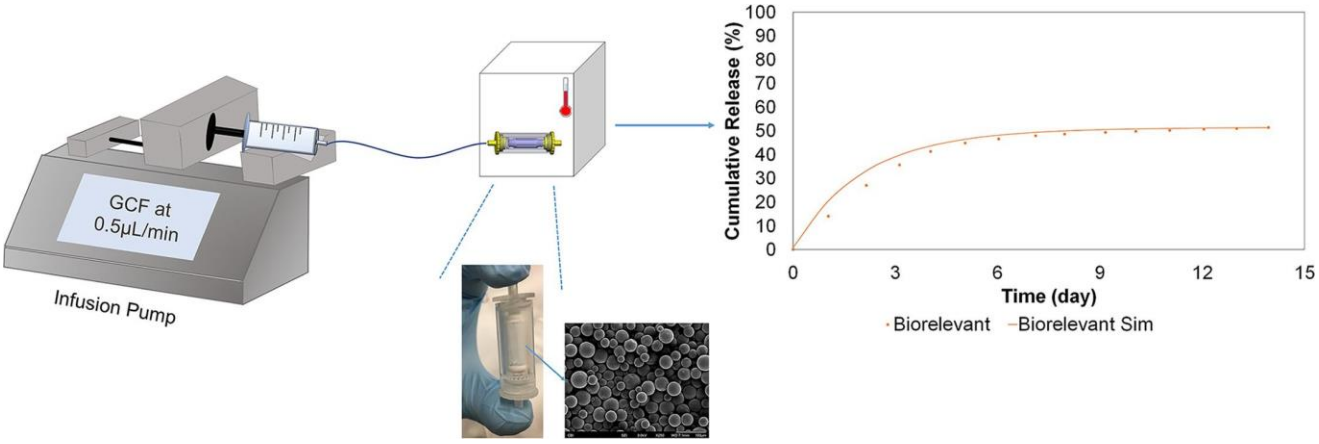

Figure 1. Graphical Abstract of Arestin comparator and small volume dissolution device (SVA) development.

2.1 Introduction

The generics industry is a multi-billion-dollar industry worldwide. In 2020, the global market was estimated at $411.6 billion and is predicted to grow to $650.3 billion by 2025[139]. With such a high influx of potential drugs, in the United States, the FDA plays a critical role in evaluating these generics for their fidelity to the reference listed drug they are intended to mimic. To do so, an assessment of similarity in performance or bioequivalence between the formulations is required. Conventionally, when a generic drug manufacturer is ready to submit their generic (ANDA) application to the FDA, they must produce dissolution data. Fittingly, the FDA provides a database with predetermined dissolution methods that are based on active ingredient and formulation dosage form, often specifying the precise compendial USP device-based method and conditions that should tested[140]. However, Arestin®, as a soon-to-be off the market reference listed drug, challenges this standard.

Arestin®, a minocycline (MIN) releasing PLGA microsphere product[43,141,142], is unique in that it is currently the only extended release microsphere product applied within the periodontal pocket. Although it is anticipated that new minocycline-releasing generics will soon take its place, these generics will first need to demonstrate bioequivalence through dissolution testing. Yet, there is no standard compendial-level dissolution method that closely mimics oral microsphere administration.

Therefore, the goal of this aim and study was to develop a panel of potential generic formulations of Arestin® to validate a new and biorelevant dissolution apparatus specifically for PLGA microspheres applied to the periodontal pocket. This device would not only simulate the small volume of the periodontal pocket but would also yield the appropriate corresponding flow

rates and media composition for a more biorelevant dissolution method. Ultimately, a rapid-screening quality control biorelevant test was developed based on a previously reported USP 4 method. The developed methods were assessed for discriminatory ability using microspheres that differed in composition and process parameters. A more biorelevant small-volume apparatus (SVA) was then fabricated and validated to better simulate the periodontal pocket in media, flow rate and to an extent, the volume.

2.2 Materials & Methods

2.2.1 Materials

Minocycline hydrochloride (MIN) was purchased from Sigma Aldrich. Arestin® was purchased from OraPharma, Bridgewater, NJ. PLGA of different molecular weights and lactic acid:glycolic acid ratios were obtained from PolySciTech, Akina, Inc. Polyvinyl alcohol (~25,000 g/mol, 98 % hydrolyzed) was obtained from Polysciences. Tetra butyl ammonium hydrogen sulphate (98%) was obtained from J. T. Baker®. Float-A-Lyzer® G2 devices of 50 kDa MWCO and dialysis tubing (1 cm flat length, 50 kDa MWCO) were obtained from Spectrum Laboratories. Phosphate-buffered saline, 10x (1.47 mM KH_2PO4, 2.68 mM KCl, 8.1 mM Na_2HPO_4 (anhydrous), and 137 mM NaCl) was obtained from Thermo Fisher Scientific. Appropriate dilutions using MilliQ water were made for use in experiments. All other chemicals including excipients used to prepare simulated GCF and HPLC mobile phase buffer were acquired from either Fisher Scientific, Sigma Aldrich or Spectrum Chemicals. Tygon tubing of 5/32” and 1/8” outer diameter was obtained from Fisher Scientific while tubing of 0.09” outer diameter was obtained from Cole-

Parmer. All small volume chambers were machined by Mr. James Scott Macpherson at Swanson School of Engineering, University of Pittsburgh.

2.2.2 Assessment of PLGA composition in Arestin® microspheres

PLGA used in Arestin® was first extracted by membrane dialysis as adapted from Garner et al. based on the drug solubility[143]. Briefly, a pre-wetted regenerated cellulose dialysis membrane (3.5 kDa MWCO, Spectrum Laboratories) was rinsed and prepared as per manufacturer's instructions. Arestin® (50 mg) was dissolved in dimethyl sulfoxide and loaded into the dialysis tubing. The solution was dialyzed against 1 L ultrapure water for a total of 10 h, after which the water was changed with fresh water, and dialysis continued for another 5 h. The remaining concentrate was centrifuged at 4°C at 1680 rcf for 10 min and then filtered with a fine porosity quantitative filter (Fisher Scientific, grade Q2). This solution was lyophilized for 24 h. Molecular weight and dispersity of the extracted PLGA were determined using a Waters GPC (gel permeation chromatography) system (THF, 0.5 mL/min) with Jordi 500 Å, 1000 Å, and 10000 Å divinylbenzene (DVB) columns and refractive index detector (Waters), which was calibrated relative to polystyrene standards. The ^{1}H and ^{13}C NMR (nuclear magnetic resonance) spectra were obtained in $CDCl_3$ using a 500 MHz Bruker Avance III spectrometer at 293 K and calibrated to the residual solvent peak at δ 7.26 ppm (1H) and δ 77.00 ppm (13C). The end group was determined using heteronuclear single quantum correlation (HSQC) 2D NMR method (1H-13C) at the United States Food and Drug Administration. Commercially available ester (Resomer RG502, Sigma Aldrich) and acid endcapped PLGA (Resomer RG502H, Sigma Aldrich) of lower molecular weight (7-17 kDa) were used as controls considering high lactic:glycolic acid (LA:GA) peaks from high molecular weight polymer could obscure results.

2.2.3 Preparation of MIN-loaded PLGA microspheres

PLGA microspheres (with distinct formulation or parameter settings) encapsulating MIN were fabricated using a single emulsion method as previously described by Jhunjhunwala et al[133]. Briefly, for the microspheres with changes in the formulation settings, 200 mg of PLGA with varied molecular weights and LA:GA ratio (Table 1), and 100 mg, 75 mg or 50 mg of MIN (to achieve a theoretical drug loading of 50%, 37.5% and 25% respectively), were dissolved in 4 mL of dichloromethane (DCM). For the microspheres with changes in the preparation parameter settings, 200mg of Resomer RG503H (LA:GA ratio 50:50, Mw 24-38kDa) and 100mg of MIN was dissolved in DCM at PLGA:solvent ratios of 0.025, 0.0625 and 0.1 (8mL, 3.2mL and 2mL respectively) per batch (Table 1). The single emulsion for these microspheres was prepared by homogenizing this solution in a 60 mL aqueous solution of 2% w/v PVA in 1X PBS for 1 min at the corresponding homogenizer speed in rpm shown in Table 1. The emulsion was then poured into an 80 mL aqueous solution of 1% w/v PVA in 1X PBS and stirred continuously using a magnetic stir plate at 600 rpm for 1.5 h to allow the DCM to evaporate. The microspheres were then collected and washed three times by centrifugation with MilliQ water before being re-suspended in 5 mL of water to be frozen and lyophilized for 48 h (VirTis BenchTop K freeze dryer; operating at 100mTorr).

Table 1. Preparation parameters for MIN-loaded microspheres.

Microsphere Name	LA:GA	Molecular Weight (kDa)	Theoretical Drug Loading (%)	Ratio of PLGA: DCM	Homogenizer Speed (RPM)
50L3	50:50	15.4	50	0.05	1500
50H1	50:50	64.14	25	0.05	1500
75L2	75:25	14.2	37.5	0.05	1500
85L1	85:15	21.8	25	0.05	1500
85H3	85:15	43.3	50	0.05	1500
Process parameter change*					
0.025H	50:50	24-38	50	0.025	1500
0.05H	50:50	24-38	50	0.05	1500
0.0625M	50:50	24-38	50	0.0625	1000
0.1L	50:50	24-38	50	0.1	500

*The molecular weight range for the 50:50 PLGA (RG503H) used in these studies is 24-38 kDa.

For compositionally different microspheres, the naming includes (from left to right) a number, letter, and a number. The number on the left correspond to ratio of LA:GA, letter indicates molecular weight (L-low, H-high), and the number on the right suggests theoretical drug loading (1-25%, 2-37.5%, and 3-50%). For microspheres with varied processing parameters, number

correspond to PLGA:DCM ratio, and the letter indicates the homogenization speed (L-500 RPM, M-1000 RPM, and H-1500 RPM).

2.2.4 Physicochemical characterization of microspheres

All microspheres, including Arestin®, were characterized for surface morphology, particle size and drug loading.

2.2.4.1 Scanning Electron Microscopy

The surface morphology was imaged using SEM (JEOL JSM6510 or JEOL JSM6335F, JEOL USA, INC. MA) at 3kV, 9-10.5mm WD and x250 magnification. Dry powder samples were mounted onto a stub with copper tape and sputter coated with palladium prior to imaging.

2.2.4.2 Particle size measurement

Size distribution of MIN-loaded microspheres was determined by a volume impedance method using Coulter Counter (Multisizer 3, Beckman Coulter). Approximately 1 mg of particles were suspended in an Isoton II diluent solution (Beckman Coulter) and readings were taken. Samples were diluted as necessary. A particle count of at least 1,000 was used to obtain number and volume averaged sizes.

2.2.4.3 Ultra-high Performance liquid chromatography (UPLC) method

An ultra-high performance liquid chromatography (UPLC) method was developed for MIN analysis in microspheres and dissolution samples. The method was based on a previously reported method for MIN tablets[144]. A Waters UPLC System (Acquity) was used for analysis. An Acquity

UPLC BEH C18 column (1.7 µm, 2.1 mm x 50 mm) fitted with a guard column and maintained at 35°C was used. The mobile phase composed of 76% of citrate-phosphate buffer at pH 7.0 and 24% of acetonitrile, combined gravimetrically. The citrate-phosphate buffer consisted of citric acid monohydrate, tetrabutylammonum hydrogen sulfate, and monobasic potassium phosphate. A flow rate of 0.2 mL/min was used for the isocratic method and analysis was carried out at 277 nm. Samples were maintained at 7°C throughout the run.

Drug loading was measured by dissolving around 10 mg particles (or 2 units of Arestin®) in 100 mL of 20% acetonitrile in MilliQ water. The particles were vortexed and stirred in the dark until clear solution was observed. The solution was then filtered using 0.22 µm PTFE syringe filters and analyzed using the developed UPLC method. This method was qualified for use by evaluating linearity, precision, and repeatability. The method was able to separate commonly observed degradants under acidic, basic, thermal, and oxidative conditions.

2.2.5 In vitro Release Study: USP Apparatus 4 Method

A USP apparatus 4 (SOTAX CP7 manual closed loop system) method was developed based on a previously reported method[73]. Float-A-Lyzer® G2 ~~devices~~ of 50 kDa molecular weight cut-off (Spectrum Laboratories) were first rinsed with 10% v/v ethanol for 10 minutes, then with purified water for 30 minutes and finally with dissolution media for another 30 minutes. Each dialysis sac contained about 10 mg of microspheres (or two Arestin® cartridges) and1.8 mL of dissolution medium (0.1% w/v sodium azide in PBS 1x, pH 7.4) and was placed in 22.6 mm clear flow-through cells. The volume of dissolution medium was 80 mL. The flow rate was set to10 mL/min. The dissolution study was carried out at 37°C for 3 days. At predetermined intervals, the cumulative amount of drug released is measured by an online UV spectrophotometer (Evolution

300, Thermo Scientific) at 292 nm. A calibration curve of MIN in the dissolution media was developed prior to analysis for quantitation.

2.2.6 In vitro Release Study: Biorelevant SVA Method

2.2.6.1 Preparation of Gingival Crevicular Fluid Simulant (sGCF)

One liter of GCF simulant (sGCF) was prepared by dissolving 0.338 g of citric acid monohydrate, 5.411 g of trisodium citrate dihydrate, 6.74 g of sodium chloride, 0.719 g of potassium chloride and 0.0559 g of bovine serum albumin in 950 mL of MilliQ water. The pH of this solution was adjusted to around 7.25 with 18% w/v of sodium hydroxide solution. Calcium chloride dihydrate (0.49 g) was dissolved separately in 5 mL MilliQ water and added to the solution dropwise. The volume was made up to 1 L with MilliQ water and the solution was filtered through 0.22 μm membrane filter. Table 4 shows a comparison between human GCF and sGCF.

2.2.6.2 Design of Small Volume Apparatus (SVA)

A novel device (Fig. 2) was fabricated at the Swanson School of Engineering, University of Pittsburgh using a clear polycarbonate (McMaster-Carr®) material. Initial prototypes were fabricated using a stereo lithography-based 3D printing method (Protolabs, MN) and employed Somos® WaterShed XC 11122 material. The design details were developed in SOLIDWORKS™ 3D CAD software. The device was designed to contain inner slotted chamber, which is 2.0 cm long and diameter around 5.7 mm that acts as a reservoir for microspheres. The slotted chamber is inserted into a cellulose dialysis membrane (Biotech CE, 1 cm flat width, 50 kDa MWCO, Spectrum Labs) and secured using an acrylic adhesive (Liquid Nails All Purpose Adhesive) and

Teflon tape. A cylindrical outer chamber (3.4 cm length) fitted with inlet and outlet caps housed the inner chamber loaded with microspheres. One end of the device was connected to a precision pump (Legato® 200, KD Scientific) for delivering sGCF, while the released drug is continuously collected via the other end of the device. Tygon tubing was used to connect the precision pump and the dissolution device. The device is placed in a 37°C oven to maintain physiological temperature (Fig. 3). As media enters the outer jacket, it distributes into several holes fabricated inside the outer jacket entry cap. This allows uniform flow of media inside the outer jacket. The small media volume in the dialysis enclosure (total volume ~0.25 mL) and a very low media flow rate (0.5 µL/min) on the exterior of dialysis membrane simulate the environment in the periodontal pocket.

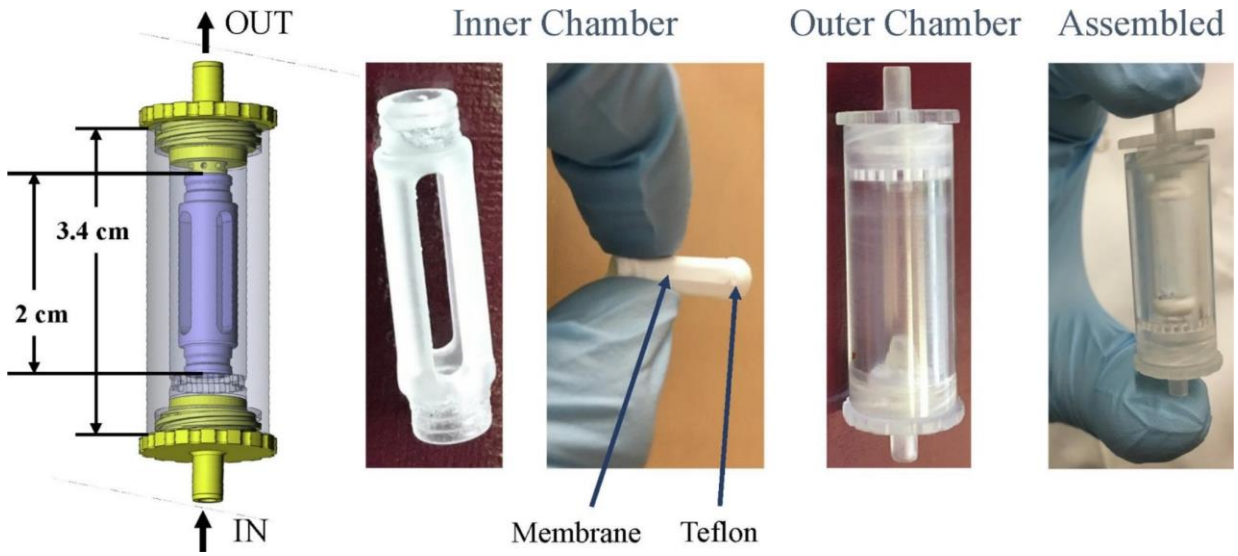

Figure 2. Design of novel dissolution device for the small volume apparatus (SVA) method. A 3D CAD image shows various parts and the dimensions of the dissolution device. The slotted inner chamber, which houses microspheres, is inserted into a dialysis membrane and is secured with Teflon and adhesive. The outer chamber and the assembled device are also shown.

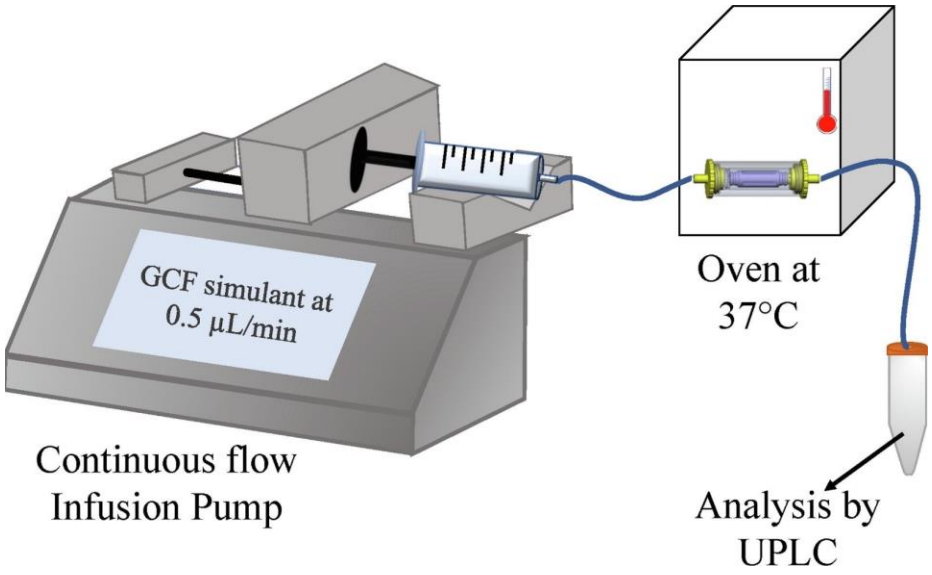

Figure 3. Schematic representation of small volume apparatus (SVA) for conducting dissolution studies. The set-up shows unidirectional flow of sGCF at 0.5 µL/min through the dissolution device maintained at 37 °C in an oven. Samples are collected at regular intervals and are analyzed using UPLC.

2.2.6.3 Dissolution Set-up and Methodology

Prior to the initiation of the experiment, syringe pumps were filled with sGCF and calibrated at 0.5 µL/min by sequential adjustments until the error was found to be less than 10%. About 10 mg of microspheres (or 1 cartridge of Arestin®) were added to the pre-made inner chamber-dialysis set-up followed by addition of 250 µL of sGCF. Arestin® powder was directly deposited through the cartridge into the inner chamber. For the in-house prepared microsphere products, the loose powder was packed into empty Arestin® cartridges and deposited similarly. The inner chamber was inserted into the outer chamber and the assembled devices connected to the syringe pump were transferred to 37°C oven. The devices were primed using sGCF at 100 µL/min. Once all the lines were filled without entrapped air, the flow rate was changed to 0.5 µL/min. Samples were collected daily for at least 14 days and diluted to a final of 20% of

acetonitrile in sGCF (v/v). The diluted samples were stored at -80°C and batched for analysis using the developed UPLC method. UPLC method and qualification parameters remained same as reported in earlier section for assay. Calibration standards were prepared in 20% acetonitrile in GCF.

2.2.7 Mathematical Model Development

Release Paradigm: The model for drug dissolution from PLGA microspheres in the SVA described herein builds upon previously published descriptions of drug release from hydrolysable, hydrophobic polymer matrices[13,145,146]. These prior models assumed perfect sink conditions at matrix surfaces, a condition that is relaxed in the present model to account for slower fluid flow in the biorelevant apparatus. Accordingly, agent concentration at the matrix surface, instead of being set to zero, becomes dictated by flux (q/A) where q is the rate of drug clearance from the matrix surface and A is the surface area of the matrix.

The rate of drug clearance (q) from the polymer matrix surface for a flow-through cell dissolution apparatus loaded with known mass of particles is proportional to the rate of fluid flow through the sample chamber relative to the volume of particles present, as follows;

$$q \propto \mathrm{n}V_p Q \qquad [2\text{-}1]$$

Where n is the number particles, Vp is the mean particle volume and Q is the fluid flow volumetric flowrate.

The matrix surface area (A) begins as a function of particle volume and grows as the polymer matrix erodes, losing molecular weight and mass. As such;

$$A \propto nV_pMw_o/Mw \quad [2\text{-}2]$$

Where *n* is the number of particles, *Vp* is the mean particle volume and *Mw* the polymer's molecular weight. In turn, change in molecular weight remaining Mw/Mw_o can be approximated by a pseudo-first order degradation rate expression:

$$\frac{Mw}{Mw_o} = e^{-kC_wt} \quad [2\text{-}3]$$

Where *kCw*, is the degradation rate constant, which is a known function of LA:GA ratio, and *t* is time.

Combining these proportionalities and equations produces a time-dependent drug (C_A) flux condition at the particle surface with constants of *Q* and kC_w.

$$\frac{\partial C_A}{\partial r}(R_P - R_{occ}, t) = F \cdot Q \cdot e^{-kC_wt} \quad [2\text{-}4]$$

Where *Rp – Rocc* is position of the particle surface along radius *r* where agent is free to release. Thus, the model of drug release from bulk eroding polymer matrices, such as PLGA microspheres, developed by Rothstein, Federspiel and Little is extended to include the small volume dissolution scenario by use of Equation 2-4 as its surface boundary condition[145,146].

Implementation: Equation 2-4 required a new fit parameter *F* which was optimized as a constant across training data for each apparatus, in this case USP 4 and small volume dissolution data for MIN-loaded PLGA microspheres. The complete model was solved via finite element method using partial differential equation script pdepe.m on MatLab v9.2.0.556344 (R2017a). Parameter *F* was calculated by non-linear regression to minimize normalized sum squared error across data sets from microspheres for a total of 10 simulations. Microsphere 85L1 was excluded from this exercise due to low drug release (≤%5).

2.2.8 Antimicrobial Testing

In order to assess the biological activity of MIN released into the dissolution media, an antimicrobial testing method was developed. Briefly, one colony of *Actinobacillus actinomycetemcomitans* (Aa) (ATCC® 29522™) was inoculated in 1 mL of pre-reduced brain heart infusion broth (BHI) (BD Biosciences 237500) and incubated anaerobically at 37°C overnight. The next day, the Aa pellet was resuspended in 1 mL broth and optical density (OD) of the suspension was adjusted by its dilution in pre-reduced BHI broth to be equivalent to 10^8 CFU/ml. The diluted suspension (1 mL) was transferred to 10 mL culture test tubes containing 100 µL of samples obtained from the dissolution apparatus at 1 and 7 days and incubated in anaerobic atmosphere at 37°C. Freshly prepared sGCF (100 µL) was used as a control. After 24 h, OD (at 600 nm) of Aa suspension in individual tubes was measured. Finally, 100 µL of serial 10-fold dilutions of bacterial suspension from each tube were inoculated on pre-reduced blood agar plates for another 24 h to determine cell viability by counting individual colony forming units.

2.2.9 Statistical Analysis

The difference between release profiles was assessed using similarity factor (f1) and difference factor (f2) described previously[147].

$$f1 = \left[\frac{\sum_{t=1}^{n}|R_t - T_t|}{\sum_{t=1}^{n} R_t}\right] \times 100 \qquad [2\text{-}5]$$

$$f2 = 50 \times \log\left[\frac{1}{\sqrt{\left[1+\frac{1}{n}\sum_{t=1}^{n}(R_t - T_t)^2\right]}} \times 100\right] \qquad [2\text{-}6]$$

Where,

n = number of time points

R_t = dissolution value of the reference at time t

T_t = dissolution value of the test at time t

2.3 Results

2.3.1 Arestin® Composition

Reverse engineering of Arestin® was attempted to determine its composition and physicochemical properties. This information was used to develop a panel of microspheres that are rationally designed based on the composition of Arestin®. Arestin® was found to be composed of PLGA and MIN at a loading of approximately 25-27% w/w. Using GPC, it was determined that the PLGA used in Arestin® has a weight average molecular weight of 24 kDa with a polydispersity index (PDI) of 1.47. Additionally, NMR analysis of Arestin® suggested that the LA:GA ratio is 50: 50. ^{1}H-^{13}C HSQC NMR analysis of the polymer purified from Arestin® confirmed that the PLGA is acid-terminated. Table 2 shows the composition and physicochemical properties of Arestin®.

Table 2. PLGA composition and physiochemical properties of Arestin®

Characterization Parameter	Result
LA:GA ratio	50:50
Molecular weight	~24 kDa
End group	Acid
Drug content	25-27 % w/w of particles
Shape	Spherical
Morphology	Uniform and non-porous
Size	~28-40 µm

2.3.2 Preparation and Characterization of Microspheres

All microspheres were fabricated using a single emulsion process and were determined to be spherical and displayed smooth surface. The particle size and drug content of the microspheres are summarized in Table 3. The SEM images of the prepared microspheres and Arestin® are shown in Figure 4. For the microspheres fabricated with changes in preparation parameters, as the stir speed increased, the microsphere size decreased. However, all microspheres had a particle size close to that of Arestin® and ranged between 28 µm and 40 µm. The UPLC method for drug content analysis showed acceptable linearity ($R^2 > 0.999$), precision (RSD < 2%), and repeatability (RSD < 2%). The actual drug loading in the microspheres was found to be proportional to the theoretical drug loading. However, the drug content of all microspheres was less than that of Arestin® and ranged from 9 % to 21 %. All microspheres including Arestin® had a glass transition temperature (Tg) between 48 – 55°C, characteristic of the PLGA used.

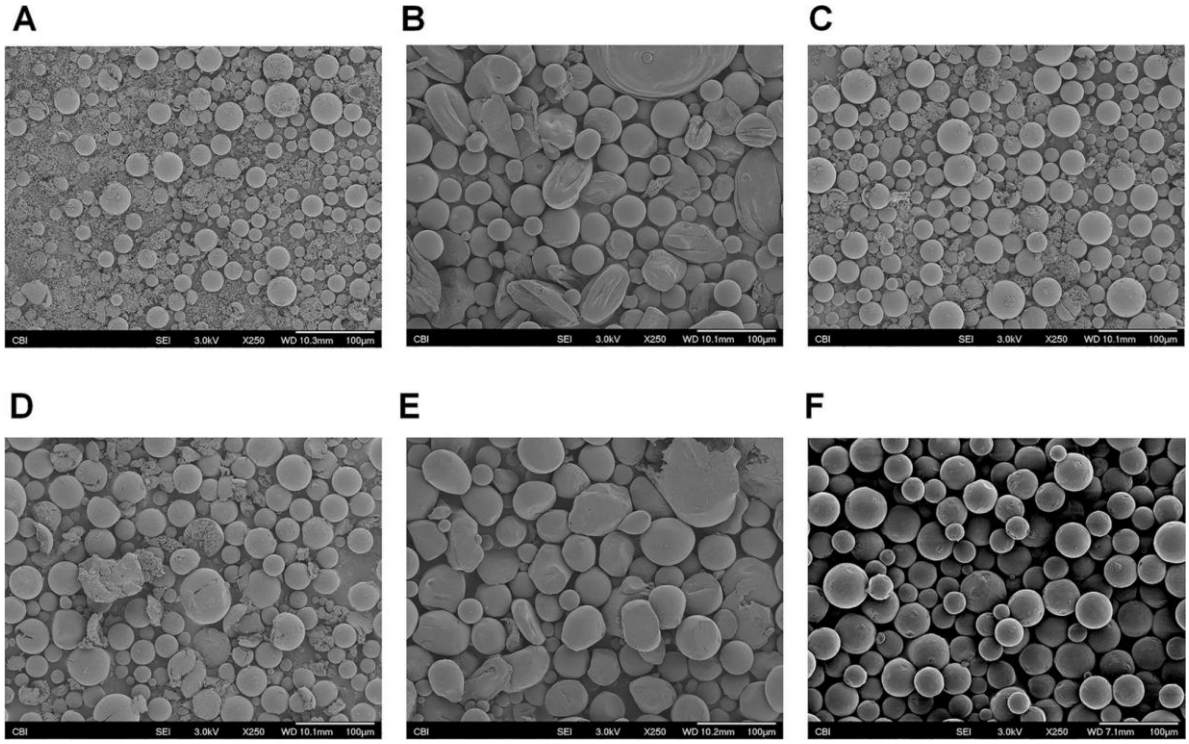

Figure 4. Scanning electron microscopy (SEM) images of microspheres (A-50L3, B-50H1, C-85L1, D-75L2, E-85H3, F-Arestin®). Scale bar = 100 µm.

Table 3. Characterization of in-house prepared microspheres

Microsphere	Particle Size – Differential Volume (µm)	Particle Size – Differential Number (µm)	Drug Loading (% w/w)
50L3	28.7 ± 9.6	9.7 ± 8.5	21.05 ± 0.09
50H1	32.9 ± 10.1	8.3 ± 9.1	9.10 ± 0.01
75L2	36.9 ± 12.8	6.4 ± 7.7	11.42 ± 0.11
85L1	33.9 ± 11.9	13.9 ± 10.9	9.90 ± 1.00
85H3	39.2 ± 11.3	10.1 ± 11.5	15.50 ± 0.20
0.025H	32.3±10.3	15.3±10.7	12.24 ± 0.05
0.05H	38.8±9.9	19.2±14.3	9.20±0.00
0.0625M	43.2±12.1	9.4±12.0	12.43 ± 0.12
0.1L	39.6±14.9	4.2±5.9	21.67 ± 0.05

2.3.3 In vitro Dissolution Study: USP Apparatus 4 Method

MIN degrades upon exposure to light and heat and showed significant degradation in dissolution media within 3 days (~76% remaining), which poses considerable challenges to obtain reliable dissolution profile. To account for drug degradation, the analysis was carried out at the isosbestic point of MIN (data not shown). The UV spectra of MIN samples (25 µg/mL in 0.1% sodium azide in PBS 1x) maintained at 37°C showed the absorption maxima of MIN at 246 nm.

Over a period of 5 days under mild shaking, the absorbance at 246 nm decreased. However, the wavelength region from 276 – 312 nm showed overlapping UV spectra indicating no or minimal changes in absorbance for samples stored for different lengths of time. This region is termed as the isosbestic region. The absorbance of the sample in this region is proportional to the total concentration of MIN and its degradants in the sample. A wavelength of 292 nm, which lies in the middle of the isosbestic region, was selected for online UV analysis. Absorbances were found to be linear from 0.5 µg/mL – 50 µg/mL at 292 nm.

A control study was performed using MIN solution to ensure that MIN degradants did not impact quantitation. A rapid and complete release of MIN from dialysis tubes was seen, which attained plateau in less than 0.5 days (data not shown). Moreover, the amount released had remained constant at the plateau levels throughout the study. Figure 5 shows dissolution of all compositionally different microspheres and Arestin® using this method. Arestin® shows a burst release and a sustained complete release within 3 days. In contrast, all microspheres plateaued before complete release. Interestingly it was observed that microspheres prepared using higher molecular weight PLGA released more MIN than microspheres fabricated with lower molecular weight PLGA. Furthermore, the impact of microsphere particle size on release was also observed, although not systematically, by comparing SEM images against dissolution profiles of comparators. The effect of particle size may be more pronounced among microspheres prepared at constant composition but varied processing parameters (Fig. 5). Microspheres 0.05H exhibited a faster release while 0.1L microspheres released in a more sustained fashion. Microspheres 0.0625M released about 60 % MIN over a period of 3 days. Microspheres 0.025H released the least cumulative amount of MIN, with about 15% of MIN released over 3 days. Comparison using difference (f1) and similarity factor (f2) further confirmed that the microspheres prepared by

varying process parameters performed differently as measured by dissolution profiles (data not shown). The reproducibility of the method was evaluated by performing dissolution of Arestin® on three occasions by two analysts (Fig. 6). Although minor differences were observed in the plateau phase, the burst release phase remained same between all the runs. Importantly, the f1/f2 statistic showed that the dissolution profiles were similar between all the runs. Overall, the USP apparatus 4 method showed discriminatory potential between microspheres of varied composition and properties.

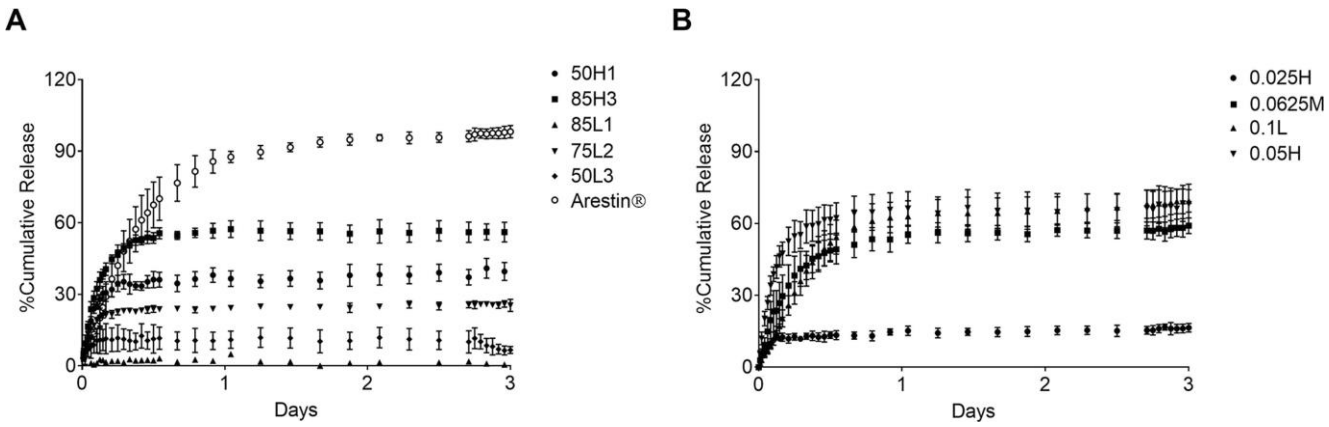

Figure 5. In vitro drug release profiles of minocycline comparators. A. microspheres with composition differences and B. compositionally equivalent microspheres with manufacturing differences obtained using USP Apparatus 4 (n = 3) at 37 °C in PBS containing 0.1% w/v sodium azide.

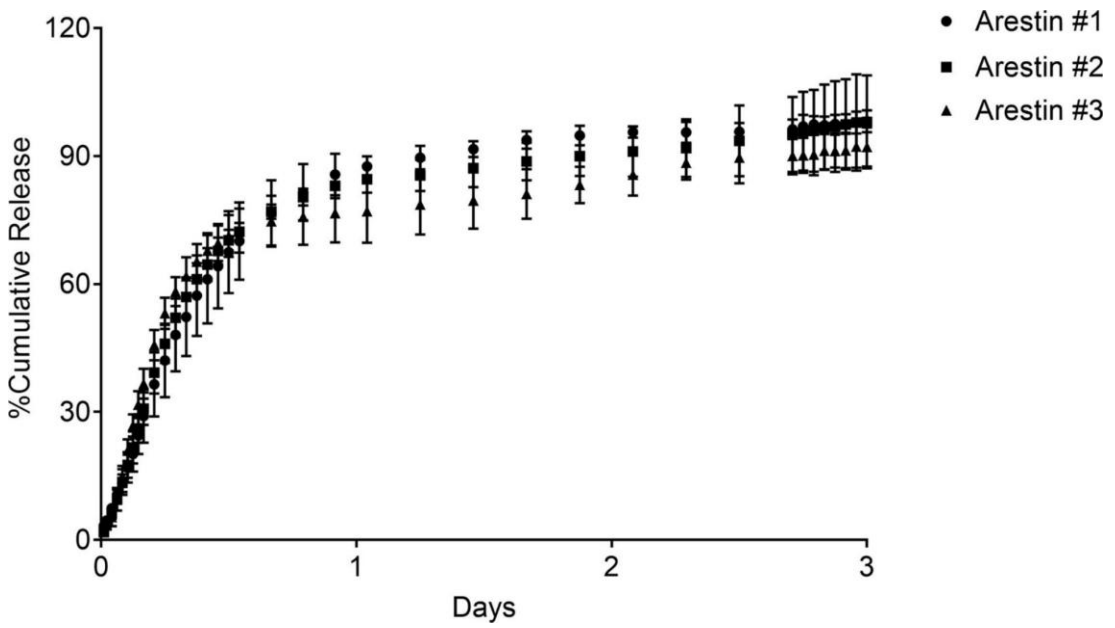

Figure 6. Overlay of in vitro drug release profiles of three Arestin® runs obtained using USP apparatus 4. Results are presented as Mean ± SD of n = 3 samples of 3 individual runs of Arestin®.

2.3.4 In vitro Release Study: Biorelevant Method (SVA)

The developed biorelevant SVA method simulated in vivo conditions to a varying degree for pH, fluid composition, and flow rate of GCF as well as the small periodontal space. The developed sGCF showed properties (Table 4) similar to the human GCF in ionic concentration, pH, and presence of proteins[148,149]. The pH of sGCF was measured to be 7.2 and osmolality around 292 mOsm/kg, which remained constant for at least 14 days when stored at 4°C, room temperature, and 37°C (Figure S5).

Table 4. Comparison between human GCF and GCF simulant (sGCF)

Component	Human GCF	sGCF
Sodium (mEq/L)	174.7 ± 18	174.5
Potassium	9.54 ± 2.4	9.52
Calcium	5.41 ± 0.37	5.44
pH	6.8-8.7	7.2

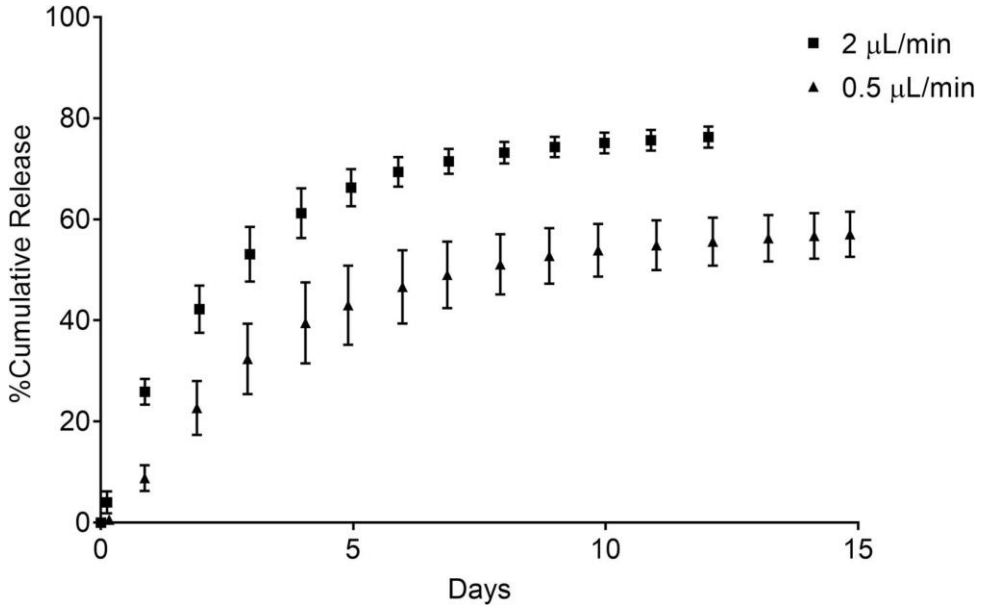

Figure 7. In vitro drug release from Arestin® using the small volume apparatus (SVA) method (n = 4) at different flow rates. Drug release was conducted at 37 °C under continuous flow of sGCF.

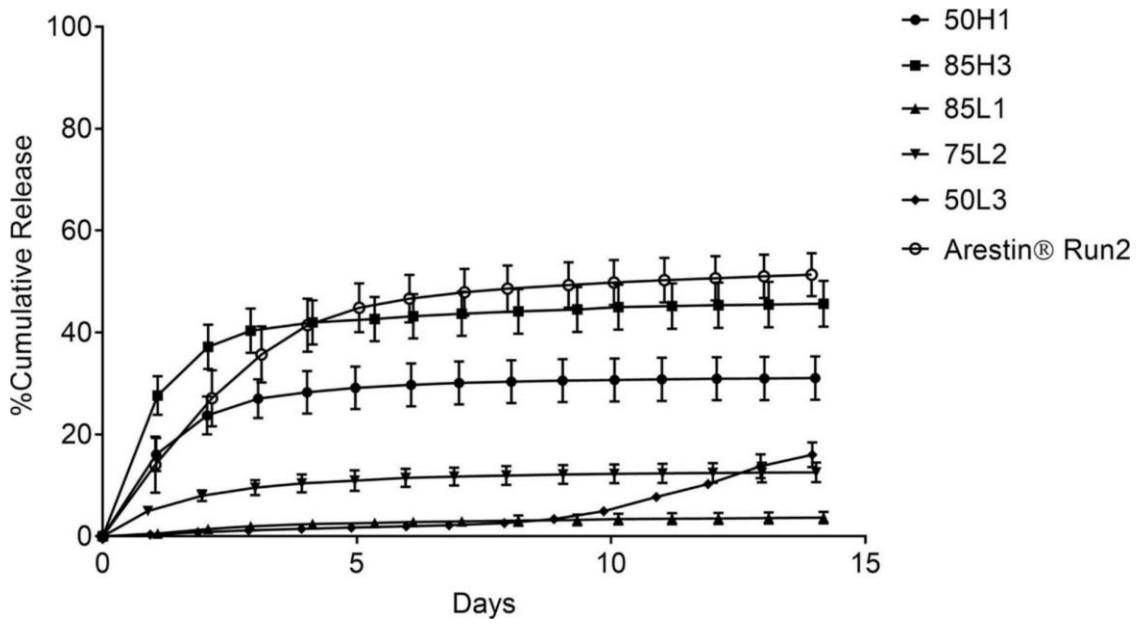

Figure 8. In vitro drug release profiles of microspheres with composition differences obtained using the biorelevant small volume apparatus (SVA) method. Results are presented as Mean ± SD of n = 3 samples.

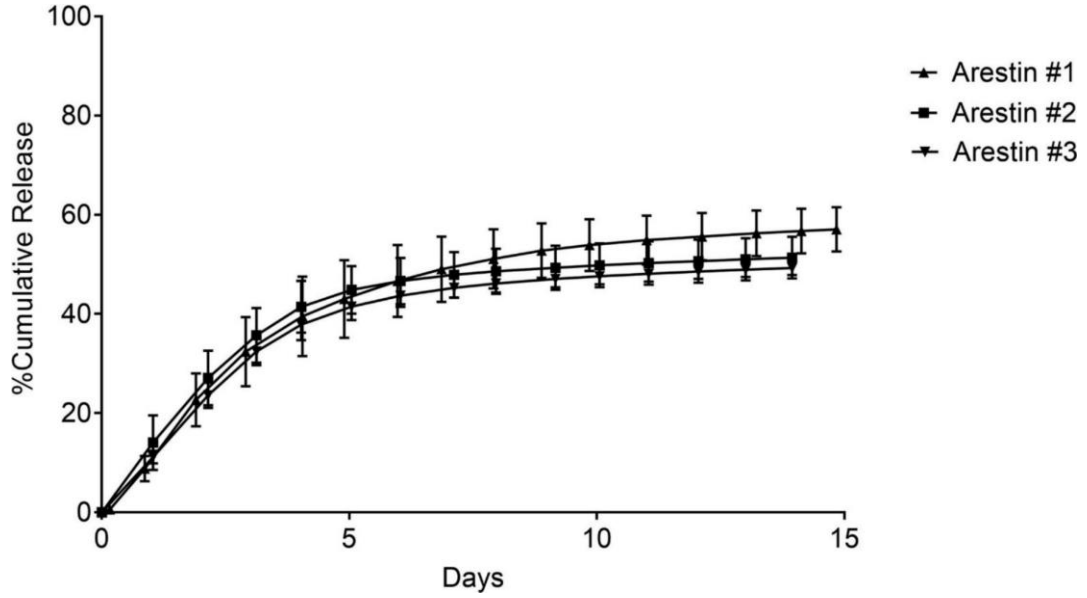

Figure 9. Dissolution profiles of three Arestin® runs obtained using the biorelevant small volume apparatus (SVA) method. Results are presented as Mean ± SD of n = 4 samples for 3 individual runs of Arestin® microspheres.

The developed UPLC method was qualified for use to assay MIN in dissolution samples. The method was found to be linear ($R^2 > 0.999$), precise (RSD < 2%), and repeatable (RSD < 2%). Importantly, the method was able to quantitate low concentrations of MIN (up to 0.25 µg/mL) in dissolution samples. The fabricated device was found to be robust and can be applied for repetitive use. In order to assess the effect of flow rate on dissolution of microspheres, Arestin® dissolution experiments were performed at 0.5 and 2 µL/min flow rates. Dissolution profiles of Arestin® at 0.5 and 2 µL/min are shown in Figure 7. Similar to MIN release from MIN solution, increased release was observed with higher flow rate.

The small volume dissolution profiles of compositionally different microspheres are shown in Figure 8. The rank order of microspheres (85H3 > 50H1 > 75L2 > 50L3 > 85L1) is same as that observed with the USP apparatus 4 method. However, the cumulative amount of MIN released within 14 days is less than the MIN amount released over 3 days in the USP apparatus 4 method. To understand the reproducibility of this method, Arestin® dissolution was performed three times. As shown in Figure 9, Arestin® dissolution from three runs showed overlapping dissolution profiles suggesting that the SVA biorelevant method set-up and use can be reproduced. Ultimately, the SVA biorelevant dissolution method effectively discriminated release profiles from prepared microspheres (similarly to the USP apparatus 4 method) supporting its applicability in the product development process.

2.3.5 Model development

A mechanistic model was developed using the dissolution data obtained from both USP apparatus 4 and SVA biorelevant methods. Simulations with the flux-degradation boundary condition account for differences in the USP apparatus 4 and SVA dissolution data from MIN-

loaded PLGA microspheres. Nonlinear regression of data from USP apparatus 4 and small volume dissolution produced constant F values of 14 and 63, respectively. This difference could be attributed to the differences in the amount of Arestin dispersed in the inner chamber and the fluid volume of the inner chamber. Table 5 highlights the major differences between these methods. In general, there was a good agreement between simulated and actual data for both USP 4 and small volume dissolution (Fig. 10).

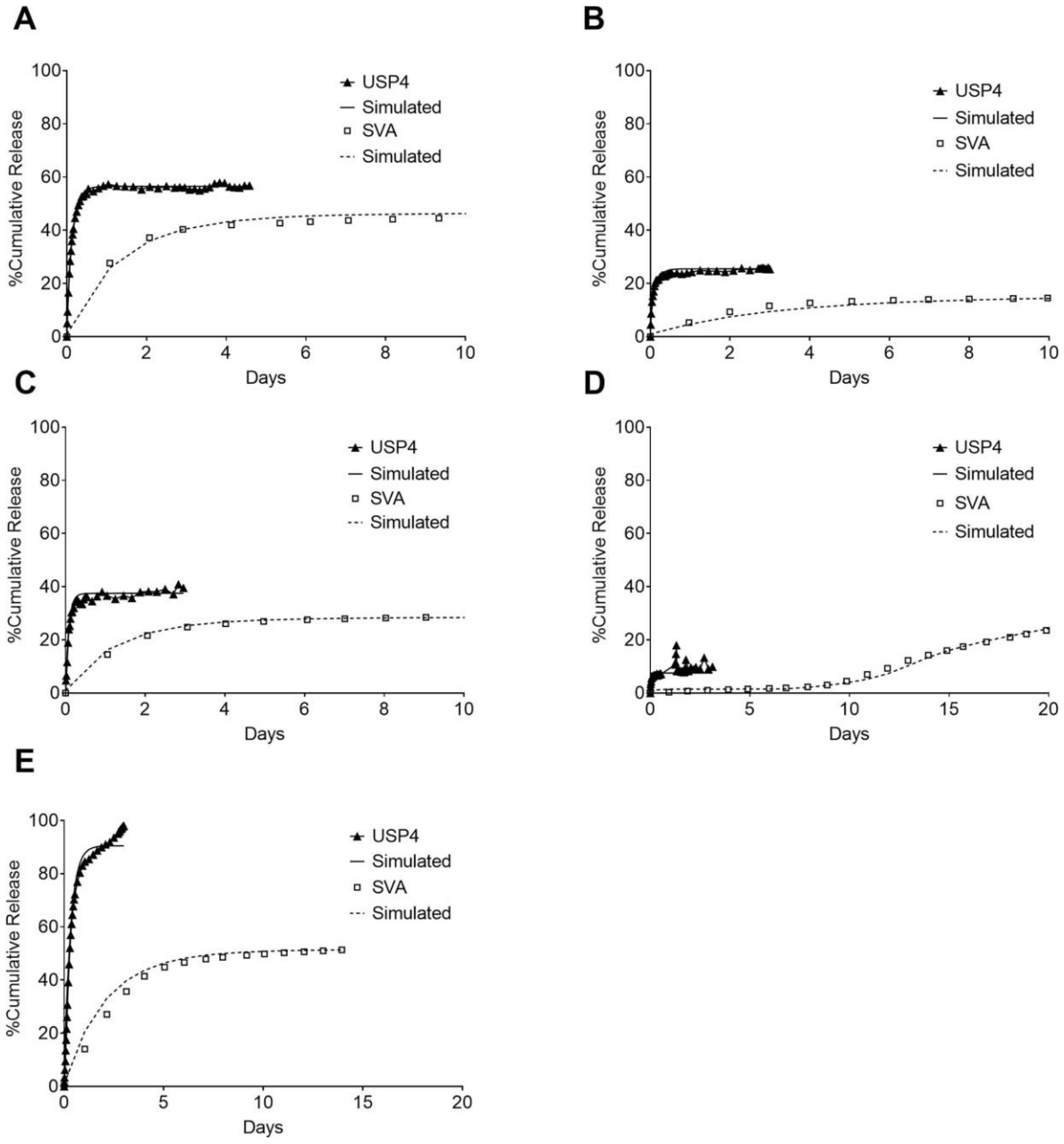

Figure 10. Simulations of minocycline release from PLGA microspheres closely follow USP Apparatus 4 and small volume apparatus (SVA) dissolution data from particle sets. Data used came from particle sets A) 85H3, B) 75L2, C) 50H1, D) 50L3, and E) Arestin®. Simulations from the original USP Apparatus 4 model (Rothstein et al.) over predict the rate of small volume dissolution (data not shown).

Table 5. Comparison between Modified USP Apparatus 4 and Small Volume Apparatus

Parameter	USP Apparatus 4	Small Volume Apparatus
Inner chamber volume	1.8 mL	250 µL
Reservoir volume	80 mL (re-circulated)	~750 µL (unidirectional)
Flow rate	10 mL/min	0.5 µL/min
Dissolution media	0.1% sodium azide in PBS 1x	sGCF
Experiment temperature	37°C	37°C
Sample volume (Arestin®)	2 units (8 mg)	1 unit (4 mg)
Experimental time	3 days	14 days
Sample analysis	On-line UV system (MIN + degradants)	UPLC (MIN peak only)

2.3.6 Antimicrobial activity of released MIN

Our antimicrobial testing data revealed that MIN released in the dissolution medium maintained its biological activity and inhibited Aa growth in a concentration dependent manner. Adding MIN released in the dissolution medium at 1 and 7 days (data not shown) to Aa suspension resulted in significant inhibition of Aa growth compared to sGCF as measured by OD at 600 nm after 24 hours. In line with the OD measurements, CFU counts were significantly lower on blood agar plates inoculated with the diluted mixture of Aa suspension and dissolution medium containing released MIN after 24 hours incubation. Altogether, the antimicrobial assays indicate that the dissolution process developed did not affect the bacteriostatic activity of MIN released from the PLGA microspheres.

2.4 Discussion

The goal of this work was to develop dissolution methods for locally acting microspheres in the periodontal pocket, that are either biologically relevant or can be used as a quality control method for routine analysis. There have been significant challenges in the development of a biorelevant dissolution method for MIN microspheres, including simulation of small periodontal space, complex fluid environment, and drug degradation under acidic, basic, thermal, and oxidative conditions[150,151]. We attempted to address these challenges and develop a novel dissolution system that is more biorelevant and discriminatory.

Initial attempts were focused on ascertaining the composition of Arestin® and physicochemical properties. Using NMR and GPC, it was identified that Arestin® is composed of acid end capped PLGA with 50:50 lactic acid to glycolic acid units and an average molecular weight of 24 kDa. Furthermore, the physicochemical properties such as drug content, particle size and morphology were determined (Fig. 4, Table 2). Based on the polymer type and composition of Arestin®, a range of microspheres were prepared (Tables 1) to assist in developing discriminatory dissolution methods. Specific formulation parameters and process conditions were varied to obtain microspheres. It has been shown previously by Rothstein et al.[13,145,146] that the investigated parameters impact the dissolution behavior of PLGA microspheres. Particle size and to a less extent the morphological features varied between comparators due to variations in composition and processing parameters. Importantly, all comparators showed lower drug content (9-21% w/w) compared to Arestin®, possibly due to difference in manufacturing procedures between comparators and Arestin®.

The USP apparatus 4 method was developed as an accelerated method that can be used to facilitate formulation screening and routine quality control analysis. This method was based on the modified USP4-dialysis method reported by the Burgess group[73]. It is known that MIN degrades rapidly in aqueous media at physiological temperature[150]. In our studies, MIN degraded rapidly (data not shown) in dissolution media (i.e., sGCF and 0.1% w/v sodium azide in PBS). This rapid degradation is especially challenging for long-acting controlled release products due to the prolonged study duration and complication arising from drug degradation that can be discounted as low or lack of release. In an attempt to simplify this process, online UV analysis of MIN at its isosbestic point was developed for the screening USP apparatus 4 dissolution method. As shown in supplemental data (not shown), the isosbestic point of MIN was found to be around 292 nm, where the absorbance changed minimally during a 5-day period. Further, dissolution of MIN solution for 3 days displayed (supplemental data not shown) constant plateau indicating that the degraded species have not reduced the absorption, thus supporting the utility of selected wavelength (292 nm). Since complete dissolution of Arestin® microspheres was observed in less than 3 days, the dissolution time scale for this method was fixed at 3 days.

The dissolution testing results of this semi-quantitative screening method showed differences in drug release profiles of the microspheres prepared with formulation and process variations. Changes in physicochemical properties such as particle size were also observed. In general, microspheres of smaller size, based on SEM, presented with reduced drug release (Fig. 4 and 5). One reason for this observation may be that the autocatalytic polymer degradation is slower for smaller microspheres due to faster clearance of generated acid[145]. For microspheres shown in Table 1 with formulation modifications, at each LA:GA, increased molecular weight led to a faster release, which is opposite to what is reported in the literature[152]. Notably, the amine groups of

minocycline have pKa of 7.8 and 9.3[153], which are ionized at pH 7.4 (PBS 1x). The ionized groups could potentially interact with the acid end groups of PLGA leading to slower release. Microspheres with increased PLGA molecular weight contain a lower number of acid groups per mole and cannot readily interact with MIN leading to faster release. Such ionic interactions for PLGA have been previously described in the literature[154]. In addition to these, the separate effect of hydrophobic lactide to hydrophilic glycolide ratio on drug release is expected but cannot be readily deduced from the limited panel of microspheres tested here. Moreover, this effect is probably confounded with particle size and inner microsphere structure. Therefore, the observed differences in drug release kinetics between these microspheres could be due to the differences in available number of acid functionalized end-groups for association with MIN as well as size, LA:GA ratio, and internal particle structure. Arestin® dissolution performed at three different times by two analysts (Fig. 6) using the USP apparatus 4 method showed similarity using f1/f2 statistic, thus confirming its reproducibility. Given the ease of use and discriminatory potential, the USP apparatus 4 dissolution method can serve as a screening method for quality control and to assess batch-to-batch variability of MIN microspheres. Moreover, rapid online analysis by the USP apparatus 4 method is less labor intense and cost-effective compared to the existing method in the USP for MIN microspheres.

Nevertheless, the USP apparatus 4 method, although facile, does not incorporate biorelevant conditions. In order to be more biorelevant, a novel small volume device with capability for continuous media flow was fabricated. Further, a biologically relevant media (sGCF) was developed to be utilized in these biorelevant dissolution studies. Markopoulos and colleagues proposed a levels pyramid scheme for developing a biorelevant dissolution media[155]. Accordingly, biorelevant media can match the in vivo media encountered by dosage forms in as little as pH to

the presence of dietary proteins and enzymes. Based on the ionic content data of human GCF from the literature, the milli-equivalent of major ions such as sodium, calcium, and potassium were established[148]. It has been shown that human GCF pH can vary between 6.8 and 8.7 for healthy and highly inflamed conditions respectively. To maintain stable pH during storage and use, buffers were introduced. Since phosphate buffers are commonly employed for pH 7.2, initial simulant preparation utilized different phosphate ingredients, which led to the precipitation of calcium. This necessitated use of a citrate buffer. The reported protein content in human GCF is very high (>70 g/L)[156]. The use of such high amounts of protein can be challenging and can lead to problems with stability, reproducibility, foaming during use and potential interference with dissolution, and downstream processing for drug analysis. Therefore, the amount of protein (bovine serum albumin) was maintained at low levels (0.05 g/L). The comparison of ionic content of sGCF and human GCF in Table 4 shows the similarities between these two media. Importantly, sGCF remained stable for the proposed duration of the dissolution study (14 days) based on monitored changes in pH, osmolality, and visual quality.

In the field of dissolution studies, efforts have been made to limit the proliferation of dissolution apparatuses and encouraged use of compendial apparatuses for biorelevant dissolution. However, using compendial apparatuses for biorelevant dissolution has not always been practical. This is especially true for small anatomical spaces where the fluid volume and hydrodynamics play a major role in dissolution, which are not closely simulated in the large volume apparatuses. Therefore, in this work, a novel dissolution apparatus was fabricated that incorporates biorelevant conditions such as physiological temperature, low fluid volume and low volumetric flow rate to assess dissolution of Arestin® and panel of microspheres. Optically clear polycarbonate material was used in the device fabrication to allow for visualization of inner components during set up and

the course of the study. A small volume device containing an inner dialysis support (slotted inner chamber) enclosed in an outer chamber containing media was fabricated. Of note, the separation of microspheres from external media using the dialysis membrane is required to maintain separation of released drug from microspheres. The design incorporated features to allow for uniform flow of fluid as it enters the outer chamber. This small volume apparatus more closely resembles the environment in the periodontal pocket as compared to the existing dissolution systems. Moreover, the continuous flow of media minimizes build of degradant species, which may complicate the analysis procedures.

To determine the effect of flow rate on release, Arestin® dissolution using the biorelevant method was compared at 0.5 and 2 µL/min (Fig. 7); the flow of GCF in the human periodontal pocket varies from 0.33 – 2.28 µL/min[77]. Arestin® is shown to release at a higher rate when the sGCF flow rate is 2 µL/min, which is in agreement with the release behavior observed from MIN solution at 0.5, 2 and 10 µL/min flow rates (data not shown), where flow rate has a significant effect on the amount of MIN released over time. This result suggests that the release of MIN is dependent on the concentration flux created inside the inner chamber of dissolution cells. The flow rate experiment results suggest that the increased flow rates deplete the inner chamber of the released MIN faster, thus maintaining fresh media within inner chamber for participation in diffusion and erosion of PLGA. The dissolution may be affected considerably with further increase (or decrease) in flow rates, which was not evaluated in this study. Based on these results, a flow rate of 0.5 µL/min was utilized for remaining studies as it provides more sustained release profile and therefore likely result in greater discriminatory potential.

The developed microsphere panel enabled testing the discriminatory potential of this system. Figure 8 confirms the discriminatory potential of the biorelevant method. Although the

rank order of MIN release is similar between USP apparatus 4 and small volume system, the potential to discriminate drug release in the initial times of release (< 5 days) is greater for the biorelevant method. It is to be noted that the contribution of epimer and other degradation products to the release profile is not included, thus underestimating the overall release from these microspheres compared to USP apparatus 4 method. MIN is likely to form similar degradation products in vivo, which are not biologically active. Therefore, the obtained drug release will help to ascertain the available drug for antimicrobial effect. Arestin® showed similar release profile between three repeated dissolution studies from two different lots suggesting high reproducibility. The antimicrobial study showed that the dissolution samples at days 1 and 7 were effective against Aa bacteria based on reduced OD and colony forming units indicating that the released drug is bioactive.

Finally, a mathematical model was developed to mechanistically understand the release of MIN from microspheres when exposed to two different dissolution environments. The mathematical model developed here in builds upon a prior model of controlled release from PLGA microspheres initially developed to describe release under perfect sink conditions, as found within the USP apparatus 4[145,146]. When applied to USP apparatus 4 data, the revised model continued to accurately describe dissolution results. These comparisons suggest that the revised flux equation specified for the particle surface effectively mimics perfect sink conditions at the 10 mL/min flow rate used in the USP apparatus 4. Critically, this new expression also allows predictions of release at slower flowrates, namely the 0.5 µL/min flow rate used in the small volume apparatus. The testing of model descriptions of release across multiple data sets, including different polymer molecular weights, polymer chemistries and particle sizes provides comparable scope of validation to prior models[145,146,157]. In these validation studies, the new model's fit parameter F was calculated

as a constant for USP apparatus 4 and for small volume system suggesting a conserved release mechanism across the tested particle types and apparatuses. The model would benefit from future studies to determine if the proposed quantification of release continues to accurately describe other drugs and other system flowrates.

Overall, two reliable and discriminatory methods were developed for periodontal microparticulate systems containing MIN. The novel biorelevant method extrapolates the versatility of the USP apparatus 4 to a micro-liter scale. The apparatus can be used with suitable media and appropriate flow rates to test any drug product that is intended for application in extremely small volumes, up to 250 µL. The apparatus can thus find applications to test ocular and nasal drug products. The biorelevant method closely mimics the conditions of the periodontal pocket and was able to discriminate between formulations with composition and process differences. Lastly, the design of microsphere products not only served to test the dissolution device but also ascertain the potential mechanism of MIN release from particulate systems with varied composition and physicochemical properties. Taken together, the developed device provides more biologically relevant drug release with effective discriminatory performance.

3.0 Controlled Release of a Natural Extract for the Treatment of Periodontal Disease

This chapter is adapted with copyright permission, from: Ashlee C. Greene, Abhinav P. Acharya1, Sang B. Lee, Riccardo Gottardi, Erin Zaleski, Steven R. Little. (2020) Cranberry extract-based formulations for preventing bacterial biofilms. *Drug Deliv. and Transl. Res.* https://doi.org/10.1007/s13346-020-00837-x

Specific Aim 2: To Develop Cranberry extracts-based Formulations for the Prevention of Oral Bacterial Biofilms and Periodontal Disease.

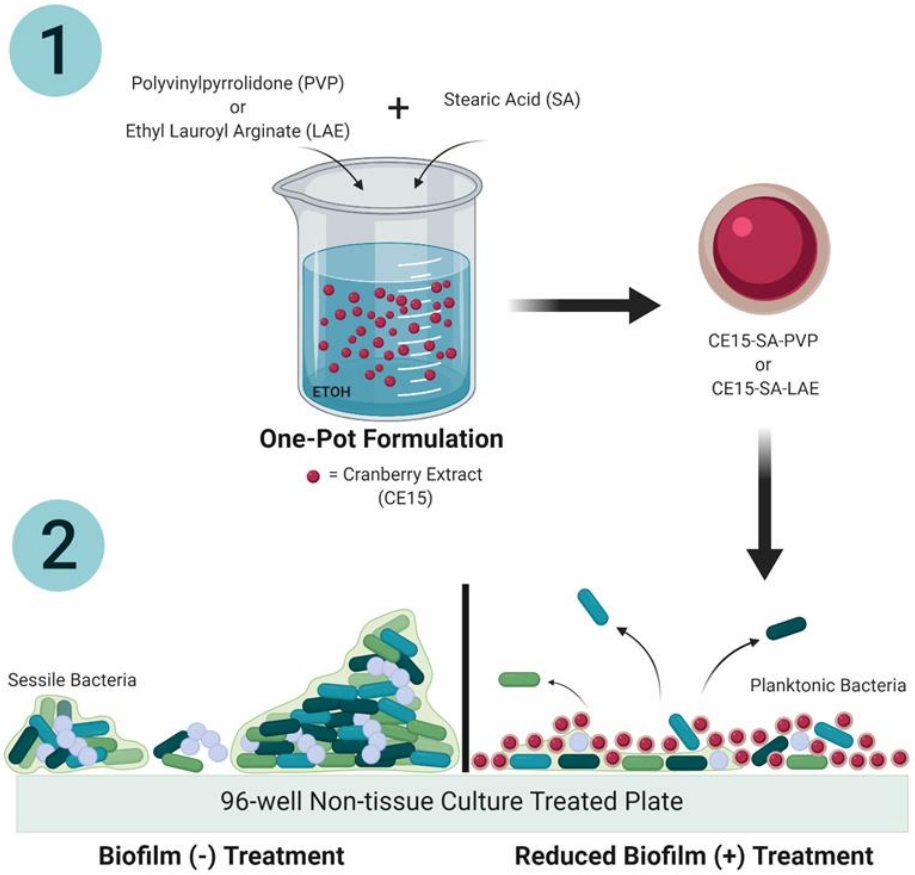

Figure 11. Graphical abstract of cranberry extract formulation anti-biofilm activity

3.1 Introduction

Antibiotic administration (aim 1) is often the first step to counteract the bacterial burden in periodontitis, although there has been an increasingly large push away from the overuse of antibiotics. Additionally, in patients with mild periodontal disease or even as a preventative, a full procedure of SRP with an adjunct antibiotic may not even be required. Mechanical means such as brushing and flossing together are quite effective at removing oral biofilm from the exposed surfaces on teeth. However, residual biofilm in hard-to-reach places can cause issues in the oral cavity over time. Oral biofilm removal through non-mechanical means may also be difficult to achieve using mouthwashes because biofilms are composed of complex communities of microorganisms that generate a robust biofilm [158,159]. While many agents have been proposed to fight oral biofilms, many agents suffer from insufficient exposure time, hindering their clinical effectiveness [158]. Therefore, an oral rinse with technologies included capable of locally adhering to biofilms and sustainably releasing anti-biofilm agents could provide a promising solution to inhibit bacterial buildup and plaque formation while retaining a convenient patient self-administration format. In order to design a treatment that can accomplish this task, it is helpful to first consider what composes an oral biofilm.

Bacterial biofilms are comprised of a complex matrix of extracellular polymeric substances (EPS) that stabilize and adhere bacterial populations to the surface of the tooth [159]. Additionally, bacterial biofilms function as extracellular digestive milieus for bacteria with the entrapment of sugar metabolic enzymes, ultimately resulting in acidic (pH 4-5) microenvironments [159,160]. Additionally, the overall structures that compose the biofilm and the pellicle (protein film formed on the surface of the tooth) are largely negatively charged, and strategies targeting these surfaces for adhesion may take advantage of ionic interactions by utilizing positively charged moieties

[158,160] such as ethyl lauroyl arginate (LAE) or inherently adhesive molecules such as polyvinylpyrrilidone (PVP). Notably, cranberry proanthocyanidins and flavonols can inhibit the growth of *Streptococcus mutans* [84], a significant contributor to tooth decay, and cranberry phenolics showed antibacterial activity against *Helicobacter pylori* [84]. Additionally, cranberry has not been shown to be bactericidal at low concentrations, but to only prevent bacterial growth [86–88,161,162]. All of this evidence suggests that cranberry extracts could be promising to prevent growth of oral bacteria and also lead to prevention of biofilm generation, while preserving buccal microbiota.

However, bulk delivery of these cranberry extract compounds would be non-trivial. To avoid bactericidal activity (10mg/mL of CE15 (which is known to kill bacteria)), concentrations of specific cranberry extracts (CE15, Naturex) between 5-10mg/mL (which is the minimum concentration to inhibit biofilm formation) would be necessary in the oral cavity (unpublished J&J data with Listerine as a control). Consequently, given the rate of human saliva production (1mL/min on average when stimulated [163–165]), a patient would require at least 7.2 grams of CE15 per day in the oral cavity in order to maintain these concentrations. This establishes an opportunity for a targeted formulation that could adhere to the pellicle or tooth surface to provide local, sustained delivery by maintaining the necessary local concentration.

Accordingly, in this aim, we explore formulations that can achieve adhesion to biofilm by utilizing chemistries that promote adhesion to negatively charged surfaces (e.g. polyvinylpyrrolidone (PVP) and also separately with ethyl lauroyl arginate (LAE)). We also explore the use of the lipid molecule stearic acid (SA) to tune controlled release properties. In addition to cranberry extract, this technique could also be a promising candidate for other natural extracts to form controlled release systems.

3.2 Materials & Methods

3.2.1 Materials

All chemicals were purchased from Fisher Scientific Inc. (Pittsburgh, PA, USA) unless otherwise mentioned. The cranberry extract used for this research (CE15) was a gift from NatureX Inc. (Avignon, France). It was chosen based on its high proanthocyanidin content. Poly(D,L-Lactide-co-Glycolide) (PLGA) Resomer® RG 502 (50:50, ester terminated, Mw ~7,000-17,000) was purchased from Sigma-Aldrich (St. Louis, MO, USA). Poly(vinyl alcohol) (PVA) was ~25,000 MW, 98 mole % hydrolyzed and purchased from PolySciences (Warrington, PA, USA). Hydroxyapatite (HA disks) from Himed Inc. (Old Bethpage, NY, USA) were provided by Johnson & Johnson. Saliva collection was approved by the University of Pittsburgh Institutional Review Board (study number: 20010259). Informed consent was obtained from all patients prior to participation in the study.

3.2.2 Formulation

CE15 was microencapsulated in poly(lactide-co-glycolide) PLGA using a double emulsion fabrication procedure. Briefly, 200mg of PLGA was dissolved in dichloromethane and 200mg of CE15 was dissolved in water. These two solutions were mixed for 1 minute using a probe sonicator to form a water-in-oil emulsion. After the sonication, the solution was transferred to a 1%, 140ml of poly (vinyl alcohol), PVA aqueous solution and homogenized to form a water-in-oil-in-water emulsion. The solution was stirred for 3-hours prior to centrifugation (2000 x *g*, 5min, 25°C) and being washed 3 times in deionized water to remove excess PVA. The microparticle solution was

then lyophilized for 72 h (VirTis BenchTop K freeze dryer; operating at -41C, 100 mTorr, no cryoprotectant) to obtain PLGA-CE15 microparticles powder.

One pot formulations were generated by mixing 10:1 wt/wt of cranberry extract: stearic acid in 100% ethanol. Next, PVP in ethanol was added to the above mixture to obtain 10:1:1, 10:1:0.5, 10:1:0.25, 10:1:0.125, 10:1:0.0625 and 10:1:0.03125 of cranberry extract: stearic acid: PVP. A 10:1:0.125 ratio of cranberry extract: stearic acid: LAE was used for the CE15-SA-LAE formulation. The slurry was then allowed to sit room temperature in a chemical hood to evaporate the ethanol. Once the ethanol was evaporated the mixture was weighed and utilized for further experiments.

3.2.3 Scanning Electron Microscopy

Scanning electron microscope JSM 6335F SEM at 3-5kV and 8mm WD, was utilized to image the formulation. Samples were mounted onto copper tape and allowed to dry prior to imaging.

3.2.4 Release Kinetics

CE15 release was determined by resuspending CE15-SA-PVP (10:1:0.125 formulation), CE15-SA-LAE (10:1:0.125 formulation), CE15-SA, CE15-PVP, CE15-LAE and CE15 only samples containing 5mg of CE15 in 1mL PBS (without calcium, magnesium) (HyClone, Marlborough, MA, USA). Samples were placed on a rotator and incubated at 37°C. At each time point, samples were centrifuged at 2500 x *g* for 5min at 22°C. All 1mL of the supernatant was

removed for full replacement with fresh PBS. CE15 content from collected supernatant samples of 150µL per well was measured by plate reader for absorbance at 525nm.

Loading of our samples was also characterized. For our PLGA formulation, 10mg of microspheres were dissolved in 5mL dichloromethane (DCM) and the CE15 was extracted into 1mL of deionized water. An addition of 1mL of ethanol (EtOH) was added to ensure complete detachment of CE15 from PLGA. The amount of extracted CE15 was quantified using a plate reader at 525nm. For our one-pot formulations, in the fabrication process, CE15 was suspended in ethanol in single vessel with coatings added sequentially to the batch. Therefore, the evaporation of ethanol after fabrication resulted in a dry formulation with essentially minimal loss of CE15 (and theoretical 100% loading). These one-pot formulation samples were then resuspended to the desired concentrations for use.

3.2.5 Saliva Collection

Saliva samples were collected according to a protocol received from Johnson & Johnson and approved by the University of Pittsburgh Institutional Review Board (STUDY20010259). Participants were instructed to conduct the saliva collection at home and not to use oral hygiene products, eat, drink or smoke starting from midnight preceding the morning collection. Brushing and/or rinsing and eating after the saliva collection was allowed. Individuals were given a sterile piece of Parafilm, approximately 4"x4" in size and a sterile, unlabeled 50mL conical tube. On the morning of the collection, participants chewed the Parafilm for several minutes to stimulate saliva production, ensuring to collect/spit ~3-5mL of saliva in the sterile 50mL unlabeled conical tube. After the collection, Parafilm was removed and discarded. Each unlabeled 50mL conical tube with ~3-5mL of saliva was then collected and samples added to a large collection container and mixed

with the other unlabeled saliva samples (at least n=5-8 to ensure heterogeneity of the saliva sample).

3.2.6 Saliva Coated HA Adhesion tests

In order to test the adhesion of the formulation to the biofilm, HA disks were utilized. Saliva pooled from four to eight subjects was incubated with the HA disks in wells of a 48-well plate at 37°C for 2 days to create a pellicle. Next, the HA disks were removed from the well and dipped in 1X PBS solution for 30 seconds. The HA disks were then dipped in a solution containing 0.5 mL of the formulation for 30 seconds. Next, the disks were dabbed on the side with kimwipes and placed in a clean well of a 48-well plate. A 0.5 mL solution of 1X PBS was then added to the well and optical images were obtained at time = 0 hours, and 24 hours using Olympus SZX10 dissection microscope.

3.2.7 Biofilm Inhibition Studies

Human saliva biofilm inhibition studies were conducted using a 96-well non-tissue culture treated plate assay, adapted from Yamanaka et al [166]. Although there are many methods to quantify various aspects of biofilms (killing of live cells, inhibition of existing biofilms), we have chosen to specifically observe the formation of new biofilms. Briefly, samples of CE15-SA-PVP, CE15-SA-LAE and CE15 were made at the formulation ratio of 10:1:0.125 as indicated above. Samples were diluted and made in triplicate containing 5mg/mL, 0.5mg/mL and 0.05mg/mL of cranberry extract and then dried for at least 72 hours. Next, 100µL of BHI media (Beckton Dickinson,

Franklin Lakes, NJ, USA) +1% glucose was added and incubated for 2 hours at 37°C to resuspend the sample wells. After 2 hours, 100µL of the incubated media + sample (or media alone for controls) was added to 100µL of saliva pooled from four to eight subjects (or PBS for the negative control) in a 96-well non-tissue culture treated plate and incubated for 48 hours at 37° C and ~5% CO_2. Next, the plate was blotted to remove media and unattached cells, rinsed three times with ultrapure water and allowed to dry for 30min. Wells were stained with 150µL of 0.1% crystal violet for 15min prior to rinsing three times with ultrapure water. Bound dye was extracted with 250µL of 99% ethanol and absorbance indicative of biofilm formation was read at 595nm.

3.2.8 Statistical Analysis

Data from the biofilm inhibition studies were analyzed using a two-way ANOVA followed by Tukey's multiple-comparisons test for simple effects between the groups. Differences were considered significant when $P < 0.05$. Statistics were performed by using GraphPad Prism.

3.3 Results

3.3.1 Cranberry Extract Characterization

As with many formulation processes, it is first extremely helpful to characterize the active ingredient. Accordingly, scanning electron microscopy (SEM) was performed to determine surface morphology. Interestingly, it was observed that the native form of the CE15 as obtained from the manufacturer is already micro-spherical in nature prior to any further processing (Fig. 12). The

solubility of CE15 microspheres was explored in various solvents in order to identify a solvent that could be utilized to resuspend the spherical CE15 with other excipients in either a traditional double emulsion microencapsulation or for coating. It was determined that 200 proof ethanol (which is originally utilized to extract CE15 from cranberries) did not dissolve the CE15 microspheres, but could effectively dissolve SA (1 mg/mL) and PVP (10 mg/mL). CE15 had a high solubility in water, and a low solubility in dichloromethane, making this solvent combination possible for a microencapsulation process.

3.3.2 Microencapsulated CE15

To microencapsulate the highly water soluble CE15, a double emulsion process with CE15 solubilized in water and PLGA in dichloromethane was used. Although these microspheres had a slight pink appearance indicating the incorporation of the CE15, many were cracked and misshaped (Fig. 12), which could result in an undesired, non-uniform release profile. Furthermore, CE15 content analysis revealed a loading (3.8%) that would be too low to inhibit biofilm formation. Therefore, alternate formulation methods that would allow for higher loading were explored.

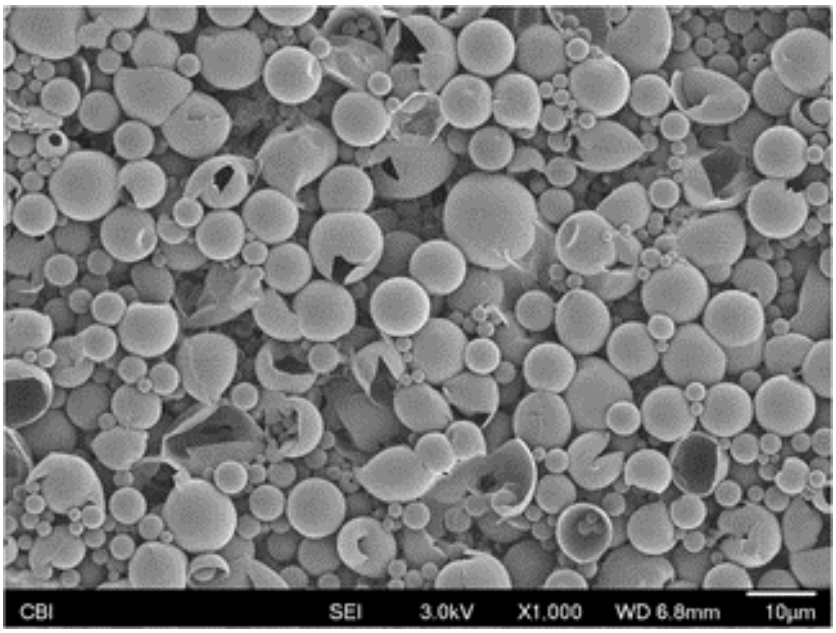

Figure 12. SEM of cracked, misshaped PLGA-CE15 at 1000x magnification.

3.3.3 One-pot formulation

In order to take advantage of the already microspherical nature of the CE15 in its native form, SA and CE15 were each dissolved in ethanol (non-solvent for CE15) then incubated with the CE15 microspheres for coating. PVP (known to have bioadhesive properties) [167–170] was then added to the ethanol solution at various concentrations. In order to retain all the active and inactive molecules of the cranberry extract, ethanol was allowed to evaporate over a period of 7 days.

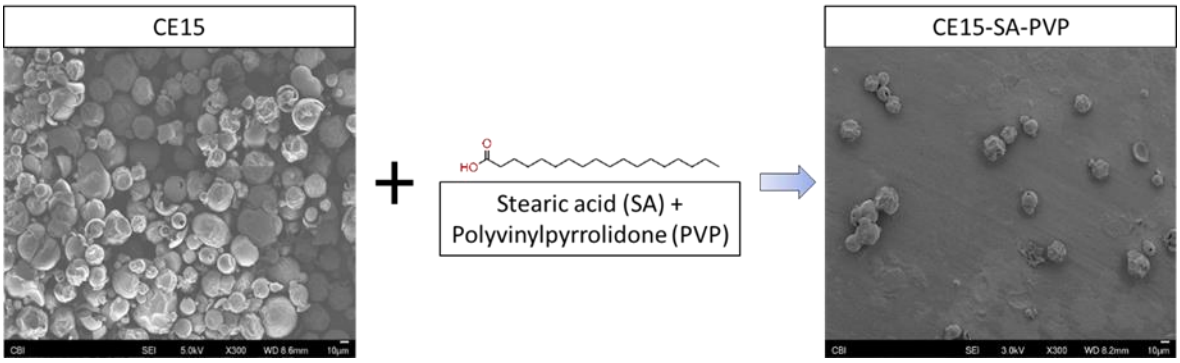

Figure 13. CE15-SA-PVP Formulation Steps. Spherical CE15 incubated with stearic acid and polyvinylpyrrolidone in ethanol produced the CE15-SA-PVP formulation; retaining all the active and inactive molecules of the cranberry extract.

The resulting CE15-SA-PVP formulation (with the inclusion of SA and PVP) allows for the controlled release of cranberry extracts and adhesion to saliva coated HA surfaces. In order to create a preventative formulation, we also explored replacing PVP with LAE, a cationic, antimicrobial surfactant [171,172] with a known ability to stick to and coat dental surfaces [173–175], which can also be easily dissolved in ethanol (10mg/mL). SA and CE15 were dissolved in ethanol together prior to the addition of LAE (with an arginine moiety pKa of 12.5) at various concentrations to provide a positive charge to the formulation and enable tooth enamel adhesion (Fig. 14). In order to retain all the active and inactive molecules of the cranberry extract, the ethanol was again allowed to evaporate over a period of 7 days.

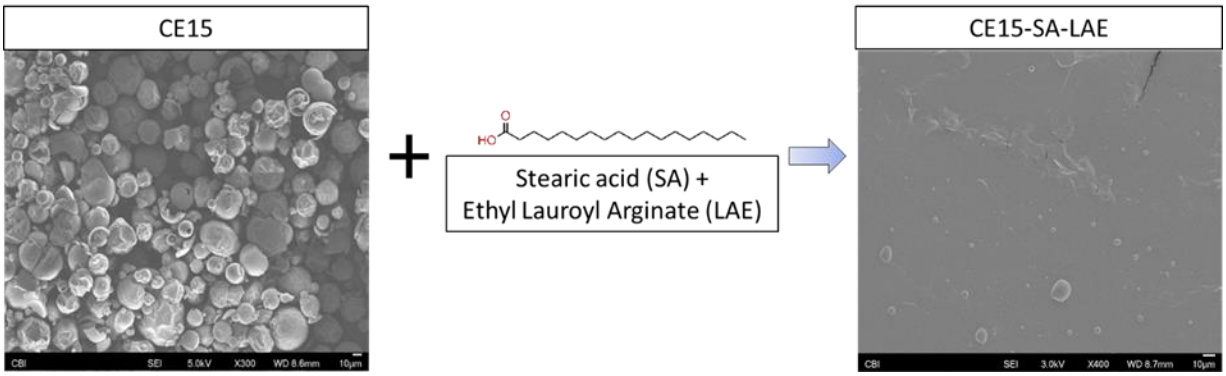

Figure 14. CE15-SA-LAE Formulation Steps. Spherical CE15 incubated with stearic acid and ethyl lauroyl arginate in ethanol produced the CE15-SA-LAE formulation

3.3.4 Release kinetics

In order to evaluate if our one-pot formulation technique could release CE15 in a sustained manner, we performed *in vitro* release assays by incubating samples in PBS and collecting the PBS at various timepoints. Specifically, we observed an overall release profile with a burst release of CE15 after 2 hours with up to 80% cumulative release of CE15 after 8 hours. Additionally, the incorporation of LAE and PVP into our formulations further modified the cumulative release profile. In the case of the CE15-SA-PVP formulation (Fig. 15) where a variety of concentrations were fabricated, a correlation between concentration of PVP and release can be seen; as the ratio of CE-SA to PVP decreases, the release of CE15 increases. For the CE15-SA-LAE formulation (Fig. 16), only one concentration of LAE was used (0.125) which also shifted the release profile as compared to the CE15 only and other controls.

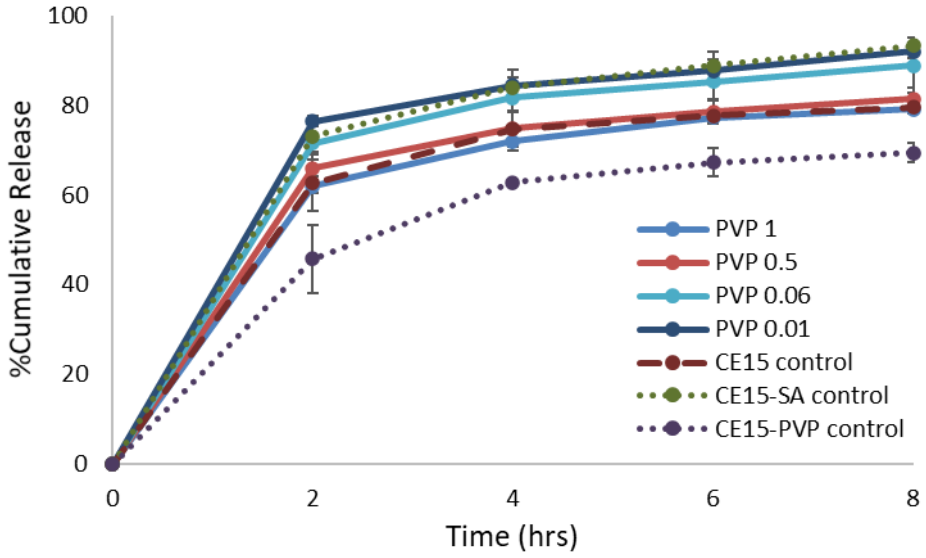

Figure 15. Release profile of percent cumulative release of CE15 from CE15-SA-PVP and controls. Error bars are based on n=3 individual samples measured for each time point.

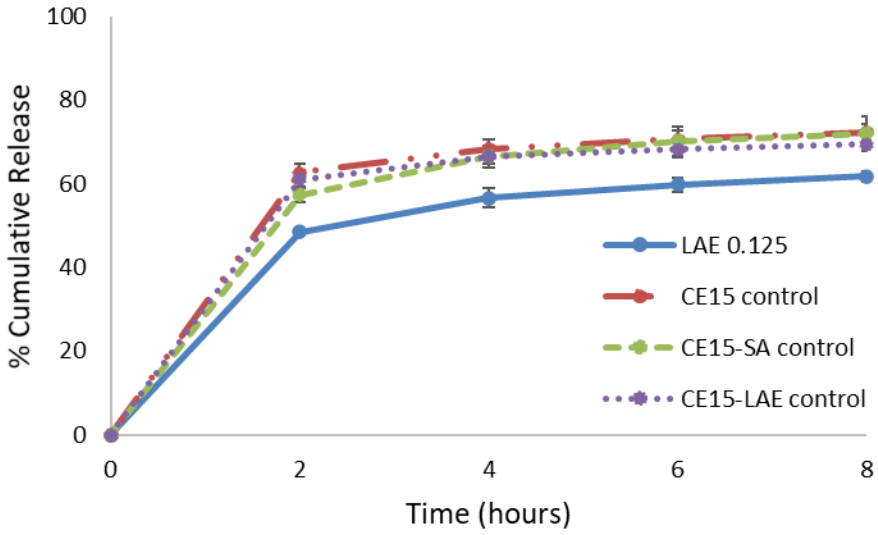

Figure 16. Release profile of percent cumulative release of CE15 from CE15-SA-LAE formulation and controls. Error bars are based on n=3 individual samples measured for each time point.

3.3.5 Adhesion to HA disk

In order to determine if CE15-SA formulations adhere to hydroxyapatite (HA) disks as a representation of teeth, a binding assay was developed (Fig. 17). It was observed that after an initial rinse with PBS at the 0 hour timepoint, the PVP and LAE formulations were the only cases where punctate dots of microspheres were still visible. Furthermore, only CE15-SA-PVP and CE15-SA-LAE samples were able to adhere to the HA disks even after 24 hours of incubation in PBS unlike the CE15 only and CE15-SA controls.

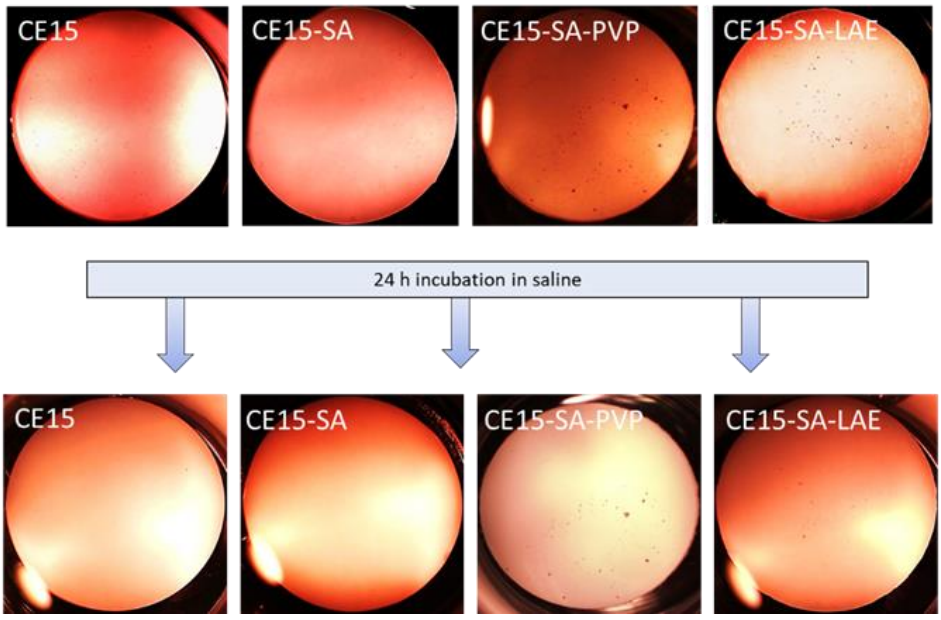

Figure 17. CE15-SA-PVP and CE15-SA-LAE adhere to hydroxyapatite disks after 24hr PBS incubation. Control samples (CE15, CE15-SA) show very little adherence (very little punctate dots present) (n=3).

3.3.6 Biofilm Inhibition

The biofilm inhibitory effects of the CE15-SA-PVP and CE15-SA-LAE formulations were determined by an *in vitro* saliva assay and compared to CE15 alone, a negative (PBS) and positive (saliva alone) control. To assess new biofilm formation only, crystal violet staining was used. At a concentration of 5 mg/mL of cranberry extract in the samples, all samples (CE15-SA-PVP, CE15-SA-LAE, CE15) significantly decreased biofilm formation compared to the positive control and were not statistically different from the negative control. At a concentration of 0.5mg/mL, all samples still had a significant decrease in biofilm formation compared to the positive control but there was a higher level of biofilm formation when compared to the CE15-SA-LAE formulation. Moreover, CE15 had a significant increase in biofilm formation compared to the negative control. At 0.05mg/mL concentration, the decrease in cranberry extract resulted in higher levels of biofilm formation for all formulations and the CE15 sample was no longer statistically different from the positive control but was statistically different than the negative control. Furthermore, at 0.05mg/mL, the CE15-SA-PVP sample was statistically different from the positive and negative controls while the CE15-SA-LAE was statistically different from all samples and resulted in the lowest biofilm formation.

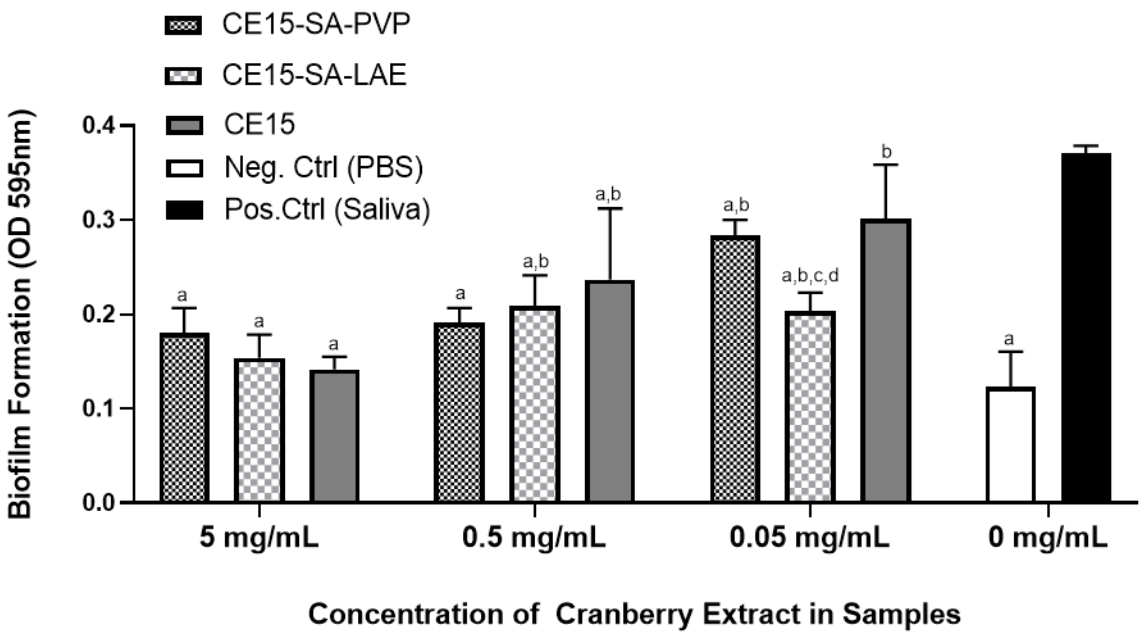

Figure 18. CE15-SA-PVP and CE15-SA-LAE inhibit saliva biofilm formation equal to or better than cranberry extract alone. Analysis (n=3) by two-way ANOVA followed by Tukey's multiple-comparisons test for simple effects. Significant differences are indicated by: "a" = difference from positive control (saliva alone) for $p < 0.05$, "b" = difference from negative control (PBS) for $p < 0.05$, "c" = difference from CE15 sample for $p < 0.01$ and "d" = difference from CE15-SA-PVP sample for $p < 0.05$.

3.4 Discussion

Prevention of disease by targeted treatment of bacterial biofilms can be difficult due to the ubiquitous nature of biofilms in the oral cavity. Commonly, dental plaque comprising bacterial biofilm can be found on most surfaces within the mouth [176] and without removal, biofilm on the teeth can calcify and become tartar. Bacterial biofilm growth on teeth and pellicle can lead to a variety of conditions such as bad breath, gingivitis, and tooth decay [177,178] and has even been implicated in serious infections such as bacterial endocarditis [179–182]as well as oral pathologies

such as periodontitis [183–185], oral caries [186–188] and peri-implantitis [189–191].Currently, to our knowledge, there are limited methods that are available that can directly target pellicle or teeth for prevention of biofilm growth in clinic. There are several effective (non-antibiotic) products available to target oral bacteria (like therapeutic mouthwashes) that often include antiseptic ingredients such as cetylpyridinium chloride, chlorohexidine, and peroxide, which work through killing bacteria that are present on oral surfaces during a short exposure time (minutes) [80,192,193] as opposed to having longer term preventative activity. As an alternative approach, we sought to design formulations to naturally prevent biofilm formation by accounting for the nature of these biofilms.

While traditional synthetic anti-microbials such as chlorohexidine, and quaternary ammonium compounds like cetylpyridinium chloride, remain effective, many natural compounds are also able to provide an inhibitory effect. Specifically, cranberry extracts are known to naturally prevent biofilm formation without being harsh and bactericidal (preserving the endogenous microflora of the oral cavity). One extract, (CE15), is composed of a mixture of polyphenol compounds [84]. Among those, three key active ingredients are working together and are effective in inhibiting biofilm formation; flavonols (FLAV), anthocyanins (A), and proanthocyanidins (PAC) [84]. Duarte et al. [84] found flavonols (FLAV) and proanthocyanidins (PAC) particularly impactful when evaluating their effect on biofilm development by *Stretptococcus mutans*, the primary microbial species associated with dental caries. Anthocyanins (A), which give cranberries their characteristic red coloring [194] have also been found by Lacombe [161] and others [195,196] to have a concentration-dependent antimicrobial effect. Together, these polyphenols provide an increased hydrophobicity [166] in addition to antiadhesion activity through the inhibition of extracellular

polysaccharide synthesis [84,197,198] . These constituents thereby prevent biofilm production and attachment although in a concentration-dependent manor.

Unfortunately, bulk concentrations of 5-10mg/mL of CE15 are needed to inhibit biofilm formation creating challenges for formulation dosing (above 10mg/mL of CE15 is bactericidal and we want to avoid this from a regulatory perspective). Specifically, even with a minimum target concentration of 5mg/mL of CE15 for delivery (and taking into account the rate of human saliva production as approximately 1mL/min when stimulated [163–165]) an unfeasible amount (approximately 7.2 grams of CE15 per day) would be required to be efficacious if delivered to the whole mouth. Notably, however, such relatively high concentration is only required in the proximity of the biofilm to be effective. Therefore, the encapsulation of these extracts into a targeted controlled release system that could be delivered locally (and modified to bind to the site of interest) could be a promising strategy, requiring a lower concentration. This could be possible if cranberry extract could be loaded into particulates (*e.g.* microparticulates) that bind directly to the biofilm.

A diverse array of encapsulation methods has been used to microencapsulate extracts, each tailored to the composition and desired extract/formulation properties. Cyclodextrin-extract complexation has been used by Hill et al. [89] and others [94,95] for various applications in food products and supplements. Specifically, this complexation has been used to increase solubility while masking taste for cinnamon and clove extracts [89]. Cyclodextrin-extract complexation has also improved the physical/chemical stability of natural and synthetic coffee flavor extracts [94] and lemon oil and peppermint oil volatile liquid aroma extracts [95] while maintaining their antioxidant or antimicrobial activity (extract dependent). Several groups have also explored alginate-based delivery [90–92], poly(lactide)/poly(lactic-co-glycolic acid) (PLA/PLGA) nano- and microsphere

delivery [96–100], liposomes [101,102] or lipid-based nanodelivery [93], to increase extract solubility, loading and antioxidant activity. Deladino et al. [92] resorted to the use of calcium alginate and calcium alginate-chitosan beads to encapsulate aqueous extracts from *Ilex paraguariensis* to retain polyphenol antioxidant activity. Separately, Kumari et al. [100] fabricated PLA nanoparticles by solvent evaporation to encapsulate the hydrophobic cranberry extract flavonoid component quercetin. Similarly, we first attempted to apply the standard PLGA, double-emulsion encapsulation platform that has worked well in our hands previously [129,133–135,199–203]. However, in the case of CE15 encapsulation, many of PLGA microspheres were cracked and misshaped (Fig. 12) and CE15 content analysis revealed a loading (3.8%); too low to inhibit biofilm formation through any reasonable dose and therefore unusable for our purposes. While these strategies of alginate-based, or PLA/PLGA delivery could be useful for the selective encapsulation of aqueous soluble polyphenols (hydrophilic) or hydrophobic/lipophilic components individually, neither of these methods allow for the full encapsulation and high loading of all components into a single formulation. CE15 is particularly challenging to encapsulate as this extract contains a variety of compounds (known and unknown) including; flavonol glycosides (primarily myricetin-3-galactoside and quercetin-3-galactoside) [103], phenolic acids (primarily 3- and 5-caffeoylquinic acid) [104] along with coumaroyl iridoid glycosides [105] and fatty acids like linolenic acid [106,107]. All of these CE15 extract components have different properties making encapsulation into a single formulation difficult.

Serendipitously, it was discovered that the CE15 extract in its native form as supplied from the manufacturer already pre-existed as encapsulated, ethanol stable microspheres ranging in size from 4 μm to 40μm which is ideal to avoid the phagocytosis limit of 1um (if injected) (left panels of Fig. 13 and Fig. 14). This is consistent with being the by-product of an emulsion extraction

process, and these newly discovered sphere-shaped extracts became the delivery vehicle for which simple coatings could be used to modulate the release of CE15 and provide adhesive properties [173,204–208]. Accordingly, a simple one-pot formulation technique (using ethanol-soluble coatings) that would allow for easy scale-up was developed to preserve the multi-component CE15 microspheres. A base coating of stearic acid (SA) to slow release and either polyvinylpyrrolidone (PVP)- a known bioadhesive [167–170] (Fig. 13) or ethyl lauroyl arginate (LAE) – a cationic polymer for direct pellicle/tooth binding and barrier creation [173](Fig. 14) were used.

Controlled release of CE15 from these microspheres is shown to include a burst release after two hours with up to 80% cumulative release of CE15 after 8 hours (Fig. 15, Fig. 16). Notably, release was monitored for 8hrs as determined by Johnson &Johnson since the formulation was desired to be potentially incorporated in a mouthwash. Internal Johnson &Johnson data has also indicated the optimal concentration of CE15 that could inhibit biofilm without killing in the critical 6-8hr timeframe. Intriguingly, the base coating of SA in both formulations contributes to the release profile although in a manor contrary to its original intended use. SA is a long chain fatty acid with a carboxyl head group (making it amphiphilic [209,210]) but is generally used as a lipid to slow release [211–216]. However, contrary to the literature [211–216] and our initial assumptions, the base coat of SA instead appears to moderately increase release (sample CE15-SA control, Fig.15, Fig. 16) as compared to the CE15 only control. This may be due to the concentration of SA used and as demonstrated by Gotzi et al [101,102], amphiphilic lipids can act as a surfactant to increase solubility of extract components. Nevertheless, for the CE-SA-PVP formulation, as the ratio of CE-SA to PVP coating decreased, the release of CE15 increased (Fig. 15). For the CE-SA-LAE formulation, although only the final formulation at a ratio of 0.125 is shown (Fig. 16), there is still

a shift in the release profile due to the LAE coating, demonstrating the tunability of these formulations.

In conjunction with the ability to controllably release CE15, these formulations were also able to adhere to hydroxyapatite disks coated in saliva pellicle to mimic actual tooth adhesion properties (Fig. 17). Adhesion studies were performed for 24hrs to determine if after a single use, the product could continue to adhere until the next day as a maximum test case. Importantly, observations at the initial 0hr and at the 24hr timepoints suggest the adhesiveness of these formulations even being able to withstand PBS incubation, which mimics saliva in the mouth. Therefore, both formulations provide adhesion and biofilm inhibition activity with the CE-SA-PVP most useful when a biofilm is already present while the CE-SA-LAE formulation provides the additional benefit of direct binding to the pellicle/tooth surface. Notably, this is the first report (to the best of our knowledge) describing a technique for controlled release of cranberry natural extract.

Moreover, the CE15-SA-PVP and CE15-SA-LAE samples also inhibit human saliva biofilm formation equal to or better than cranberry extract alone; a trend that becomes clear even at lower concentrations (Fig. 18). Demonstrably, the literature has already shown cranberry extract to have concentration-dependent antibacterial/anti-biofilm properties [84,86,161,166,196] and our data supports biofilm formation increasing as the concentration of cranberry extract decreases. However, our data further suggests the importance of the PVP and LAE addition (known to prevent bacterial attachment and plaque formation) [173] to prevent biofilm. Herein, crystal violet staining was used to specifically capture new biofilm formation. When all samples (CE15-SA-PVP, CE15-SA-LAE and CE15 alone) were made to contain the same concentration of cranberry extract (5mg/mL), our CE15-SA-PVP and CE15-SA-LAE samples inhibited biofilm formation

comparable to CE15 alone. Furthermore, at the lowest concentration (0.05mg/mL), our CE15-SA-LAE outperforms both CE15-SA-PVP and CE15 alone. Hence, these biofilm inhibition characteristics (equal to or better than CE15 alone) combined with the engineered controlled release and adhesion properties highlight the potential use of our formulations for inhibition of oral biofilms.

This simple and facile technique of generating a formulation that utilizes FDA approved excipients, allows for easy scale-up for testing in humans and has the potential to be broadly applied to generate controlled release formulations of a variety of other multi-component natural extracts such as neem, turmeric, and ginger extracts.

4.0 Controlled Release of Treg Inducing Microspheres for the Treatment of Periodontal Disease

This chapter is adapted from; Ashlee C. Greene, Mostafa Shehabeldin, Jin Gao, Stephen C. Balmert, Michelle Ratay, Charles Sfeir, Steven R. Little. (2021) Local Induction of Regulatory T cells Prevents Inflammatory Bone Loss in Ligature-Induced Experimental Periodontitis in Mice. Manuscript submitted for publication.

Specific Aim 3: To Develop Controlled Release Drug Delivery Formulations for Immune Modulation and Treatment of Periodontal Disease.

4.1 Introduction

In the previous aims, treatment strategies targeting bacterial pathogens through the encapsulation of an antibiotic API (aim 1) and a natural extract API (aim 2) were investigated. However, while an overburden of periodontal pathogens can initiate oral dysbiosis of the microbiome, literature suggests the root cause is actually an unbalanced inflammatory response that produces the severity of symptoms that leads to both hard and soft tissue destruction [112].

In the healthy steady state, the body employs natural immune regulatory mechanisms that restore unbalanced inflammatory responses back to homeostasis. A subset of T lymphocytes, regulatory T cells (Tregs), are professional, regulatory immune cells that function through both

direct cell-cell contact and secreted signals [126]. Our previous studies [129] have suggested that these cells can be locally recruited in the local periodontium environment, leading to the reestablishment of homeostasis in periodontal disease. Notably, endogenous Tregs exist as a relatively small percentage of lymphocyte populations in the periphery (5%-10%)[217], and therefore recruitment strategies are limited by the number of Treg, and also could be less effective in patients with systemic diseases that may alter the prevalence of endogenous Tregs [130–132].

Herein, we build on previous demonstrations that a combination of factors (IL2, TGFβ and Rapamycin) can lead to the local induction of a highly prevalent population of CD4+ naïve T cells, differentiating them into Tregs at the site of administration [133–135]. Notably, IL2 and TGFβ (in small quantities delivered locally) are cytokines known to promote the growth and differentiation of naïve T cells into regulatory T cells [136]. Rapamycin is a small molecule, mTorr inhibitor capable of preventing the differentiation of naïve T cells into other T-cell types [137]. Therefore, we hypothesize that the local delivery of a formulation with this combination of factors could reduce inflammatory bone loss even in the ligature-induced model of periodontal disease. Accordingly, we have tested the local delivery of a combination of TGFβ, rapamycin and IL2 encapsulated in degradable microspheres (TRI MPs) in a ligature-induced murine model for periodontal disease. These formulations (as well as previously explored Treg recruitment strategies) may serve as a platform to treat a number of inflammation-based oral diseases.

4.2 Materials & Methods

4.2.1 Microsphere fabrication

For IL-2 microspheres, a water-oil-water double emulsion was used. Two hundred (200) mg of acid terminated Poly (lactic-co-glycolic) acid (PLGA) (RG502H; 50:50 lactide:glycolide, MW: 7-17kDa, Sigma Aldrich) was dissolved in 4mL of dichloromethane (DCM). For the 200uL inner aqueous phase, 5ug of recombinant mouse IL-2 (R&D Systems, Minneapolis, MN) aliquoted in 50uL of phosphate buffered saline without calcium or magnesium (PBS (-)) was added to 150uL of PBS (-). The first water-in-oil emulsion was prepared by sonicating the 200uL inner aqueous solution of IL-2 in the 4mL of dissolved polymer at 55% amplitude for 10s (Active Motif, Carlsbad, CA). The resulting primary emulsion is then poured into 60mL of 2% w/v Poly(vinyl alcohol)(PVA, MW ~25 kDa, 98% hydrolyzed, Polysciences, Warrington, PA) with 51.6mM NaCl and homogenized at 3,000rpm for 1min (L4RT-1, Silverson, East Longmeadow, MA). The resulting double emulsion was then poured into 80mL of 1% w/v PVA with 51.6mM NaCl and with a stir bar and stir plate, stirred on ice at 600rpm for 3hrs to allow for the DCM to evaporate.

For TGF-β microspheres, similarly, 170mg of ester terminated Poly (lactic-co-glycolic) acid (PLGA) (RG502; 50:50 lactide:glycolide, MW: 7-17kDa, Sigma Aldrich) and 30mg of mPEG-PLGA (50:50 lactide:glycolide, 5-20 kDa, PolySciTech, West Lafayette, IN) were dissolved in 4mL of dichloromethane (DCM). For the 200uL inner aqueous phase, 10ug of recombinant human TGF-β (Peprotech, Rocky Hill, NJ) aliquoted in 100uL of deionized (DI) water was added to 100uL of DI water. The first water-in-oil emulsion was prepared by sonicating the 200uL inner aqueous solution of TGF-β in the 4mL of dissolved polymer at 55% amplitude for 10s (Active Motif, Carlsbad, CA). The resulting primary emulsion is then poured into 60mL

of 2% w/v PVA in DI water and homogenized at 3,000rpm for 1min. The resulting double emulsion was then poured into 80mL of 1% w/v PVA in DI water and, with a stir bar and stir plate, stirred on ice at 600rpm for 3hrs to allow for the DCM to evaporate.

For rapamycin microspheres, an oil-water single emulsion was used. Two hundred (200) mg of acid terminated Poly (lactic-co-glycolic) acid (PLGA) (RG502H; 50:50 lactide:glycolide, MW: 7-17kDa, Sigma Aldrich) was dissolved in 4mL of dichloromethane (DCM). Next, the polymer solution was poured into 60mL of 2% w/v Poly(vinyl alcohol)(PVA, MW ~25 kDa, 98% hydrolyzed, Polysciences, Warrington, PA) in DI water and homogenized at 3,000rpm for 1min (L4RT-1, Silverson, East Longmeadow, MA). The resulting single emulsion was then poured into 80mL of 1% w/v PVA in DI water and, with a stir bar and stir plate, stirred on ice at room temperature for 3hrs to allow for the DCM to evaporate.

For all microspheres, a polymer only control microsphere (blank) was also prepared. After stirring to allow for solvent evaporation, all microspheres were collected by centrifugation (200g, 5min, 4C) and washed 4 times with DI water. In a final suspension of >5mL DI water, samples were then flash frozen by liquid nitrogen and lyophilized for at least 48 hours (Virtis Benchtop K freeze dryer, Gardiner, NY; operating at 100mTorr).

4.2.2 Microsphere characterization

Sizing- Size distribution of the microspheres was measured by volume impedance method performed on a Beckman Coulter Counter (Multisizer-3, Beckman Coulter, Fullerton, CA). Approximately 1 mg of particles were suspended in 20mL of Isoton II diluent solution (Beckman Coulter) and readings were taken. Samples were diluted as necessary. A particle count of at least 1,000 was used to obtain number and volume averaged sizes.

In vitro release studies were carried out by incubating 10mg of microspheres placed in 1mL PBS (without calcium, magnesium) (HyClone, Cytiva, Marlborough, MA) with either 1% w/v bovine serum albumin (BSA) (for TGFB and IL2 MPs) or 0.2% Tween-80 (for Rapamycin MPs) on an end-over-end rotator at 37°C. At each time point, samples were centrifuged at 22°C at 371rcf for 5min and 800uL of supernatant was collected and replaced. Supernatant samples were quantified using an enzyme-linked immunosorbent assay (ELISA) (R&D Systems, Minneapolis, MN). For rapamycin MPs, cumulative release was quantified by UV-vis spectroscopy on a microplate reader (absorbance at 278nm).

Scanning electron microscopy (SEM) (JEOL, JSM-6330F, Peabody, MA) at 3kV, 8-8.5mm WD and x2000 magnification was performed to assess the morphology of the microspheres. Dry powder samples were mounted onto a stub with copper tape and sputter coated with palladium prior to imaging.

4.2.3 Disease induction Model and Treatment

Male Balb/c wild type mice aged 6-8weeks old were purchased from Charles River (Wilmington, MA). All procedures were performed in accordance with a protocol approved by the Institutional Animal Care and Use Committee at the University of Pittsburgh (protocol number: 20077447). First, mice were randomly assigned to experimental groups; age control, diseased untreated (ligature only), vehicle control (ligature + blank MPs) and treated (ligature + TRI MPs). Next, for disease induction, mice were anesthetized by I.P. injection of Ketamine/Xylazine. A 6-0 silk suture (Henry Schein, Melville, NY) was then tied around the left maxillary second molars using a stereomicroscope, similar to as previously described[218]. Following ligature placement, microspheres (either Blank MPs or TRI MPs), at 20mg MPs/mL suspended in 2%

carboxymethylcellulose in PBS were locally injected. An injection of 30 uL was distributed along the palatal side and an additional 20 uL injection was placed on the buccal side of the ligated molar. Ligatures were left in place for 7 days before sacrifice (Fig. 19).

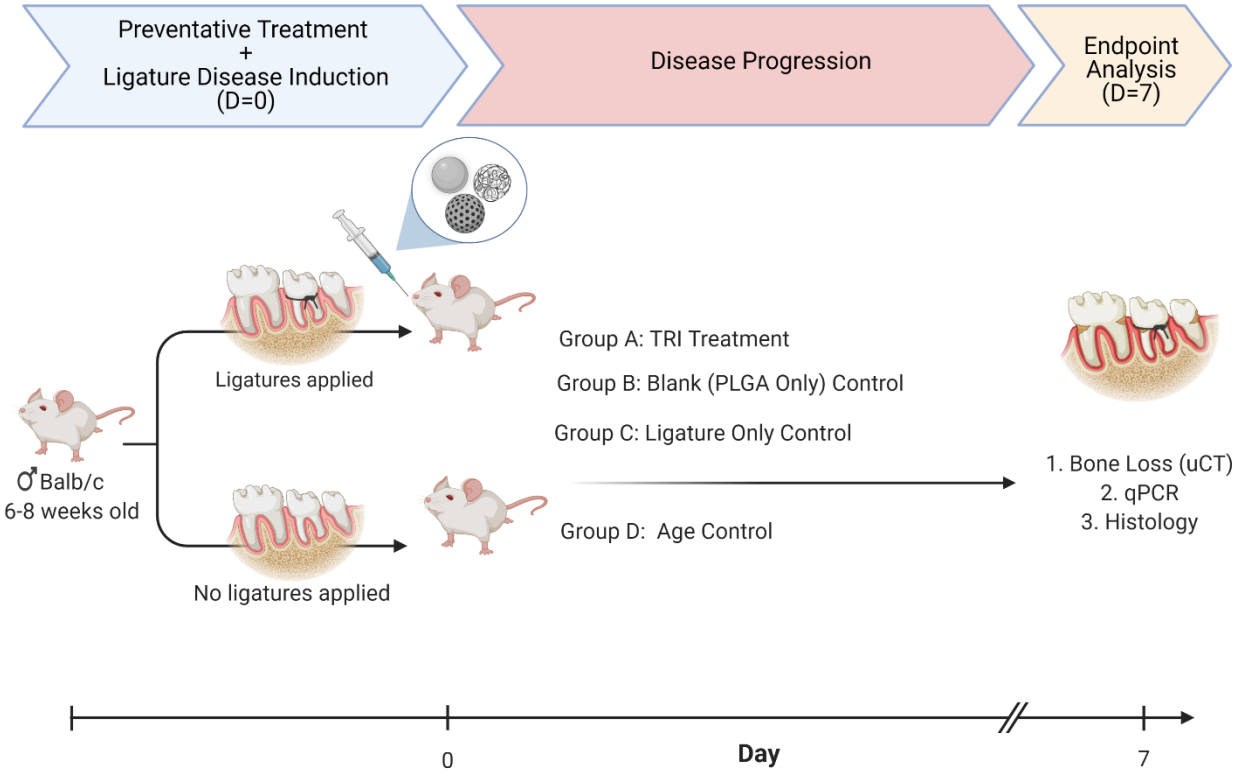

Figure 19. Murine Ligature-Induced Periodontal Disease. Experimental design where male Balb/c mice (6-8 weeks old) on Day 0 are either in; Group A-ligatures applied with a TRI microsphere injection, Group B-ligatures applied with blank PLGA (vehicle only) microsphere injection, Group C- ligatures applied only or Group D- no ligatures applied (age control). On Day 7, samples were collected to quantify bone loss by micro-CT (uCT), qPCR and histology as endpoint analyses.

4.2.4 Alveolar Bone loss analysis

Micro-computed tomography (uCT) was used to assess bone loss. Mice maxillae were first harvested and fixed in 10% buffered formalin overnight prior to being transferred to 70% ethanol for uCT scanning with a resolution of 10um voxel size (Scanco uCT 50, Scanco Medical, Switzerland). Scans were then reoriented using DataViewer software (GE Healthcare) to a standardized orientation. CTAN software (Bruker, Massachusetts) was then used to perform blinded measurements of the distance between the cementoenamel junction (CEJ) of the maxillary second molar and the alveolar bone crest (ABC) at mesial and distal aspects. A total of 8 measurement slices with 40um in between were used for each sample. Results of the distances from the ligated side were normalized to the corresponding average from the healthy, right side of the same maxillae.

4.2.5 Histological Analysis

To prepare for histological analysis, mice maxillae were demineralized in 10% EDTA solution for 2 weeks. Samples were then embedded in paraffin and cut into sagittal sections 5um thick for immunohistochemistry and immunofluorescence staining. For tissue and bone contrast, tissue sections were stained with Masson-Goldner according to the manufacturer instructions. Samples we qualitatively assessed for bone loss and changes in gingiva and periodontal ligament for comparison. To determine changes in total T cells and FOXP3 T cells after TRI administration, samples were first deparaffinized followed by an antigen retrieval step using 10mM pH 6 Na Citrate with 0.05% Tween 20. Next, an autofluorescence reduction step was performed using 10mM Copper Sulfate and 50mM NH4 Acetate. Sections were then blocked with PBS containing

5% donkey serum and 1% Tween20 and treated with a streptavidin/biotin blocking kit (Vector Labs, Burlingame, CA). The blocked sections were then incubated overnight at 4°C with primary antibodies; biotin-FoxP3 (FJK-16s; eBio) and CD3 (SP7, monoclonal rabbit IgG; Thermo Scientific, Waltham, MA). Sections were then incubated with secondary antibodies Cy3-streptavidin (Jackson ImmunoResearch Laboratories, West Grove PA) and Alexa Fluor 555 donkey anti-rabbit IgG (Thermo Scientific) for 1 hr at room temperature, counter stained with DAPI and fixed with 2% paraformaldehyde, similar to as previously described[135]. Samples were imaged with a fluorescent microscope (Eclipse TE200-E; Nikon Instruments) and a blinded quantification was performed of the ratio of FOXP3 positive cells (Tregs) to CD3 positive cells (total T cells).

4.2.6 Quantitative Polymerase Chain Reaction (qPCR)

To analyze gene expression, maxillae were flash frozen in liquid nitrogen for storage at -80C until RNA extraction. The day before RNA extraction, each sample was thawed in RNA later solution at 4°C overnight. Then, gingival tissue was resected from the ligated side of the maxilla under a dissection microscope and Trizol reagent (Life Technologies) was used to extract total RNA from the gingiva samples. Purification was performed using RNeasy Mini Kit (Qiagen). For each reverse transcription reaction, 450ng of RNA was converted to cDNA using a High-Capacity RNA-to-cDNA Kit (Applied Biosystems). Quantitative polymerase chain reaction was then performed using TaqMan Gene Expression Master Mix and markers specific for RANKL (Mm00441906_m1; FAM-MGB), NCF1 (Mm00447921_m1; FAM-MGB), IFNG (Mm01168134_m1; FAM-MGB), IL4 (Mm00432102_m1; FAM-MGB), TGFβ (Mm01178820_m1; FAM-MGB), IL10 (Mm01288386_m1; FAM-MGB),

COL1A1(Mm00801666_g1; FAM-MGB), TIMP1(Mm01341361_m1; FAM-MGB) and GAPDH as the endogenous control (Mm99999915_g1; FAM-MGB). Reactions were run on a QuantStudio 6 Flex Real-Time PCR system (Thermo Fisher Scientific) and the delta-delta Ct method was used for analysis.

4.2.7 Statistics

Statistical analyses were performed using GraphPad Prism Software v9. A One-way ANOVA with a Tukey post-hoc test was used to compare the mean of each experimental group with the mean of every other group. A ROUT outlier test with a threshold for outlier removal (Q = 0.1%) was used to remove outliers from the graph of average interdental bone loss. Data are expressed as a scatter plot with the mean or bar graph with the mean ± standard deviation. The following cutoffs were used for statistical significance; * $p \leq 0.05$, ** $p \leq 0.01$, *** $p \leq 0.001$, **** $p \leq 0.0001$.

4.3 Results

4.3.1 TRI MPs demonstrate morphology consistent with their 1-week release profiles

Microspheres were first measured for size by volume-impedance method with a Coulter counter. Volume-average diameters were: TGFβ MPs (21.5um ± 6.8um), Rapamycin MPs (14.6um ± 6.8um), and IL2 MPs (20.8um ± 6.1um) (Fig. 20A). After sizing, release was assessed for 7 days to span the length of the ligature model timeline. For TGFβ MPs, approximately 5.5ng

were released before the profile reaches a plateau as compared to IL2 MPs with a burst release of approximately 28ng before plateauing. Rapamycin MPs have a steadier, more linear release profile, reaching approximately 3,500ng by day 7 (Fig. 20B). Lastly, surface morphology was detected with scanning electron microscopy (SEM). As demonstrated in the representative SEM images, TGFβ MPs with the addition of poly (ethylene glycol) (PEG)-PLGA di-block copolymer, are spherical with an uneven or bumpy surface. Rapamycin MPs have a smooth and spherical appearance. IL2 MPs have a porous surface morphology (Fig. 20C).

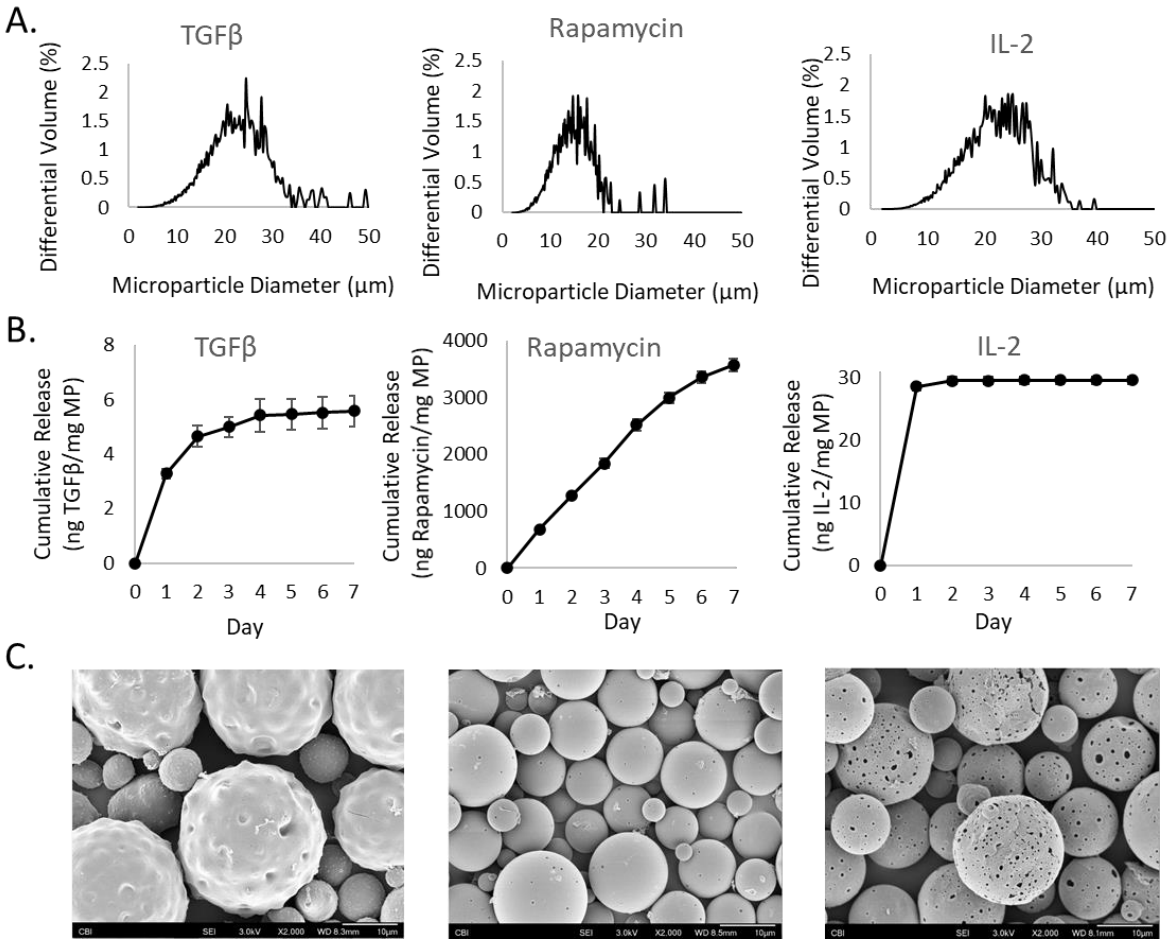

Figure 20. Characterization of the TRI (TGFβ, Rapamycin and IL-2) MPs. (A) Size distributions of microspheres (MPs) as measured by volume-impedance method with a Coulter Counter as mean ± standard deviation for TGFβ MPs (21.5um ± 6.8um), Rapamycin MPs (14.6um ± 6.8um), and IL-2 MPs (20.8um ± 6.1um). All Coulter Counter sigma counts were greater than 1000. (B) In-vitro release kinetics at 37°C (n=3) presented as the mean ± standard error of the mean for TGFβ MPs in PBS + 1%BSA , Rapamycin MPs in PBS + 0.2% Tween80 , and IL-2 MPs in PBS + 1%BSA . (C) Representative scanning electron microscopy (SEM) images to observe surface morphology of TGFβ MPs, Rapamycin MPs, and IL-2 MPs at 2000x (scale bar = 10um).

4.3.2 TRI MPs reduce alveolar bone resorption in an aggressive periodontitis model

Next, local treatment with TRI MPs was evaluated in regard to the impact on alveolar bone resorption in an aggressive, ligature-induced periodontitis model. Interdental bone loss was assessed for age control, diseased untreated (ligature only), vehicle control (ligature + blank MPs) and treated (ligature + TRI MPs) groups. Representative 3D reconstructed images reveal a visual difference in the bone level between the groups (Fig. 21A). Blinded analysis of the interdental measurements show our TRI MPs successfully reduced interdental alveolar bone loss by approximately ~30-40% when compared to the ligature only group and ~10-20% when compared to the vehicle control (Fig. 21B). This is further validated with Masson-Goldner trichrome immunohistochemical staining. In performing tissue morphological identification, differences in the periodontal ligament, gingiva tissue and alveolar bone can be observed (Fig. 22A,B).

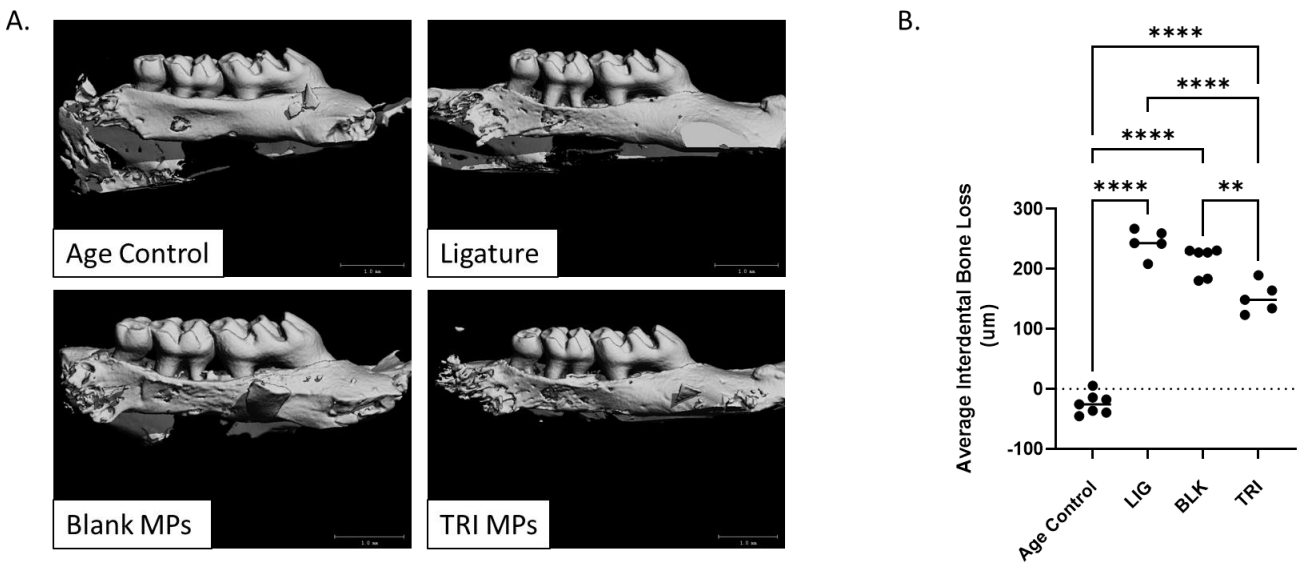

Figure 21. TRI MPs reduce ligature-induced alveolar bone resorption. An injection of MPs was administered to male Balb/c mice (6-8 weeks old) at the same time as ligature placement around the maxillary second molar. After 7 days, bone loss was assessed by micro-CT. (A) Representative 3D reconstructed micro-CT scans of the age control, ligature (diseased untreated), blank MPs (PLGA vehicle-only control) and TRI MPs experimental groups (scale bar = 1nm). (B) Average bone loss quantified by linear interdental measurements between the cementoenamel junction and alveolar bone crest (CEJ-ABC) of the ligated maxillary second molar for each experimental group (n=5-7 mice). A One-way ANOVA was performed followed by Tukey post-hoc analysis to compare the mean of every group with the mean of every other group to determine statistical significance where; ** $p \leq 0.01$, *** $p \leq 0.001$, **** $p \leq 0.0001$.

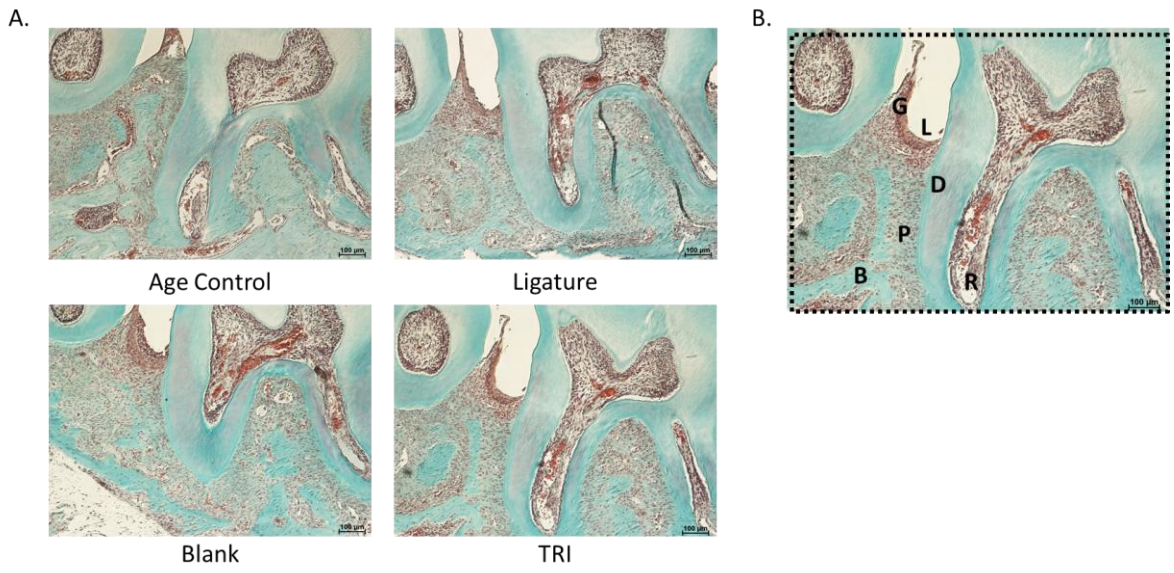

Figure 22. Representative immunohistochemistry of tissue sections near the ligated second maxillary molar. Maxilla from each group were paraffin embedded, cut into sagittal sections and stained. A) Masson-Goldner trichrome immunohistochemical staining. Scale bars are 100um. B) Representative labeled Masson-Goldner stained sagittal section where G; gingiva, L; ligature demarcation, D; dentin, P; periodontal ligament, B; alveolar bone and R; root.

4.3.3 Immunofluorescence supports Treg induction capability of TRI treatment

In order to determine the Treg induction capability of the TRI MPs, total T cells (CD3 positive cells) and Tregs (FOXP3 positive cells) were stained by immunofluorescence. A blinded quantification of the percent FOXP3 positive cells of total T cells (CD3 positive cells) (representative images Fig. 23A) reveals an increase in this ratio when TRI MPs are administered (Fig. 23B). While there is only (on average) approximately 23.1% Tregs for the age control, there is 37.0% and 37.8% Tregs for the ligature and blank groups. However, the average percentage of Tregs for the TRI group was 48%.

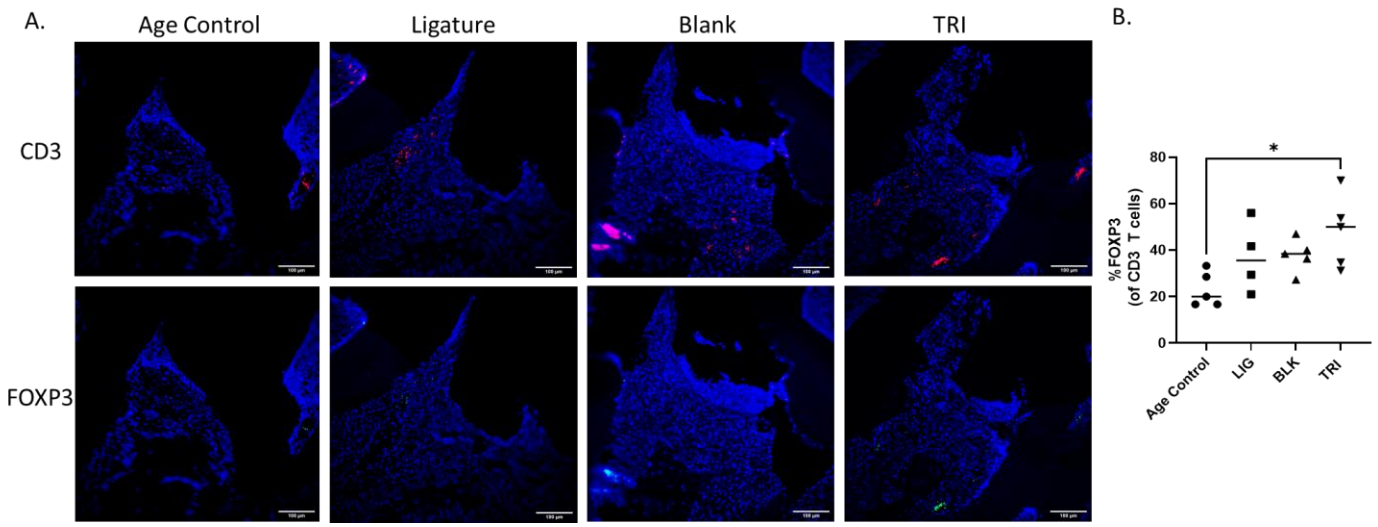

Figure 23. TRI MPs increase the ratio of Tregs to effector T cells. A) Representative immunofluorescence staining for CD3 (total T cells), FOXP3 (Tregs), and DAPI (nuclei). Scale bars are 100um. B) Blinded quantification of the %FOXP3 of CD3 total T cells (n= 4-5 per group) where a One-way ANOVA was performed followed by Tukey post-hoc analysis ; * $p \leq 0.05$.

4.3.4 Expression of pro-inflammatory vs. pro-regenerative markers varied following treatment

Changes in gene expression of local markers in response to ligature administration and TRI MP treatment were also assessed. The expression of RANKL, NCF1, IFNγ, and IL4 was examined to capture the local pro-inflammatory context (Fig. 24A). Concurrently, the expression of TGFβ, IL10, COL1A1 and TIMP1 was examined to capture the local pro-regenerative context (Fig. 24B). An upregulation in expression of pro-inflammatory markers was observed with the ligature group, blank group or both for IFNγ, NCF1 and RANKL, respectively. There was also a trend toward an increase in pro-inflammatory IL4 for the ligature group although not significant. For the anti-inflammatory markers, TGFβ and IL10 expression was upregulated for all groups that had received

ligatures regardless of the treatment. Furthermore, while there was more of a bias towards upregulation of COL1A1 and TIMP1 in the blank MP and TRI MP treatment groups, the difference between these two groups appeared to be minimal.

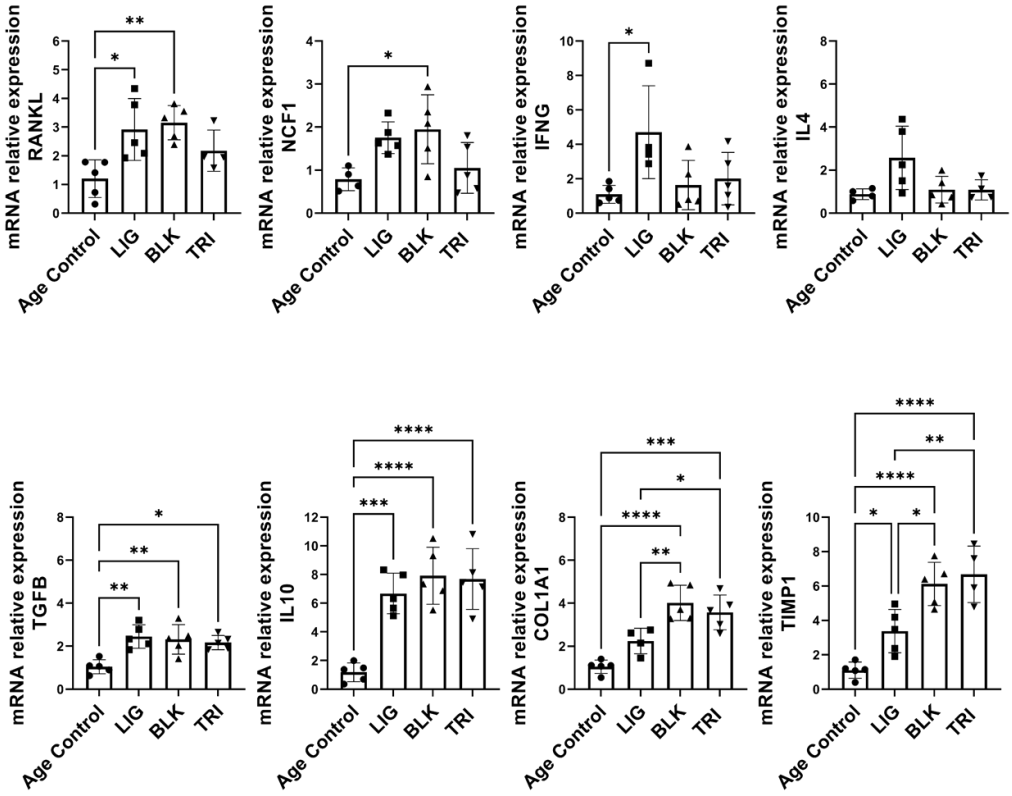

Figure 24. Expression of pro-inflammatory vs. pro-regenerative markers following treatment. Balb/c mice from Group A-ligatures applied with a TRI microsphere injection (TRI), Group B- ligatures applied with blank PLGA (vehicle only) microsphere injection (BLK), Group C- ligatures applied only (LIG) or Group D- no ligatures applied (age control) were sacrificed after 7 days. Periodontal gingival tissues were resected and mRNA expression was assed by qPCR for (A) markers indicative of a pro-inflammatory environment (RANKL, NCF1, IFNG and IL4) vs. (B) anti-inflammatory and pro-regenerative markers (TGFB,IL10,COL1A1 and TIMP1). mRNA expression levels were compared by the value of $2^{(-\Delta\Delta Ct)}$ with GAPDH as the endogenous control. A One-way ANOVA was performed followed by Tukey post-hoc analysis to compare the mean of every group with the mean of every other group to determine statistical significance where; ** $p \leq 0.01$, *** $p \leq 0.001$, **** $p \leq 0.0001$.

4.4 Discussion

Periodontitis is a common but complex oral disease that has historically been characterized by the presence of a bacterial assault [219,220]. Yet, in recent years, literature has elucidated a more nuanced but critical interplay between oral bacteria and the host response. Specifically, it is not just the microbial dysbiosis but an underlying unbalanced host immune response that is ultimately responsible for the inflammatory destruction and disease progression of periodontitis [221,222]. This renewed understanding has made way for a multitude of new immunomodulatory approaches as potential treatments; from the use of pro-resolving molecules like lipoxins and resolvins [116] to strategies of modulating innate immune cells such as macrophages [223] and cytokine signaling such as Del-1 or anti-IL17 [224,225]. Therefore, in this study, we evaluated the effect of re-balancing the host immune response through an immune cell modulation strategy of locally inducing regulatory T cells (Tregs) for its impact on inflammatory bone loss in periodontitis.

Regulatory T cells (Tregs) are naturally positioned to counteract immune imbalance and inflammatory destruction [127]. Previously, we demonstrated the modulatory potential of Tregs in periodontitis through the local enrichment of Tregs using a *recruitment* strategy in a murine oral gavage model [129]. When Tregs were locally recruited and enriched such that the ratio of Treg to effector T cells favored resolution of inflammation, bone loss was reduced and there was a microenvironment shift towards regeneration. Furthermore, this strategy of harnessing the immunomodulatory power of Tregs did not have a negative pathogenic effect; it did not lead to an increase in total bacterial counts. Additionally, several mechanistic studies have also shown disease improvement could be disabled upon Treg inhibition. A reduction in Treg to effector T cell ratios due to the depletion of Tregs instead enabled further disease progression [129,200,226]. Therefore, while the potent ability of Tregs to counteract inflammation in periodontitis has been

established, the efficacy of a Treg recruitment strategy is ultimately constrained by the pre-existence of local Tregs in sufficient numbers for recruitment.

A Treg *induction* strategy was developed to serve as an alternative (or potentially even an option to accompany) the Treg recruitment strategy. This induction strategy enables flexibility to increase the abundance of local Tregs through the induced differentiation of naïve T cells. As demonstrated previously, a combination of TGFβ, rapamycin and IL2 encapsulated microspheres (TRI MPs) were utilized; known for their roles in the development and differentiation of Tregs, ability to decrease effector T cell populations and as a T cell proliferative agent, respectively. Although we have previously shown the ability of these factors (combined but not the factors individually) to induce Tregs from naïve T cells in-vitro [133] and in the context other disease models [134,135,227,228], this is the first time that this induction strategy has been used in the context of periodontitis.

Accordingly, we investigated the effect of this induction strategy (with TRI MP treatment) on alveolar bone resorption. While there is no singular, ideal in-vivo animal model for murine induction of periodontitis and bone resorption, for this study, we utilized the ligature-induced murine model. Unlike the oral gavage model that has a long timeline for disease establishment and is based on the initial bacterial inoculation's ability to take hold and locally colonize, the ligature-induced periodontitis model is advantageous in that disease can be initiated at a known time with a predictable, albeit more aggressive, disease propagation time course (when compared to the oral gavage model) of just a few days [218]. Therefore, the benefits of the ligature-induced model provide an optimal yet aggressive testing condition to rigorously evaluate the upper limits of the immunomodulatory capabilities of TRI MP treatment on periodontitis disease symptoms. On Day 0 (Figure 19), mice either received no ligatures (age control), or received ligatures without

treatment (ligature only), received ligatures with blank MPs injection (vehicle control) or received ligatures with a TRI injection (consisting of TGFβ, Rapamycin and IL2 microspheres delivered together) since previous studies utilizing TRI MPs demonstrated the effect with all three factors was greater than any single factor or double factor combination. The 'TRI' formulation was adapted for use in the 7-day ligature-induced periodontitis murine model and the in-vitro results were consistent with our previous findings of characterization profiles that have demonstrated successful Treg induction (Fig. 20) [134,135,227,228]. Importantly, TRI MPs were able to demonstrate significant bone loss reduction when compared to the ligature group by approximately 30% (Fig. 21B). Unexpectedly, there was also a reduction in bone loss with Blank MPs (albeit to a lesser degree) when compared to the ligature group, by about 10-20%. Although this seemingly protective effect from the Blank MPs may not have been anticipated, this effect has actually been reported in other disease model applications of TRI MPs in the past [134,228] and by others in the literature [229–231]. These findings may be due to PLGA-derived lactic acid and it's latent immunomodulatory properties at the local site of administration [232]. Nevertheless, our studies show that TRI MP treatment produced a significant reduction in bone loss in an extremely acute model of periodontitis.

However, even with substantiated bone loss indicative of the benefit of an increased Treg presence, the immunomodulatory ability of Tregs ultimately depends upon the ratio of Tregs to effector T cells in the local environment, as observed in other disease models (allergic contact dermatitis, dry eye disease, transplant) with TRI MP treatment [134,135,227]. For this reason, we quantitatively assessed the ratio of Tregs to effector T cells after TRI MP administration in the ligature-induced periodontitis model. In the blinded quantification of immunofluorescence staining for FOXP3 (Tregs) and CD3 (total T cells), there was an increase in the ratio of Tregs to

CD3 cells (Fig. 23B). This effect could be driven in part by the model itself; the presence of ligatures is supposed to increases inflammation as compared to the age control group , and this general increase in inflammation can increase the overall presence of responding lymphocytes (including Tregs) in the local area [233]. Nevertheless, the TRI MP group demonstrates the highest ratio of all measured groups, on average ~48%. This promising Treg induction by TRI MP lays the groundwork for future studies where we can even further bolster this ratio and explore its effects.

In previous findings, the immunomodulatory impact of TRI MP-induced Tregs was not only a reduction in key signs of disease but also a decrease in pro-inflammatory cytokine expression and increase pro-regenerative cytokine expression in the local microenvironment [134,135,227]. An inspection of sample sagittal sections that were stained using Masson-Goldner (Fig. 22) qualitatively supports some preservation of the periodontal ligament space for all groups with a mix of tissue necrosis and regeneration of the gingiva tissues where ligatures were applied specifically for Blank and TRI MP groups. Importantly, upon further quantitative assessment of local cytokines and cell markers there was a trend of a decrease in pro-inflammatory cytokines (Fig. 24A) and an increase of pro-regenerative factors upon TRI MP treatment, notably with some variability (Fig. 24B). While there were some inconsistent fluctuations in marker expression outside of these trends, it may again be due to the inherent acute nature of the ligature-induced model. As noted in the literature, the ligature-induced periodontitis model expedites disease progression and enables visible bone loss in as little as a few days [218]. Such acute inflammation aggressively expedites and increases the natural influx of lymphocytes to that site. This change in an already immunologically complex microenvironment, also influences the process of differentiation for that influx and local accumulation of lymphocytes (including T cells)[234].

Therefore, administering a preventative treatment on the same day an acutely inflamed microenvironment is developing, may detract from the effectiveness of the treatment. Instead, based on the data we have presented here, a stronger Treg induction response may be necessary (to counteract the inherent acute nature of the model and its effects) to yield more consistent trends in pro-inflammatory and pro-regenerative markers. Future studies would be needed to investigate how to further bolster the Treg induction response whether through dose escalation studies or increased dendritic cell (antigen-presenting cell) stimulation time to aid in a more robust Treg induction etc. Nevertheless, it is promising that in such complex conditions, TRI MP treatment is still able to have a detectable impact, indicating the feasibility of this approach.

Overall, findings of reduced bone loss, increase in Treg to T effector ratio and trends of decreasing pro-inflammatory factors and increasing pro-regenerative factors with TRI MP treatment, suggest that there could be potential for a Treg induction strategy for immunomodulation in the context of periodontitis. This strategy to increase the local concentration of Tregs for the regulation of inflammation-based destruction could be used as the basis for treatment of other inflammation driven diseases.

5.0 Conclusions and Future Work

The overarching goal of this thesis was to engineer three types of extended release, bioerodible microsphere formulations. Each of these formulations were centered around a different active ingredient (antibiotic, natural extract, proteins) but all were successful in addressing some of the unmet needs of currently available treatments while also providing translational value for patients with varying forms of periodontitis.

5.1 Specific Aim 1: To Engineer Arestin® Comparator Products for Biorelevant Dissolution Testing Mimicking the Periodontal Pocket for the FDA.

In aim 1, in anticipation of FDA generic drug applications to replace a common periodontal adjunct antibiotic therapy (Arestin®), we used reverse engineering to determine critical microsphere design parameters. We then used an emulsion fabrication technique to generate a direct comparator (direct mimic of Arestin®) along with alternative comparator panels meant to simulate generic formulations of Arestin® the FDA may see in future ANDA applications. These comparator panels were then tested for bioequivalence (qualitative (Q1) and quantitative (Q2) sameness and change) to Arestin®. As a final measure, the comparator panels were used to validate and determine the discriminatory power of a novel biorelevant dissolution device that better simulates the periodontal pocket than traditional methods.

The significance of the generation of these comparator panels is two-fold. First, these panels demonstrated which variations in process parameters vs physiochemical parameters

(qualitative (Q1) and quantitative (Q2) sameness and change) could predictably change formulation characteristics (size, drug loading, morphology, release/dissolution kinetics). Process parameters like the homogenization and solvent type were found to be the most influential on particle size (increase in homogenization rate decreased particle size) and drug content (ethyl acetate resulted in lower loading as compared to DCM). However, the second significance of the generation of these panels comes from our elucidation that physiochemical parameters most strongly influence release/dissolution kinetics. Intriguingly, our dissolution kinetics trends were unexpected. Opposite to what has been reported in the literature, at each LA:GA ratio, we observed an increase in molecular weight led to a faster release profile. While we hypothesized this phenomenon was due to ionic interactions between our API-minocycline and the PLGA, future work would be needed for better understanding of this trend. Incorporating more molecular weight polymers within each LA:GA ratio in addition to looking at other APIs with different potentials of ionic interaction with PLGA would be impactful to better understand the underlying mechanism and better predict in-vitro outcomes. Additionally, quality control measures should also be incorporated into the fabrication process to ensure the variability that has been observed is not a result of process changes or operator changes. This would help to eliminate any man-made interference in observed trends for more predictable formulation outcomes.

Overall, our increased understanding of how to predictably change formulation characteristics- especially dissolution kinetics-has the potential for tremendous applications in the development of better translational in-vitro/in-vivo correlations. With a better simulation of the periodontal pocket using our novel small volume dissolution device and as a result, more accurate in-vitro data, theoretically, better correlations between in-vitro release and in-vivo bioavailability can be made. However, these correlation studies in addition to further validation of the small

volume dissolution device with other oral periodontal drugs also remain to be performed in future work. Additionally, several parameters such as flow rates, dissolution media and membrane permeance of the device could be modified to make this dissolution device more applicable to other desired and difficult to replicate physiological milieus.

5.2 Specific Aim 2: To Develop Cranberry extracts-based Formulations for the Prevention of Oral Bacterial Biofilms and Periodontal Disease.

In aim 2, as an alternative approach to bacterial biofilm treatment with antibiotics/ antimicrobials or harsh antiseptic mouthwashes prescribed to mild/moderate periodontitis patients, we developed oral delivery formulations with natural biofilm prevention properties by encapsulating cranberry extract. We determined an optimal fabrication method that resulted in high loading and coated our selected formulations with stearic acid (SA) and a bioadhesive (polyvinylpyrrolidone (PVP) or ethyl lauroyl arginate (LAE)). We then characterized our formulations for in-vitro controlled release, followed by bioactivity and adhesion to oral pellicle/biofilm using a saliva-based assay and crystal violet staining for quantification of new biofilms.

One of the most pivotal findings in this work was the multi-component, hydrophilic/hydrophobic nature of the cranberry extract that was also surprisingly already spherical in shape, which all strongly influenced the fabrication method. Our initial attempts with a traditional technique of PLGA encapsulation resulted in extremely low loading with most of the extract settling out or leaching out of the formulation throughout the fabrication process. Therefore, we adapted our approach to take advantage of the already spherical nature of the

cranberry extract and used a one pot fabrication process with coatings to tune the release kinetics and the adhesion properties.

The one pot fabrication approach enabled us to fully capture all the hydrophilic/hydrophobic components of the cranberry extract but there will need to be future studies to determine the final use/packaging and its impact on activity. These formulations were originally intended as a consumer oral health care product with varied potential applications like mouth wash, floss or a chewable gum. Each of these final product formats have different benefits but it is unknown how these formats and their corresponding additional excipients would impact release rate and activity. Nevertheless, this one pot fabrication process is highly attractive due to its high yield especially for multi-component APIs of interest. This fabrication method also could be used as a strategy to encapsulate other hard to formulate natural extracts.

5.3 Specific Aim 3: To Develop Controlled Release Drug Delivery Formulations for Immune Modulation and Treatment of Periodontal Disease.

Lastly, in aim 3, we took an immunomodulation approach to address the root cause of periodontitis, an underlying immune imbalance. Here, we hypothesized that enrichment of the local presence of regulatory lymphocytes (Tregs) could restore local, immunological homeostasis. This approach has been attempted with other inflammation driven diseases, but we had not yet studied this approach in periodontitis. Accordingly, we locally delivered a combination of TGFβ (cytokine- growth factor essential for Treg differentiation), Rapamycin (small molecule- mTorr inhibitor to prevent differentiation into effector T-cell types) and IL2 (cytokine- promotes the differentiation of immature T cells into regulatory T cells) microspheres to increase the local

number and ratio of Tregs in the periodontium. Using a ligature-induced murine periodontitis model, we demonstrated that this combination of factors significantly decreased alveolar bone loss in mice. A shift in the local ratio of Tregs to T effector cells and a microenvironment change of pro-inflammatory and anti-inflammatory markers, was also demonstrated. However, we also stumbled upon some unexpected findings that merit more understanding through future work.

We believe many of the unexpected findings in this work may be attributed back to our selected murine ligature induced periodontitis model. While we initially attempted to use the bacterial gavage model as had been performed in previous studies, after several years of attempting to replicate the model, it only worked moderately at best. We have since determined that there were some environment-based (and possibly even genetic) differences in mouse strain and bacterial susceptibility between here in the US and in Brazil where the previous successful studies were performed. Therefore, to perform the studies here in aim 3, we switched to the murine ligature induce periodontitis model which is more aggressive (in comparison to the gavage model) with a very short 1-week timeline for disease induction that was more easily reproducible. However, this model is not without its disadvantages. An unintended consequence of the rapid escalation in disease progression for this model, is the increased influx of key inflammatory players present, their influence/signaling changes on the local microenvironment and Treg induction. However, it remains to be seen through future studies, if this is just a temporary effect that could be both better understood and better separated from Treg induction events by making the experimental timepoints earlier or later. Future studies should also monitor the other key cellular players like dendritic cell stimulation that would directly impact the resulting Treg induction for any time-dependent changes as well. Nevertheless, the use of these Treg-inducing microspheres appears to

significantly improve periodontitis outcomes and may be able to serve as another platform delivery system to treat other inflammatory diseases.

Bibliography

1. Malerba, F. & Orsenigo, L. The evolution of the pharmaceutical industry. *http://dx.doi.org/10.1080/00076791.2014.975119* **57**, 664–687 (2015).
2. Campisi, B., Chicco, D., Vojnovic, D. & Phan-Tan-Luu, R. Experimental design for a pharmaceutical formulation: optimisation and robustness. *J. Pharm. Biomed. Anal.* **18**, 57–65 (1998).
3. Hirshfield, L., Giridhar, A., Taylor, L. S., Harris, M. T. & Reklaitis, G. V. Dropwise Additive Manufacturing of Pharmaceutical Products for Solvent-Based Dosage Forms. *J. Pharm. Sci.* **103**, 496–506 (2014).
4. Constantinides, P. P. *et al.* Formulation Development and Antitumor Activity of a Filter-Sterilizable Emulsion of Paclitaxel. *Pharm. Res. 2000 172* **17**, 175–182 (2000).
5. Dosage Forms | FDA. https://www.fda.gov/industry/structured-product-labeling-resources/dosage-forms.
6. Suchomel, M., Weinlich, M. & Kundi, M. Influence of glycerol and an alternative humectant on the immediate and 3-hours bactericidal efficacies of two isopropanol-based antiseptics in laboratory experiments in vivo according to EN 12791. *Antimicrob. Resist. Infect. Control 2017 61* **6**, 1–5 (2017).
7. Domínguez-Robles, J. *et al.* Lignin and Cellulose Blends as Pharmaceutical Excipient for Tablet Manufacturing via Direct Compression. *Biomol. 2019, Vol. 9, Page 423* **9**, 423 (2019).

8. Mullarney, M. P., Hancock, B. C., Carlson, G. T., Ladipo, D. D. & Langdon, B. A. The powder flow and compact mechanical properties of sucrose and three high-intensity sweeteners used in chewable tablets. *Int. J. Pharm.* **257**, 227–236 (2003).

9. Nande, V. S., Barabde, U. V., Morkhade, D. M., Joshi, S. B. & Patil, A. T. Investigation of PEGylated Derivatives of Rosin as Sustained Release Film Formers. *AAPS PharmSciTech 2007 91* **9**, 105–111 (2008).

10. Varde, N. K. & Pack, D. W. Microspheres for controlled release drug delivery. *http://dx.doi.org/10.1517/14712598.4.1.35* **4**, 35–51 (2005).

11. Kim, K. K. & Pack, D. W. Microspheres for Drug Delivery. *BioMEMS Biomed. Nanotechnol.* 19 (2006) doi:10.1007/978-0-387-25842-3_2.

12. Berkland, C., Kipper, M. J., Narasimhan, B., Kim, K. (Kevin) & Pack, D. W. Microsphere size, precipitation kinetics and drug distribution control drug release from biodegradable polyanhydride microspheres. *J. Control. Release* **94**, 129–141 (2004).

13. Rothstein, S. N., Kay, J. E., Schopfer, F. J., Freeman, B. A. & Little, S. R. A Retrospective Mathematical Analysis of Controlled Release Design and Experimentation. *Mol. Pharm.* **9**, 3003–3011 (2012).

14. Rothstein, S. N. *et al.* A “tool box” for rational design of degradable controlled release formulations. *J. Mater. Chem.* **21**, 29–39 (2011).

15. Tyrer, J. H., Eadie, M. J., Sutherland, J. M. & Hooper, W. D. Outbreak of Anticonvulsant Intoxication in an Australian City. *Br. Med. J.* **4**, 271 (1970).

16. Kassebaum, N. J. *et al.* Global Burden of Severe Periodontitis in 1990-2010. *J. Dent. Res.* **93**, 1045–1053 (2014).

17. Petersen, P. E. The World Oral Health Report 2003: continuous improvement of oral health in the 21st century - the approach of the WHO Global Oral Health Programme. *Community Dent. Oral Epidemiol.* **31**, 3–24 (2003).

18. Eke, P. I. *et al.* Update on Prevalence of Periodontitis in Adults in the United States: NHANES 2009 to 2012. *J. Periodontol.* **86**, 611–622 (2015).

19. Eke, P. I., Dye, B. A., Wei, L., Thornton-Evans, G. O. & Genco, R. J. Prevalence of Periodontitis in Adults in the United States: 2009 and 2010. *J. Dent. Res.* **91**, 914–920 (2012).

20. Listl, S., Galloway, J., Mossey, P. A. & Marcenes, W. Global Economic Impact of Dental Diseases: *http://dx.doi.org/10.1177/0022034515602879* **94**, 1355–1361 (2015).

21. PAGE, R. C. & KORNMAN, K. S. The pathogenesis of human periodontitis: an introduction. *Periodontol. 2000* **14**, 9–11 (1997).

22. Borrell, L. N. & Crawford, N. D. Social disparities in periodontitis among United States adults 1999–2004. *Community Dent. Oral Epidemiol.* **36**, 383–391 (2008).

23. Fisher, M. A. *et al.* Periodontal disease and other nontraditional risk factors for CKD. *Am. J. Kidney Dis.* **51**, 45–52 (2008).

24. Backes, J. M., Howard, P. A. & Moriarty, P. M. Role of C-Reactive Protein in Cardiovascular Disease*. *Ann. Pharmacother.* **38**, 110–118 (2004).

25. Seymour, G. J., Ford, P. J., Cullinan, M. P., Leishman, S. & Yamazaki, K. Relationship between periodontal infections and systemic disease. *Clin. Microbiol. Infect.* **13 Suppl 4**, 3–10 (2007).

26. Offenbacher, S. *et al.* A perspective on the potential cardioprotective benefits of periodontal therapy. *Am. Heart J.* **149**, 950–954 (2005).

27. Boggess, K. A. *et al.* Maternal periodontal disease in early pregnancy and risk for a small-for-gestational-age infant. *Am. J. Obstet. Gynecol.* **194**, 1316–1322 (2006).

28. Riviere, G. R., Riviere, K. H. & Smith, K. S. Molecular and immunological evidence of oral Treponema in the human brain and their association with Alzheimer's disease. *Oral Microbiol. Immunol.* **17**, 113–118 (2002).

29. Kamer, A. R. *et al.* Periodontal disease associates with higher brain amyloid load in normal elderly. *Neurobiol. Aging* **36**, 627–633 (2015).

30. Sparks Stein, P. *et al.* Serum antibodies to periodontal pathogens are a risk factor for Alzheimer's disease. *Alzheimer's Dement.* **8**, 196–203 (2012).

31. Marouf, N. *et al.* Association between periodontitis and severity of COVID-19 infection: A case–control study. *J. Clin. Periodontol.* **48**, 483–491 (2021).

32. Mancini, L., Quinzi, V., Mummolo, S., Marzo, G. & Marchetti, E. Angiotensin-Converting Enzyme 2 as a Possible Correlation between COVID-19 and Periodontal Disease. *Appl. Sci. 2020, Vol. 10, Page 6224* **10**, 6224 (2020).

33. Ready, D. *et al.* Disease severity associated with presence in subgingival plaque of Porphyromonas gingivalis, Aggregatibacter actinomycetemcomitans, and Tannerella forsythia, singly or in combination, as detected by nested multiplex PCR. *J. Clin. Microbiol.* **46**, 3380–3 (2008).

34. Lindhe, J. *et al.* Consensus Report: Chronic Periodontitis. *Ann. Periodontol.* **4**, 38–38 (1999).

35. Consensus Report Periodontal Diseases: Pathogenesis and Microbial Factors. *Ann. Periodontol.* **1**, 926–932 (1996).

36. Listgarten, M. A. Pathogenesis of periodontitis. *J. Clin. Periodontol.* **13**, 418–30 (1986).

37. Comprehensive Periodontal Therapy: A Statement by the American Academy of Periodontology. *J. Periodontol.* **82**, 943–949 (2011).

38. *The Journal of Dental Hygiene Special supplement*. http://jdh.adha.org/content/jdenthyg/82/suppl_2/16.full.pdf.

39. AMERICAN ACADEMY OF PEDIATRIC DENTISTRY ENDORSEMENTS 453. (2001) doi:10.1902/jop.2001.72.11.1624.

40. Armitage, G. C. Development of a Classification System for Periodontal Diseases and Conditions. *Ann. Periodontol.* **4**, 1–6 (1999).

41. Krebs, K. A., Clem, D. S. & American Academy of Periodontology. Guidelines for the Management of Patients With Periodontal Diseases. *J. Periodontol.* **77**, 1607–1611 (2006).

42. Periodontal Scaling and Root Planing Policy. (2014).

43. Smiley, C. J. *et al.* Evidence-based clinical practice guideline on the nonsurgical treatment of chronic periodontitis by means of scaling and root planing with or without adjuncts. *J. Am. Dent. Assoc.* **146**, 525–535 (2015).

44. G. Caton, J. *et al.* A new classification scheme for periodontal and peri-implant diseases and conditions – Introduction and key changes from the 1999 classification. *J. Clin. Periodontol.* **45**, S1–S8 (2018).

45. Cobb, C. M. Clinical significance of non-surgical periodontal therapy: an evidence-based perspective of scaling and root planing. *J. Clin. Periodontol.* **29**, 22–32 (2002).

46. Rabbani, G. M., Ash, M. M. & Caffesse, R. G. The Effectiveness of Subgingival Scaling and Root Planing in Calculus Removal. *J. Periodontol.* **52**, 119–123 (1981).

47. Costerton, J. W., Stewart, P. S., Greenberg, E. P. & Mattick, J. S. Bacterial biofilms: a common cause of persistent infections. *Science* **284**, 1318–22 (1999).

48. Nishihara, T. & Koseki, T. Microbial etiology of periodontitis. *Periodontol. 2000* **36**, 14–26 (2004).

49. Olson, M. E., Ceri, H., Morck, D. W., Buret, A. G. & Read, R. R. Biofilm bacteria: formation and comparative susceptibility to antibiotics. *Can. J. Vet. Res.* **66**, 86–92 (2002).

50. Desrosiers, M., Bendouah, Z. & Barbeau, J. Effectiveness of Topical Antibiotics on *Staphylococcus Aureus* Biofilm *in Vitro*. *Am. J. Rhinol.* **21**, 149–153 (2007).

51. Smith, K., Perez, A., Ramage, G., Gemmell, C. G. & Lang, S. Comparison of biofilm-associated cell survival following in vitro exposure of meticillin-resistant Staphylococcus aureus biofilms to the antibiotics clindamycin, daptomycin, linezolid, tigecycline and vancomycin. *Int. J. Antimicrob. Agents* **33**, 374–378 (2009).

52. Li, Y. & Zhang, Y. PhoU Is a Persistence Switch Involved in Persister Formation and Tolerance to Multiple Antibiotics and Stresses in Escherichia coli †. *Antimicrob. Agents Chemother.* **51**, 2092–2099 (2007).

53. Hoffman, L. R. *et al.* Aminoglycoside antibiotics induce bacterial biofilm formation. *Nature* **436**, 1171–1175 (2005).

54. Anderl, J. N., Franklin, M. J. & Stewart, P. S. Role of antibiotic penetration limitation in Klebsiella pneumoniae biofilm resistance to ampicillin and ciprofloxacin. *Antimicrob. Agents Chemother.* **44**, 1818–24 (2000).

55. Vrany, J. D., Stewart, P. S. & Suci, P. A. Comparison of recalcitrance to ciprofloxacin and levofloxacin exhibited by Pseudomonas aeruginosa bofilms displaying rapid-transport characteristics. *Antimicrob. Agents Chemother.* **41**, 1352–8 (1997).

56. Stewart, P. S. Theoretical aspects of antibiotic diffusion into microbial biofilms. *Antimicrob. Agents Chemother.* **40**, 2517–22 (1996).

57. Dunne, W. M., Mason, E. O., Kaplan, S. L., Jr & Kaplan, S. L. Diffusion of rifampin and vancomycin through a Staphylococcus epidermidis biofilm. *Antimicrob. Agents Chemother.* **37**, 2522–6 (1993).

58. Hoyle, B. D., Alcantara, J. & Costerton, J. W. Pseudomonas aeruginosa biofilm as a diffusion barrier to piperacillin. *Antimicrob. Agents Chemother.* **36**, 2054–6 (1992).

59. Stabholz, A. *et al.* Using the PerioChip in treating adult periodontitis: an interim report. *Compend. Contin. Educ. Dent.* **21**, 325–8, 330, 332 passim; quiz 338 (2000).

60. Heasman, P. A., Heasman, L., Stacey, F. & McCracken, G. I. Local delivery of chlorhexidine gluconate (PerioChipTM) in periodontal maintenance patients. *J. Clin. Periodontol.* **28**, 90–95 (2008).

61. Soskolne, W. A. *et al.* An in vivo Study of the chlorhexidine release profile of the PerioChipTM in the gingival crevicular fluid, plasma and urine. *J. Clin. Periodontol.* **25**, 1017–1021 (1998).

62. Tomasi, C. & Wennstrom, J. L. Locally delivered doxycycline improves the healing following non-surgical periodontal therapy in smokers. *J. Clin. Periodontol.* **31**, 589–595 (2004).

63. Salvi, G. E. *et al.* Local antimicrobial therapy after initial periodontal treatment. A randomized clinical trial comparing three biodegradable sustained release polymers. *J. Clin. Periodontol.* **29**, 540–550 (2002).

64. Thomas, J. G., Metheny, R. J., Karakiozis, J. M., Wetzel, J. M. & Crout, R. J. Long-Term Sub-Antimicrobial Doxycycline (Periostat®) as Adjunctive Management in Adult

Periodontitis: Effects on Subgingival Bacterial Population Dynamics. *Adv. Dent. Res.* **12**, 32–39 (1998).

65. Haffajee, A. D., Torresyap, G. & Socransky, S. S. Clinical changes following four different periodontal therapies for the treatment of chronic periodontitis: 1-year results. *J. Clin. Periodontol.* **34**, 243–253 (2007).

66. Page, R. C. The microbiological case for adjunctive therapy for periodontitis. *J. Int. Acad. Periodontol.* **6**, 143–9 (2004).

67. Valeant Pharmaceuticals North America. *Arestin Education Card*. www.fda.gov/medwatch (2017).

68. Orapharma, I. ARESTIN-minocycline hydrochloride powder.

69. Abbreviated New Drug Application (ANDA) | FDA. https://www.fda.gov/drugs/types-applications/abbreviated-new-drug-application-anda.

70. Dokoumetzidis, A. & Macheras, P. A century of dissolution research: From Noyes and Whitney to the Biopharmaceutics Classification System. *Int. J. Pharm.* **321**, 1–11 (2006).

71. Fotaki, N. & Vertzoni, M. *Biorelevant Dissolution Methods and Their Applications in In Vitro-In Vivo Correlations for Oral Formulations*. *The Open Drug Delivery Journal* vol. 4 (2010).

72. Grady, H. *et al.* Industry's view on using quality control, biorelevant, and clinically relevant dissolution tests for pharmaceutical development, registration, and. *Elsevier*.

73. Bhardwaj, U. & Burgess, D. J. A novel USP apparatus 4 based release testing method for dispersed systems. *Int. J. Pharm.* **388**, 287–294 (2010).

74. Shen, J. & Burgess, D. J. Accelerated in-vitro release testing methods for extended-release parenteral dosage forms. *Journal of Pharmacy and Pharmacology* vol. 64 986–996 (2012).

75. Shen, J. *et al.* A reproducible accelerated in vitro release testing method for PLGA microspheres. *Elsevier*.

76. Ren, W. *et al.* Dissolution Chamber for Small Drug Delivery System in the Periodontal Pocket. *AAPS J.* **21**, (2019).

77. Goodson, J. M. Gingival crevice fluid flow. *Periodontol. 2000* **31**, 43–54 (2003).

78. Lindhe, J., Westfelt, E., Nyman, S., Socransky, S. S. & Haffajee, A. D. Long-term effect of surgical/non-surgical treatment of periodontal disease. *J. Clin. Periodontol.* **11**, 448–458 (1984).

79. Chapple, I. L. C. *et al.* Primary prevention of periodontitis: managing gingivitis. *J. Clin. Periodontol.* **42**, S71–S76 (2015).

80. Charles, C. H., Mostler, K. M., Bartels, L. L. & Mankodi, S. M. Comparative antiplaque and antigingivitis effectiveness of a chlorhexidine and an essential oil mouthrinse: 6-month clinical trial. *J. Clin. Periodontol.* **31**, 878–884 (2004).

81. Mankodi, S. *et al.* A 6-month clinical trial to study the effects of a cetylpyridinium chloride mouthrinse on gingivitis and plaque. *Am. J. Dent.* **18 Spec No**, 9A-14A (2005).

82. Fine, D. H. *et al.* Effect of an essential oilcontaining antiseptic mouthrinse on plaque and salivary *Streptococcus mutans* levels. *J. Clin. Periodontol.* **27**, 157–161 (2000).

83. Pan, P., Barnett, M. L., Coelho, J., Brogdon, C. & Finnegan, M. B. Determination of the in situ bactericidal activity of an essential oil mouthrinse using a vital stain method. *J. Clin. Periodontol.* **27**, 256–261 (2000).

84. Duarte, S. *et al.* Inhibitory effects of cranberry polyphenols on formation and acidogenicity of *Streptococcus mutans* biofilms. *FEMS Microbiol. Lett.* **257**, 50–56 (2006).

85. Lee, Y. L., Owens, J., Thrupp, L. & Cesario, T. C. Does cranberry juice have antibacterial activity? *JAMA* **283**, 1691 (2000).

86. Weiss, E. I. *et al.* A high molecular mass cranberry constituent reduces mutans streptococci level in saliva and inhibits in vitro adhesion to hydroxyapatite. *FEMS Microbiol. Lett.* **232**, 89–92 (2004).

87. Gregoire, S., Singh, A. P., Vorsa, N. & Koo, H. Influence of cranberry phenolics on glucan synthesis by glucosyltransferases and Streptococcus mutans acidogenicity. *J. Appl. Microbiol.* **103**, 1960–1968 (2007).

88. H.R., R. *et al.* Formulation of thermoreversible gel of cranberry juice concentrate: Evaluation, biocompatibility studies and its antimicrobial activity against periodontal pathogens. *Mater. Sci. Eng. C* **75**, 1506–1514 (2017).

89. Hill, L. E., Gomes, C. & Taylor, T. M. Characterization of beta-cyclodextrin inclusion complexes containing essential oils (trans-cinnamaldehyde, eugenol, cinnamon bark, and clove bud extracts) for antimicrobial delivery applications. *LWT - Food Sci. Technol.* **51**, 86–93 (2013).

90. Belščak-Cvitanović, A. *et al.* Encapsulation of polyphenolic antioxidants from medicinal plant extracts in alginate–chitosan system enhanced with ascorbic acid by electrostatic extrusion. *Food Res. Int.* **44**, 1094–1101 (2011).

91. Chan, E.-S., Yim, Z.-H., Phan, S.-H., Mansa, R. F. & Ravindra, P. Encapsulation of herbal aqueous extract through absorption with ca-alginate hydrogel beads. *Food Bioprod. Process.* **88**, 195–201 (2010).

92. Deladino, L., Anbinder, P. S., Navarro, A. S. & Martino, M. N. Encapsulation of natural antioxidants extracted from Ilex paraguariensis. *Carbohydr. Polym.* **71**, 126–134 (2008).

93. Sessa, M. *et al.* Exploitation of Polyphenolic Extracts from Grape Marc as Natural Antioxidants by Encapsulation in Lipid-Based Nanodelivery Systems. *Food Bioprocess Technol.* **6**, 2609–2620 (2013).

94. SZENTE, L. & SZEJTLI, J. Molecular Encapsulation of Natural and Synthetic Coffee Flavor with B-Cyclodextrin. *J. Food Sci.* **51**, 1024–1027 (1986).

95. Szejtli, J., Szente, L. & Hung, E. B.-E. Molecular encapsulation of volatile, easily oxidizable labile flavour substances by cyclodextrins. *Acta Chim. Acad. Sci.* (1979).

96. Ganea, G. M. *et al.* Delivery of phytochemical thymoquinone using molecular micelle modified poly(D, L lactide- *co* -glycolide) (PLGA) nanoparticles. *Nanotechnology* **21**, 285104 (2010).

97. Silva, L. M., Hill, L. E., Figueiredo, E. & Gomes, C. L. Delivery of phytochemicals of tropical fruit by-products using poly (dl-lactide-co-glycolide) (PLGA) nanoparticles: Synthesis, characterization, and antimicrobial activity. *Food Chem.* **165**, 362–370 (2014).

98. Pereira, M. C. *et al.* Nanoencapsulation of hydrophobic phytochemicals using poly (dl-lactide-co-glycolide) (PLGA) for antioxidant and antimicrobial delivery applications: Guabiroba fruit (Campomanesia xanthocarpa O. Berg) study. *LWT - Food Sci. Technol.* **63**, 100–107 (2015).

99. Pool, H., Mendoza, S., Xiao, H. & McClements, D. J. Encapsulation and release of hydrophobic bioactive components in nanoemulsion-based delivery systems: impact of physical form on quercetin bioaccessibility. *Food Funct.* **4**, 162–174 (2013).

100. Kumari, A., Yadav, S. K., Pakade, Y. B., Singh, B. & Yadav, S. C. Development of biodegradable nanoparticles for delivery of quercetin. *Colloids Surfaces B Biointerfaces* **80**, 184–192 (2010).

101. GORTZI, O., LALAS, S., CHINOU, I. & TSAKNIS, J. Reevaluation of Antimicrobial and Antioxidant Activity of Thymus spp. Extracts before and after Encapsulation in Liposomes. *J. Food Prot.* **69**, 2998–3005 (2006).

102. Gortzi, O., Lalas, S., Chinou, I. & Tsaknis, J. Reevaluation of bioactivity and antioxidant activity of Myrtus communis extract before and after encapsulation in liposomes. *Eur. Food Res. Technol.* **226**, 583–590 (2008).

103. Lin, L.-Z. & Harnly, J. M. A Screening Method for the Identification of Glycosylated Flavonoids and Other Phenolic Compounds Using a Standard Analytical Approach for All Plant Materials. *J. Agric. Food Chem.* **55**, 1084–1096 (2007).

104. Wilson, T. *et al.* Human Glycemic Response and Phenolic Content of Unsweetened Cranberry Juice. *J. Med. FOOD J Med Food* **11**, 46–54 (2008).

105. Allison Turner, † *et al.* Coumaroyl Iridoids and a Depside from Cranberry (Vaccinium macrocarpon). *J. Nat. Prod.* **70**, 253–258 (2007).

106. Yu, L. L., Zhou, K. K. & Parry, J. Antioxidant properties of cold-pressed black caraway, carrot, cranberry, and hemp seed oils. *Food Chem.* **91**, 723–729 (2005).

107. Parker, T. D., Adams, D. A., Zhou, K., Harris, M. & Yu, L. Fatty Acid Composition and Oxidative Stability of Cold-pressed Edible Seed Oils. *J. Food Sci.* **68**, 1240–1243 (2003).

108. Caffesse, R. G., Sweeney, P. L. & Smith, B. A. Scaling and root planing with and without periodontal flap surgery. *J. Clin. Periodontol.* **13**, 205–210 (1986).

109. Roccuzzo, M., Bunino, M., Needleman, I. & Sanz, M. Periodontal plastic surgery for treatment of localized gingival recessions: a systematic review. *J. Clin. Periodontol.* **29**, 178–194 (2002).

110. van Steenberghe, D. *et al.* The rehabilitation of the severely resorbed maxilla by simultaneous placement of autogenous bone grafts and implants: a 10-year evaluation. *Clin. Oral Investig.* **1**, 102–108 (1997).

111. Dutzan, N. *et al.* A dysbiotic microbiome triggers TH17 cells to mediate oral mucosal immunopathology in mice and humans. *Sci. Transl. Med.* **10**, eaat0797 (2018).

112. Graves, D. T., Oates, T. & Garlet, G. P. Review of osteoimmunology and the host response in endodontic and periodontal lesions. *J. Oral Microbiol.* **3**, 5304 (2011).

113. Baker, P. J. The role of immune responses in bone loss during periodontal disease. *Microbes Infect.* **2**, 1181–1192 (2000).

114. Reuter, B. K., Davies, N. M. & Wallace, J. L. Nonsteroidal anti-inflammatory drug enteropathy in rats: role of permeability, bacteria, and enterohepatic circulation. *Gastroenterology* **112**, 109–17 (1997).

115. Kantarci, A., Hasturk, H. & Dyke, T. E. Host-mediated resolution of inflammation in periodontal diseases. *Periodontol. 2000* **40**, 144–163 (2006).

116. Hasturk, H. *et al.* Resolvin E1 regulates inflammation at the cellular and tissue level and restores tissue homeostasis in vivo. *J. Immunol.* **179**, 7021–9 (2007).

117. Hasturk, H. *et al.* RvE1 protects from local inflammation and osteoclast-mediated bone destruction in periodontitis. *FASEB J.* **20**, 401–3 (2005).

118. Ramamurthy, N. S. *et al.* Inhibition of Matrix Metalloproteinase-Mediated Periodontal Bone Loss in Rats: A Comparison of 6 Chemically Modified Tetracyclines. *J. Periodontol.* **73**, 726–734 (2002).

119. Giannobile, W. V. Host-response therapeutics for periodontal diseases. *J. Periodontol.* **79**, 1592–600 (2008).

120. Lee, D. E. *et al.* Periodontitis mainly increases osteoclast formation via enhancing the differentiation of quiescent osteoclast precursors into osteoclasts. *J. Periodontal Res.* **50**, 256–264 (2015).

121. Cutler, C. W. & Jotwani, R. Antigen-presentation and the role of dendritic cells in periodontitis.

122. Jotwani, R. *et al.* Mature Dendritic Cells Infiltrate the T Cell-Rich Region of Oral Mucosa in Chronic Periodontitis: In Situ, In Vivo, and In Vitro Studies. *J. Immunol.* **167**, 4693–4700 (2001).

123. Ni, C. *et al.* Gold nanoparticles modulate the crosstalk between macrophages and periodontal ligament cells for periodontitis treatment. *Biomaterials* **206**, 115–132 (2019).

124. Z, Z. *et al.* Induction of M2 Macrophages Prevents Bone Loss in Murine Periodontitis Models. *J. Dent. Res.* **98**, 200–208 (2019).

125. Tang, Q. & Bluestone, J. A. The Foxp3+ regulatory T cell: a jack of all trades, master of regulation. *Nat. Immunol.* **9**, 239–44 (2008).

126. Vignali, D. A. A., Collison, L. W. & Workman, C. J. How regulatory T cells work. *Nat. Rev. Immunol.* **8**, 523–32 (2008).

127. Francisconi, C. F. *et al.* Characterization of the Protective Role of Regulatory T Cells in Experimental Periapical Lesion Development and Their Chemoattraction Manipulation as a Therapeutic Tool. *J. Endod.* **42**, 120–126 (2016).

128. Cardoso, C. R. *et al.* Characterization of CD4+CD25+ natural regulatory T cells in the inflammatory infiltrate of human chronic periodontitis. *J. Leukoc. Biol.* **84**, 311–318 (2008).

129. Glowacki, A. J. *et al.* Prevention of inflammation-mediated bone loss in murine and canine periodontal disease via recruitment of regulatory lymphocytes. *Proc. Natl. Acad. Sci. U. S. A.* **110**, 18525–30 (2013).

130. Abdulahad, W. H. *et al.* Functional defect of circulating regulatory CD4+ T cells in patients with Wegener's granulomatosis in remission. *Arthritis Rheum.* **56**, 2080–2091 (2007).

131. Viglietta, V., Baecher-Allan, C., Weiner, H. L. & Hafler, D. A. Loss of Functional Suppression by CD4+CD25+ Regulatory T Cells in Patients with Multiple Sclerosis. *J. Exp. Med.* **199**, (2004).

132. Baecher-Allan, C. & Hafler, D. A. Human regulatory T cells and their role in autoimmune disease. *Immunol. Rev.* **212**, 203–216 (2006).

133. Jhunjhunwala, S. *et al.* Controlled release formulations of IL-2, TGF-B1 and rapamycin for the induction of regulatory T cells. *J. Control. Release* **159**, 78–84 (2012).

134. Ratay, M. L. *et al.* TRI Microspheres prevent key signs of dry eye disease in a murine, inflammatory model. *Sci. Rep.* **7**, 17527 (2017).

135. Balmert, S. C. *et al.* In vivo induction of regulatory T cells promotes allergen tolerance and suppresses allergic contact dermatitis. *J. Control. Release* **261**, 223–233 (2017).

136. Horwitz, D. A., Zheng, S. G., Wang, J. & Gray, J. D. Critical role of IL-2 and TGF-β in generation, function and stabilization of Foxp3+CD4+ Treg. *Eur. J. Immunol.* **38**, 912–915 (2008).

137. Kopf, H., de la Rosa, G. M., Howard, O. M. Z. & Chen, X. Rapamycin inhibits differentiation of Th17 cells and promotes generation of FoxP3+ T regulatory cells. *Int. Immunopharmacol.* **7**, 1819–1824 (2007).

138. Haxhinasto, S., Mathis, D. & Benoist, C. The AKT-mTOR axis regulates de novo differentiation of CD4+Foxp3+ cells. *J. Exp. Med.* **205**, 565–74 (2008).

139. Global Generic Drugs Market Report 2021: The New Generics Era - The Patent Cliff, Types of Generic Drugs, Simple Generics, Super Generics, Biosimilars, ANDA Approvals - ResearchAndMarkets.com | Business Wire. https://www.businesswire.com/news/home/20210528005253/en/Global-Generic-Drugs-Market-Report-2021-The-New-Generics-Era---The-Patent-Cliff-Types-of-Generic-Drugs-Simple-Generics-Super-Generics-Biosimilars-ANDA-Approvals---ResearchAndMarkets.com.

140. Dissolution Methods. https://www.accessdata.fda.gov/scripts/cder/dissolution/dsp_SearchResults.cfm.

141. Observations on Current Controversies in Dentistry | Dentistry Today. https://www.dentistrytoday.com/new-directions/10128-observations-on-current-controversies-in-dentistry.

142. OraPharma, Inc.'s ARESTIN receives accolades | DentistryIQ. https://www.dentistryiq.com/products/hygiene/article/16370346/orapharma-incs-arestin-receives-accolades.

143. Garner, J. *et al.* A protocol for assay of poly(lactide-co-glycolide) in clinical products. *Int. J. Pharm.* **495**, 87–92 (2015).

144. Pharmacopeia US. *Minocycline Hydrochloride Extended-Release Tablets*. (2015).

145. Rothstein, S. N., Federspiel, W. J. & Little, S. R. A simple model framework for the prediction of controlled release from bulk eroding polymer matrices. *J. Mater. Chem.* **18**, 1873–80 (2008).

146. Rothstein, S. N., Federspiel, W. J. & Little, S. R. A unified mathematical model for the prediction of controlled release from surface and bulk eroding polymer matrices. *Biomaterials* **30**, 1657–64 (2009).

147. Polli, J. E., Rekhi, G. S., Augsburger, L. L. & Shah, V. P. Methods to Compare Dissolution Profiles and a Rationale for Wide Dissolution Specifications for Metoprolol Tartrate tablets. *J. Pharm. Sci.* **86**, 690–700 (1997).

148. Bang, J., Cimasoni, G., Rosenbusch, C. & Duckert, A. Sodium, Potassium and Calcium Contents of Crevicular Exudate: Their Relations to Gingivitis and Periodontitis. *J. Periodontol.* **44**, 770–774 (1973).

149. Bickel, M. & Cimasoni, G. The pH of human crevicular fluid measured by a new microanalytical technique. *J. Periodontal Res.* **20**, 35–40 (1985).

150. Aoyagi, S., Onishi, H. & Machida, Y. Novel chitosan wound dressing loaded with minocycline for the treatment of severe burn wounds. *Int. J. Pharm.* **330**, 138–145 (2007).

151. Jain, N., Jain, G. K., Ahmad, F. J. & Khar, R. K. Validated stability-indicating densitometric thin-layer chromatography: Application to stress degradation studies of minocycline. *Anal. Chim. Acta* **599**, 302–309 (2007).

152. Park, T. G. Degradation of poly(lactic-co-glycolic acid) microspheres: effect of copolymer composition. *Biomaterials* **16**, 1123–30 (1995).

153. Arias, K. *et al.* Minocycline and tigecycline form higher-order Ca2+ complexes of stronger affinity than tetracycline. *Inorganica Chim. Acta* **441**, 181–191 (2016).

154. Balmert, S. C. *et al.* Positive charge of '"sticky"' peptides and proteins impedes release from negatively charged PLGA matrices. *J. Mater. Chem. B* **3**, 4723–4734 (2015).

155. Markopoulos, C., Andreas, C. J., Vertzoni, M., Dressman, J. & Reppas, C. In-vitro simulation of luminal conditions for evaluation of performance of oral drug products: Choosing the appropriate test media. *Eur. J. Pharm. Biopharm.* **93**, 173–182 (2015).

156. Khurshid, Z., Mali, M., Naseem, M., Najeeb, S. & Zafar, M. S. Human Gingival Crevicular Fluids (GCF) Proteomics: An Overview. *Dent. J. 2017, Vol. 5, Page 12* **5**, 12 (2017).

157. Raman, C., Berkland, C., Kim, K. & Pack, D. W. Modeling small-molecule release from PLG microspheres: effects of polymer degradation and nonuniform drug distribution. *J. Control. Release* **103**, 149–158 (2005).

158. del Pozo, J. L. & Patel, R. The Challenge of Treating Biofilm-associated Bacterial Infections. *Clin. Pharmacol. Ther.* **82**, 204–209 (2007).

159. Flemming, H.-C. & Wingender, J. The biofilm matrix. *Nat. Rev. Microbiol.* **8**, 623–633 (2010).

160. Horev, B. *et al.* pH-Activated Nanoparticles for Controlled Topical Delivery of Farnesol To Disrupt Oral Biofilm Virulence. *ACS Nano* **9**, 2390–2404 (2015).

161. Lacombe, A., Wu, V. C. H., Tyler, S. & Edwards, K. Antimicrobial action of the American cranberry constituents; phenolics, anthocyanins, and organic acids, against Escherichia coli O157:H7. *Int. J. Food Microbiol.* **139**, 102–107 (2010).

162. ENACHE, E. & CHEN, Y. Survival of Escherichia coli O157:H7, Salmonella, and Listeria monocytogenes in Cranberry Juice Concentrates at Different °Brix Levels. *J. Food Prot.* **70**, 2072–2077 (2007).

163. Baum, B. J. *CLINICAL SCIENCE Evaluation of Stimulated Parotid Saliva Flow Rate in Different Age Groups*. *J Dent Res* vol. 60 http://journals.sagepub.com/doi/pdf/10.1177/00220345810600070101 (1981).

164. Emeritus, M. E. & Dawes, C. *Saliva and oral health Fourth edition*. https://pdfs.semanticscholar.org/e483/571214ba40121071a143f100e2fe9f7fc7d8.pdf.

165. Heft1, M. W. & Baum2, B. J. *BASIC BIOLOGICAL SCIENCES Unstimulated and Stimulated Parotid Salivary Flow Rate in Individuals of Different Ages*. *J Dent Res* vol. 63 http://journals.sagepub.com/doi/pdf/10.1177/00220345840630100101 (1984).

166. Yamanaka, A., Kimizuka, R., Kato, T. & Okuda, K. Inhibitory effects of cranberry juice on attachment of oral streptococci and biofilm formation. *Oral Microbiol. Immunol.* **19**, 150–154 (2004).

167. Diaz del Consuelo, I., Falson, F., Guy, R. H. & Jacques, Y. Ex vivo evaluation of bioadhesive films for buccal delivery of fentanyl. *J. Control. Release* **122**, 135–140 (2007).

168. Smart, J. D., Kellaway, I. W. & Worthington, H. E. C. An in-vitro investigation of mucosa-adhesive materials for use in controlled drug delivery. *J. Pharm. Pharmacol.* **36**, 295–299 (1984).

169. Jones, D. S., Woolfson, A. D., Djokic, J. & Coulter, W. A. Development and Mechanical Characterization of Bioadhesive Semi-Solid, Polymeric Systems Containing Tetracycline for the Treatment of Periodontal Diseases. *Pharm. Res.* **13**, 1734–1738 (1996).

170. Do, M. P. *et al.* In situ forming implants for periodontitis treatment with improved adhesive properties. *Eur. J. Pharm. Biopharm.* **88**, 342–350 (2014).

171. Aznar, M., Gómez-Estaca, J., Vélez, D., Devesa, V. & Nerín, C. Migrants determination and bioaccessibility study of ethyl lauroyl arginate (LAE) from a LAE based antimicrobial food packaging material. *Food Chem. Toxicol.* **56**, 363–370 (2013).

172. Woodcock, N. H., Hammond, B. H., Ralyea, R. D. & Boor, K. J. Short communication: Nalpha-lauroyl-L-arginine ethylester monohydrochloride reduces bacterial growth in pasteurized milk. *J. Dairy Sci.* **92**, 4207–10 (2009).

173. Gallob, J. T. *et al.* A randomized trial of ethyl lauroyl arginate-containing mouthrinse in the control of gingivitis. *J. Clin. Periodontol.* **42**, 740–747 (2015).

174. Auschill, T. M., Sculean, A., Hellwig, E., Haug, M. & Arweiler, N. B. Clinical and antibacterial effect of toothpastes with a new ingredient. *J. Dent. Res.* **86**, (2007).

175. Giertsen, E., Guggenheim, B. & Gmür, R. Antiplaque effects of ethyl lauroyl arginine in situ. *J. Dent. Res.* **86**, (2007).

176. Zijnge, V. *et al.* Oral Biofilm Architecture on Natural Teeth. *PLoS One* **5**, e9321 (2010).

177. Mariotti, A. Dental Plaque-Induced Gingival Diseases. *Ann. Periodontol.* **4**, 7–17 (1999).

178. Axelsson, P. & Lindhe, J. The effect of a preventive programme on dental plaque, gingivitis and caries in schoolchildren. Results after one and two years. *J. Clin. Periodontol.* **1**, 126–138 (1974).

179. Durack, D. T. Prevention of Infective Endocarditis. *N. Engl. J. Med.* **332**, 38–44 (1995).

180. Strom, B. L. *et al.* Dental and Cardiac Risk Factors for Infective Endocarditis: A Population-Based, Case-Control Study. *Ann. Intern. Med.* **129**, 761 (1998).

181. Lockhart DDS, P. B. *et al. Poor oral hygiene as a risk factor for infective endocarditis–related bacteremia*. http://jada.ada.org (2014) doi:10.14219/jada.archive.2009.0046.

182. Dajani, A. S. *et al. Prevention of Bacterial Endocarditis: Recommendations by the American Heart Association*. *American Medical Association* vol. 277 https://academic.oup.com/cid/article-abstract/25/6/1448/363787 (1997).

183. Noiri, Y., Ehara, A., Kawahara, T., Takemura, N. & Ebisu, S. Participation of Bacterial Biofilms in Refractory and Chronic Periapical Periodontitis. *J. Endod.* **28**, 679–683 (2002).

184. Ricucci, D. & Siqueira, J. F. Biofilms and Apical Periodontitis: Study of Prevalence and Association with Clinical and Histopathologic Findings. *J. Endod.* **36**, 1277–1288 (2010).

185. Nair, P. N. R., Henry, S., Cano, V. & Vera, J. Microbial status of apical root canal system of human mandibular first molars with primary apical periodontitis after "one-visit" endodontic treatment. *Oral Surgery, Oral Med. Oral Pathol. Oral Radiol. Endodontology* **99**, 231–252 (2005).

186. Kidd, E. A. M. & Fejerskov, O. *WHAT CONSITUTUTES DENTAL CARIES? What Constitutes Dental Caries? Histopathology of Carious Enamel and Dentin Related to the Action of Cariogenic Biofilms PROCEEDINGS*. http://journals.sagepub.com/doi/pdf/10.1177/154405910408301s07.

187. Shu, M., Wong, L., Miller, J. H. & Sissons, C. H. Development of multi-species consortia biofilms of oral bacteria as an enamel and root caries model system. *Arch. Oral Biol.* **45**, 27–40 (2000).

188. Giacaman, R. A., Campos, P., Muñoz-Sandoval, C. & Castro, R. J. Cariogenic potential of commercial sweeteners in an experimental biofilm caries model on enamel. *Arch. Oral Biol.* **58**, 1116–1122 (2013).

189. Hayek, R. R. A. *et al.* Comparative Study Between the Effects of Photodynamic Therapy and Conventional Therapy on Microbial Reduction in Ligature-Induced Peri-Implantitis in Dogs. *J. Periodontol.* **76**, 1275–1281 (2005).

190. Mombelli, A., Müller, N. & Cionca, N. The epidemiology of peri-implantitis. *Clin. Oral Implants Res.* **23**, 67–76 (2012).

191. Mombelli, A. & Décaillet, F. The characteristics of biofilms in peri-implant disease. *J. Clin. Periodontol.* **38**, 203–213 (2011).

192. Carlin, V. *et al.* Cytogenetic damage induced by mouthrinses formulations in vivo and in vitro. *Clin. Oral Investig.* **16**, 813–820 (2012).

193. Silverman, S. & Wilder, R. Antimicrobial mouthrinse as part of a comprehensive oral care regimen: Safety and compliance factors. *J. Am. Dent. Assoc.* **137**, S22–S26 (2006).

194. Hong, V. & Wrolstad, R. E. Use of HPLC separation/photodiode array detection for characterization of anthocyanins. *J. Agric. Food Chem.* **38**, 708–715 (1990).

195. Gopu, V., Kothandapani, S. & Shetty, P. H. Quorum quenching activity of Syzygium cumini (L.) Skeels and its anthocyanin malvidin against Klebsiella pneumoniae. *Microb. Pathog.* **79**, 61–69 (2015).

196. Viskelis, P. *et al.* Anthocyanins, Antioxidative, and Antimicrobial Properties of American Cranberry (*Vaccinium macrocarpon* Ait.) and their Press Cakes. *J. Food Sci.* **74**, C157–C161 (2009).

197. Weiss, E. I., Lev-Dor, R., Sharon, N. & Ofek, I. Inhibitory Effect of a High-Molecular-Weight Constituent of Cranberry on Adhesion of Oral Bacteria. *Crit. Rev. Food Sci. Nutr.* **42**, 285–292 (2002).

198. Steinberg, D., Feldman, M., Ofek, I. & Weiss, E. I. Effect of a high-molecular-weight component of cranberry on constituents of dental biofilm. *J. Antimicrob. Chemother.* **54**, 86–89 (2004).

199. Jhunjhunwala, S. *et al.* Bioinspired controlled release of CCL22 recruits regulatory T cells in vivo. *Adv. Mater.* **24**, 4735–8 (2012).

200. Ratay, M. L. *et al.* Treg-recruiting microspheres prevent inflammation in a murine model of dry eye disease. *J. Control. Release* **258**, 208–217 (2017).

201. Ratay, M. L., Balmert, S. C., Bassin, E. J. & Little, S. R. Controlled release of an HDAC inhibitor for reduction of inflammation in dry eye disease. *Acta Biomater.* **71**, 261–270 (2018).

202. Fedorchak, M. V. *et al.* 28-day intraocular pressure reduction with a single dose of brimonidine tartrate-loaded microspheres. *Exp. Eye Res.* **125**, 210–216 (2014).

203. Balmert, S. C. *et al.* Positive charge of "sticky" peptides and proteins impedes release from negatively charged PLGA matrices. *J. Mater. Chem. B* **3**, 4723–4734 (2015).

204. Angadi, S. C., Manjeshwar, L. S. & Aminabhavi, T. M. Stearic Acid-Coated Chitosan-Based Interpenetrating Polymer Network Microspheres: Controlled Release Characteristics. *Ind. Eng. Chem. Res.* **50**, 4504–4514 (2011).

205. Robson, H. ., Craig, D. Q. . & Deutsch, D. An investigation into the release of cefuroxime axetil from taste-masked stearic acid microspheres: Part 1: The influence of the dissolution medium on the drug release profile and the physical integrity of the microspheres. *Int. J. Pharm.* **190**, 183–192 (1999).

206. Chary, R. B., Vani, G. & Rao, Y. M. In vitro and in vivo adhesion testing of mucoadhesive drug delivery systems. *Drug Dev. Ind. Pharm.* **25**, 685–90 (1999).

207. Hayama, M. *et al.* Nanoscopic behavior of polyvinylpyrrolidone particles on polysulfone/polyvinylpyrrolidone film. *Biomaterials* **25**, 1019–1028 (2004).

208. Yang, S., Sadekuzzaman, M. & Ha, S.-D. Treatment with lauric arginate ethyl ester and commercial bacteriophage, alone or in combination, inhibits Listeria monocytogenes in chicken breast tissue. *Food Control* **78**, 57–63 (2017).

209. Yordanov, G. G., Yoshimura, H. & Dushkin, C. D. Fine control of the growth and optical properties of CdSe quantum dots by varying the amount of stearic acid in a liquid paraffin matrix. *Colloids Surfaces A Physicochem. Eng. Asp.* **322**, 177–182 (2008).

210. Morigaki, K. & Walde, P. Fatty acid vesicles. *Curr. Opin. Colloid Interface Sci.* **12**, 75–80 (2007).

211. Lavasanifar, A., Samuel, J. & Kwon, G. S. The effect of fatty acid substitution on the in vitro release of amphotericin B from micelles composed of poly(ethylene oxide)-block-poly(N-hexyl stearate-l-aspartamide). *J. Control. Release* **79**, 165–172 (2002).

212. Hu, F.-Q., Ren, G.-F., Yuan, H., Du, Y.-Z. & Zeng, S. Shell cross-linked stearic acid grafted chitosan oligosaccharide self-aggregated micelles for controlled release of paclitaxel. *Colloids Surfaces B Biointerfaces* **50**, 97–103 (2006).

213. Hu, F.-Q. *et al.* Preparation and characterization of stearic acid nanostructured lipid carriers by solvent diffusion method in an aqueous system. *Colloids Surfaces B Biointerfaces* **45**, 167–173 (2005).

214. Hu, F.-Q. *et al.* A novel chitosan oligosaccharide–stearic acid micelles for gene delivery: Properties and in vitro transfection studies. *Int. J. Pharm.* **315**, 158–166 (2006).

215. Hu, F.-Q., Liu, L.-N., Du, Y.-Z. & Yuan, H. Synthesis and antitumor activity of doxorubicin conjugated stearic acid-g-chitosan oligosaccharide polymeric micelles. *Biomaterials* **30**, 6955–6963 (2009).

216. Zhang, Q., Yie, G., Li, Y., Yang, Q. & Nagai, T. Studies on the cyclosporin A loaded stearic acid nanoparticles. *Int. J. Pharm.* **200**, 153–159 (2000).

217. Ito, T. *et al.* Two Functional Subsets of FOXP3+ Regulatory T Cells in Human Thymus and Periphery. *Immunity* **28**, 870–880 (2008).

218. Abe, T. & Hajishengallis, G. Optimization of the ligature-induced periodontitis model in mice. *J. Immunol. Methods* **394**, 49–54 (2013).

219. Hajishengallis, G. & Lamont, R. J. Beyond the red complex and into more complexity: the polymicrobial synergy and dysbiosis (PSD) model of periodontal disease etiology. *Mol. Oral Microbiol.* **27**, 409–419 (2012).

220. Darveau, R. P. Periodontitis: a polymicrobial disruption of host homeostasis. *Nat. Rev. Microbiol.* **8**, 481–490 (2010).

221. Cekici, A., Kantarci, A., Hasturk, H. & Van Dyke, T. E. Inflammatory and immune pathways in the pathogenesis of periodontal disease. *Periodontol. 2000* **64**, 57–80 (2014).

222. Hajishengallis, G. Immunomicrobial pathogenesis of periodontitis: keystones, pathobionts, and host response. *Trends Immunol.* **35**, 3–11 (2014).

223. Zhuang, Z. *et al.* Induction of M2 Macrophages Prevents Bone Loss in Murine Periodontitis Models. *J. Dent. Res.* **98**, 200–208 (2019).

224. Eskan, M. A. *et al.* The leukocyte integrin antagonist Del-1 inhibits IL-17-mediated inflammatory bone loss. *Nat. Immunol.* **13**, 465–473 (2012).

225. Pacheco, C. M. F. *et al.* Local Sustained Delivery of Anti–IL-17A Antibodies Limits Inflammatory Bone Loss in Murine Experimental Periodontitis. *J. Immunol.* **206**, 2386–2392 (2021).

226. Araujo-Pires, A. C. *et al.* IL-4/CCL22/CCR4 axis controls regulatory T-cell migration that suppresses inflammatory bone loss in murine experimental periodontitis. *J. Bone Miner. Res.* **30**, 412–22 (2015).

227. Fisher, J. D. *et al.* Treg-inducing microparticles promote donor-specific tolerance in experimental vascularized composite allotransplantation. *Proc. Natl. Acad. Sci. U. S. A.* **116**, 25784–25789 (2019).

228. Bassin, E. J., Buckley, A. R., Piganelli, J. D. & Little, S. R. TRI microparticles prevent inflammatory arthritis in a collagen-induced arthritis model. *PLoS One* **15**, e0239396 (2020).

229. Casey, L. M. *et al.* Cargo-less nanoparticles program innate immune cell responses to toll-like receptor activation. *Biomaterials* **218**, 119333 (2019).

230. Look, M., Saltzman, W. M., Craft, J. & Fahmy, T. M. The nanomaterial-dependent modulation of dendritic cells and its potential influence on therapeutic immunosuppression in lupus. *Biomaterials* **35**, 1089–1095 (2014).

231. Liu, M. *et al.* Old Dog New Tricks: PLGA Microparticles as an Adjuvant for Insulin Peptide Fragment-Induced Immune Tolerance against Type 1 Diabetes. *Mol. Pharm.* **17**, 3513–3525 (2020).

232. Allen, R. P., Bolandparvaz, A., Ma, J. A., Manickam, V. A. & Lewis, J. S. Latent, Immunosuppressive Nature of Poly(lactic-co-glycolic acid) Microparticles. *ACS Biomater. Sci. Eng.* **4**, 900 (2018).

233. O'Boyle, C. *et al.* Ligature-induced periodontitis induces systemic inflammation but does not alter acute outcome after stroke in mice: *https://doi.org/10.1177/1747493019834191* **15**, 175–187 (2019).

234. Moro-García, M. A., Mayo, J. C., Sainz, R. M. & Alonso-Arias, R. Influence of Inflammation in the Process of T Lymphocyte Differentiation: Proliferative, Metabolic, and Oxidative Changes. *Front. Immunol.* **9**, 1 (2018).